UNIVERSIDADE FEDERAL DE PERNAMBUCO

CENTRO DE TECNOLOGIA E GEOCIÊNCIAS

DEPARTAMENTO DE GEOLOGIA

PROGRAMA DE PÓS-GRADUAÇÃO EM GEOCIÊNCIAS

JOSÉ VICTOR ANTUNES DE AMORIM

MAGMATISMO FERROSO NA ZONA TRANSVERSAL DA PROVÍNCIA BORBOREMA: PETROGÊNESE E IMPLICAÇÕES GEODINÂMICAS

RECIFE

2018

JOSÉ VICTOR ANTUNES DE AMORIM

MAGMATISMO FERROSO NA ZONA TRANSVERSAL DA PROVÍNCIA BORBOREMA: PETROGÊNESE E IMPLICAÇÕES GEODINÂMICAS

Dissertação de Mestrado apresentada ao Pro- grama de Pós-Graduação em Geociências - PPGEOC, da Universidade Federal de Pernambuco, como parte dos requisitos necessários à obtenção do título de Mestre em Geociências.

Área de concentração: Geoquímica, Geofísica e Evolução Crustal.

Linha de pesquisa: Processos ígneos, metalogênese e evolução crustal.

Orientadora: Profª. Drª. Ignez de Pinho Guimarães

Coorientadora: Profª. Drª. Vanessa Biondo Ribeiro

RECIFE

2018

Catalogação na fonte
Bibliotecária: Rosineide Mesquita Gonçalves Luz / CRB4-1361 (BCTG)

A524m Amorim, José Victor Antunes de.
Magmatismo ferroso na Zona Transversal da Província da Borborema: petrogênese e implicações geodinâmicas / José Victor Antunes de Amorim. – Recife, 2018.
131folhas, il., figs., gráfs., tabs.

Orientadora: Profª. Drª. Ignez de Pinho Guimarães.
Coorientadora: Profª Drª Vanessa Biondo Ribeiro.
Dissertação (Mestrado) – Universidade Federal de Pernambuco. CTG. Programa de Pós-Graduação em Geociências - PPGEOC, 2018.
Inclui Referências Apêndices e Anexo.

1. Geociências. 2. Granitos ferrosos. 3. Província Borborema. 4. Subprovíncia Transversal. 5. Geoquímica. 6. Geocronologia. I.Guimarães, Ignez de Pinho (Orientadora). II. Ribeiro, Vanessa Biondo (Coorientadora). III. Título.

551CDD (22.ed) UFPE/BCTG-2018/ 286

JOSÉ VICTOR ANTUNES DE AMORIM

MAGMATISMO FERROSO NA ZONA TRANSVERSAL DA PROVÍNCIA BORBOREMA: PETROGÊNESE E IMPLICAÇÕES GEODINÂMICAS

Dissertação apresentada ao Programa de Pós-Graduação em Geociências da Universidade Federal de Pernambuco, como requisito parcial para a obtenção do título de Mestre em Geociências.

Aprovada em: 20/02/2018

BANCA EXAMINADORA

Prof.ª Dr.ª Ignez de Pinho Guimarães (Orientadora)
Universidade Federal de Pernambuco

Prof. Dr. Adejardo Francisco da Silva Filho (Examinador Interno)
Universidade Federal de Pernambuco

Prof. Dr. Herbet Conceição (Examinador Externo)
Universidade Federal de Sergipe

Dedico esta dissertação aos meus pais, que sempre estiveram presentes na minha jornada acadêmica.

AGRADECIMENTOS

Agradeço a Fundação de Amparo à Ciencia e Tecnologia do estado de Pernambuco, por financiar o mestrado, através do projeto IBPG-1074-1.07/15.

Agradeço aos meus amigos da sala de pós-graduação no Departamento de Geologia, pelas discussões produtivas.

Aos meus colegas do Grupo de Geotectônica e Geoquímica Aplicada (GEG), pela disposição em me ajudar.

Aos meus amigos de longa data Anna, Ana, Mirella, Nayara, Natália, Áureo, Gabriel, Thales, Rodrigo, Flávio, Douglas, Jefferson, Lucilene, Rafaella e Aldine, por me incentivar a ir além.

Às minhas orientadoras, Ignez de Pinho Guimarães e Vanessa Biondo Ribeiro, pela incansável paciência e disposição.

“É fácil se posicionar na multidão, mas é preciso coragem para se posicionar sozinho” - Mahatma Gandhi

RESUMO

Granitos ferrosos possuem número de ferro mais alto que granitóides cordilheranos, estão comumente associados a ambientes extensionais, e são enriquecidos em LILE e HFSE. Granitos ferrosos (580 - 530 Ma) foram descritos na subprovíncia Transversal da Província da Borborema (PB) e na África. Compreendem dois grupos: G1 - levemente peraluminosos a metaluminosos, álcali-cálcicos, com mica pobre em annita e cristalizados sob condições intermediárias de fO_2 (Complexo Aroeiras e enxames de diques Serra Branca - Coxixola); G2 - metaluminosos a levemente peraluminosos, alcalinos a álcali-cálcicos, com mica rica em annita e cristalizados sob condições de baixa fO_2. G1 marca a transição da colisão para transcorrências (~585 Ma), ou da transcorrência para uplift e transtensão (~545 Ma). G2 respresenta os granitóides intrudidos durante tectonica extensional associada a fase transcorrente (~550 Ma), ou sincrônica com a deposição de bacias intracratônicas transtensionais (~530 Ma). Idades modelo de Hf e Nd são mais antigas que 2,0 Ga, sugerindo que a geração dos granitóides ferrosos envolveu fusão parcial de rochas Paleoproterozoicas. O fato destes grantóides serem enriquecdidos em LILE e HFSE, como esperado, é reconhecível em mapas gamaespectrométricos de escala regional, valores mais altos de K(%), eTh (ppm) e eU (ppm) contrastam significativamente com as rochas encaixantes e com granitos magnesianos. Alguns destes granitóides encontram-se associados com gabros e dioritos, resultando em associações heterogêneas de rochas. Essas heterogeneidades, em mapas gamaespectrométricos, são possíveis de serem identificadas e correlacionadas com processos geológicos (mistura, deformação em zonas de cisalhamento), geoquímica, e petrografia. Dioritos e gabros mostram valores médios a baixos de K (1 - 3%), eTh (5 - 20ppm) e eU (0,2 - 2ppm), contrastando com valores altos em regiões que dominam granitóides ferrosos (K, 3 - 6%; eTh, 15 - 60ppm; eU, 2 - 4ppm).

Palavras-chave: Granitos ferrosos. Província Borborema. Subprovíncia Transversal. Geoquímica. Geocronologia.

ABSTRACT

Ferroan granites have higher Fe-number than cordilleran granitoids, often emplaced in extensional settings, and are LILE and HFSE enriched. Ferroan granites (585 – 530 Ma) have been described in the Transversal subprovince of the Borborema Province (BP) and in Africa. They comprise two groups: G1 - slightly peraluminous to metaluminous, alkali-calcic rocks, with annite-poor mica and crystallized under intermediate fO_2 (Aroeiras Complex and Serra Branca – Coxixola dike swarms); G2 metaluminous to slightly peraluminous, alkalic to alkali-calcic rocks, with annite rich mica and crystallized under low fO_2 (Queimadas and Prata intrusions). G1 marks the transition from collision to transcurrence (ca. 585 Ma), or from transcurrence to uplift and transtension (ca. 545 Ma). G2 represents the granitoids intruded during extensional tectonics in transcurrent setting (ca. 550 Ma), or coeval with deposition of transtensional intracratonic basins (ca. 530 Ma). Hf and Nd model ages are older than 2.0 Ga, suggesting that the ferroan granitoids involved partial melting of Paleoproterozoic rocks. The LILE and HFSE enriched nature of these granitoids, as expected, is recognizable in gamma spectrometric maps of regional scale, highest values of K(%), eTh (ppm) and eU (ppm) contrasts significantly with country rocks and magnesian granites. Some of the ferroan granitoids are associated with coeval diorites and gabbros, comprising heterogeneous rock associations. In gamma spectrometric maps it is possible to identify these heterogeneities and link to geological processes (mingling, shear zone deformation), geochemistry, as well as, petrography. Diorites and gabbros show low to medium values of K (1 – 3%), eTh (5 – 20ppm) and eU (0.2 – 2ppm), contrasting with the high values of regions with dominance of ferroan granitoids (K, 3 – 6%; eTh, 15 – 60ppm; eU, 2 –4ppm).

Keywords: Ferroan granites. Borborema Province. Transversal subprovince. Geochemistry. Geochronology.

LISTA DE FIGURAS

SUMÁRIO

1 INTRODUÇÃO

Granitos (*sensu lato*) são as rochas mais abundantes da crosta continental superior (WEDEPOHL, 1991). O entendimento dos processos que geram esse tipo rocha têm importante papel na differenciação geoquímica da crosta continental, e estão intimamente conectados com tectônica e geodinâmica.

Parte da complexidade associada ao estudo de granitos é que a mesma associação mineral (quartzo, feldpatos e minerais ferromagnesianos), pode ser alcançada através de inúmeros processos (FROST et al., 2001). Fusão parcial de rochas crustais é referido como o principal mecanismo para a geração de magmas graniticos (STEVENS; CLEMENS, 1993), contudo *melts* graníticos podem ser gerados também a partir derivados mantélicos evoluídos, ou a partir da mistura de fusões crustais e mantélicas (PITCHER, 1993; BONIN; DUBOIS; GOHAU, 1997; YOUNG, 2003).

Devido a complexidade e quantidade de processos envolvidos, classificações geoquímicas tem sido utilizadas por petrólogos como parâmetro para distinção dos tipos de granitos (BARBARIN, 1999; FROST et al., 2001).

1.1 CLASSIFICAÇÃO DE GRANITOS

Barbarin (1990) mostra que aproximadamente vinte esquemas genéticos de classificação de granitóides foram propostos, contudo nenhum obteve aceitação unânime.

1.1.1 Classificação alfabética (S-I-M-A)

Chappell e White (1974) propuseram o primeiro esquema moderno de classificação geoquímica de rochas graníticas (Tabela 1), quando reconheceram dois tipos de granitos contrastantes (Tipo-I e Tipo-S) no *Lachlan Fold Belt*. Granitos tipo-I são metaluminosos a levemente peraluminosos, relativamente sódicos, com ampla variação de sílica (56 - 77% SiO_2), formados a partir de uma fonte metaígnea máfica. Granitos tipo-S são fortemente peraluminosos relativamente potássicos e restritos a altas concentrações de sílica (64 - 77% SiO_2), formados a partir da fusão de rochas metassedimentares.

Posteriormente, Loiselle e Wones (1979) introduziram um novo termo a classificação, eles reconheceram um tipo de granito relativamente potássico, com alta razão $\frac{FeOt}{(FeOt+MgO)}$, elevados teores de Zr e outros elementos de alto potencial iônico. Como estas intrusões geralmente eram fracamente ou raramente deformadas, inferia-se que intrudiam durante último evento deformacional e eram chamadas de “anorogênicas”. Os autores chamaram estes

granitóides de tipo-A, em função da sua alcalinidade, caráter “anidro” e ambiente tectônico anorogênico. Desde então diversos artigos acerca de granitos tipo-A foram publicados, em especial discutindo o significado geotectônico to termo anorogênico, entretanto a maioria dos autores consideram que este tipo de granitóide está associado a processos extensionais (FROST; FROST, 1997; EBY, 1990; EBY, 1992; WHALEN; CURRIE; CHAPPELL, 1987).

Outros tipos propostos incluem o tipo-M (WHITE, 1979) e o tipo-C (KILPATRICK; ELLIS, 1992). Os tipo-M ditas que ascendem do manto, especificamente em ambientes de arco de ilha, enquanto os granitóides tipo-C compreendem rochas charnoquíticas como uma população distinta e reconhecível em ambientes plutônicos e vulcânicos.

O maior problema desta classificação está associado ao fato de presumir fontes simples e únicas para a geração de rochas graníticas, na realidade granitos raramente são gerados a partir de fontes únicas, tais processos são amplamente discutidos e revisados por Clemens e Stevens (2016).

Tabela 1 – Classificação alfabética dos tipos de granitos

Tipos de granito	Características químicas	Minerais específicos	Rochas Fonte
S	Peraluminoso ASI≥1.1	Minerais Máficos peraluminosos (Cordierita, granada, etc.)	Sequências metassedimentares
I	Metaluminoso ASI<1.1	Sem a presença de minerais máficos peraluminosos, ocorrência de hornblenda	Materiais ígneos em níveis crustais profundos
M	Assinatura de arco vulcânico		Crosta oceânica subductada
Sem letra atribuída	Afinidades alcalinas e anorogênicas	Silicatos máficos ricos em Fe	Resíduo granulítico de fusão pretérita

White (1979)

1.1.2 Granitos da série Magnetita e Ilmenita

Ishihara (1977) reconheceu que no Japão existe uma distribuição distinta de rochas graníticas que contém magnetita coexistindo com ilmenita, em relação as que possuem ilmenita como único óxido de Fe-Ti.

Granitos que possuem magnetita são relativamente oxidados, enquanto os que possuem ilmenita, reduzidos. Ambos os tipos relacionados com depósitos minerais distintos. O sistema não é estritamente geoquímico, mas baseado em reações que inibem a formação de magnetita durante a cristalização de rochas graníticas. Três reações possíveis controlam a estabilidade da magnetita em rochas graníticas:

- Redução por combustão de carbono durante fusão de rochas metassedimentares (ISHIHARA, 1977);
- Em rochas reduzidas, desestabilização por reações com silicatos de Fe-Mg (FROST; LINDSLEY; ANDERSEN, 1988);
- Em rochas peralcalinas, consumo de magnetita para formação de piroxênios e anfibólios sódicos.

Entretanto, a classificação de Ishihara (1977) reconhece apenas o primeiro processo, como resultado só pode ser aplicada a rochas graníticas de arcos magmáticos, apesar de ser válida para granitos Cordilheiranos, é menos aplicável a granitóides de outros ambientes tectônicos.

1.1.3 Diagramas discriminantes tectônicos

Compilando mais de 600 análises, Pearce, Harris e Tindle (1984) introduz um método geoquímico para caracterizar granitóides provenientes de quatro ambientes tectônicos: granitos de dorsais oceânicas, de arcos vulcânicos, intra-placa e colisionais.

Contudo, as composições de elementos traços em granitóides são função de suas fontes e da história do líquido, sendo o ambiente tectônico um fator secundário. O maior exemplo são os granitóides pós-colisionais, que podem plotar em qualquer um dos campos definidos, por serem derivados inúmeras fontes, dependendo da composição da crosta espessada durante a orogênese.

1.1.4 Classificação química não-tectônica e não-genética

Frost et al. (2001), baseando-se em três variáveis, propôs uma classificação estritamente geoquímica, sem conotação genética ou tectônica. As três variáveis são:

- Fe# $\frac{FeOt}{(FeOt+MgO)}$, esta variável está associada aos processos que participaram da história de diferenciação da rocha e distingue dois *trends*, um ferroso, o outro magnesiano, antes referidos como toleítico e cálcio-alcalino (MIYASHIRO, 1970). Maniar e Piccoli (1989), Frost e Frost (1997) até então haviam usado o enriquecimento em ferro como fator para

distinção entre granitos de diferentes ambientes tectônicos, em particular granitos tipo-A que se mostravam mais enriquecidos que granitos cordilheiranos;

- MALI (*modified alkali-lime index*), ($Na_2O + K_2O - CaO$), uma versão, para um intervalo maior de variação de sílica, da classificação de (PEACOCK, 1931), que expressa as quantidades de feldspatos na rocha e pode estar relacionado às fontes das rochas;

- ASI (índice de saturação em alumina), que corresponde à razão molecular $\frac{Al}{Ca-1,67P+Na+K}$, essa razão leva em consideração a presença de apatita, isso significa que rochas com ASI>1 possuem conríndon na norma e alguma fase aluminosa presente. Para rochas fracamente peraluminosas essa fase pode ser biotita, para rochas fortemente peraluminosas, cordierita, granada ou polimorfos de Al_2SiO_5.

1.2 GRANITOS FERROSOS

Granitos ferrosos representam um distinto grupo de granitos. Ocorrem em diversos contextos geodinâmicos (ambientes intra-placa a limites de placa), e seu alojamento e localização não são arbitrários (BONIN, 2007).

Possuem maiores razões $\frac{FeOt}{(FeOt+MgO)}$ que granitos cordilheiranos, e portanto, são mais reduzidos. Apesar de ambientes extensionais não produzirem necessariamente granitoides ferrosos (BEA et al., 2007), sua origem está usualmente associada a sítios ou ambientes do tipo (GUIMARÃES et al., 2005; FROST; FROST, 1997; BONIN, 2007).

São suítes geralmente ricas em LILE (Large Ion Lithophile Elements) e HSFE (High Field Strength Elements), entrentanto empobrecidas em elementos compatíveis (Co, Sc, Cr, Ni) e elementos traços compatíveis em feldspatos (Ba, Sr, Eu). Cristalizam comumente em níveis crustais rasos, sob baixas fugacidades de H_2O e oxigênio e altas razões HF/H_2O no magma.

Whalen, Currie e Chappell (1987) sugeriram que altas razões Ga/Al poderiam ser diagnósticas para a identificação de granitos ferrosos. (EBY, 1992) subdividiu granitos tipo-A em dois tipos, com base na abundância em elementos traços, particularmente a razão Y/Nb. Grupo A1, com razões Y/Nb < 12 derivados de um basaltos de ilha oceânica em ambientes intraplaca ou de rifte. Grupo A2, com razões Y/Nb > 12 associados a diversos mecanismos de fusão, desde basaltos de arcos de ilha à fontes crustais como granodioritos e tonalitos.

Frost e Frost (2011) identificaram 8 tipos de granitóides ferrosos, com base na química de elementos maiores, utilizando os parâmetros de (FROST et al., 2001):

Tabela 2 – Classificação de granitos ferrosos de acordo com a química de elementos maiores

ASI/MALI	Metaluminosos	Peraluminosos	Peralcalinos
Alcalinos	X	X	X
Álcali-cálcicos	X	X	X
Cálcio-alcalinos	X	X	
Cálcicos	raros		

Frost & Frost (2011)

Os autores também resumiram os principais modos de geração de granitos ferrosos: 1) fusão parcial de crosta quarto-feldspática (SKJERLIE; JOHNSTON, 1993; DOUCE, 1997; BOGAERTS; SCAILLET; AUWERA, 2006); 2) diferenciação a partir de magma basáltico (FROST; FROST, 1997); 3) combinação dos dois primeiros modelos, envolvendo processos de mistura incompleta e/ou assimilação crustal (HILDRETH; HALLIDAY; CHRISTIANSEN, 1991).

1.3 APRESENTAÇÃO E OBJETIVOS

O presente trabalho consiste de uma coletânea de artigos, submetidos a periódicos internacionais que somados resultam nesta dissertação. Esta, que é requisito para a obtenção do título de Mestre em Geociências, na área de concentração Geoquímica, Geofísica e Evolução Crustal do Programa de Pós-Graduação em Geociências da Universidade Federal de Pernambuco.

O primeiro trabalho, submetido ao periódico *International Geology Review* aborda os aspectos mineralógicos, geoquímicos e isotópicos das suítes ferrosas, modos de ocorrência e suas relações com as fases deformacionais do evento Brasiliano - Pan-Africano. Granitos ferrosos da subprovíncia Transversal foram comparados granitos similares nas subprovíncias Norte e Sul, e equivalentes em cinturões Pan-Africanos. O trabalho faz uma revisão regional e traz uma nova perspectiva a respeito da ocorrência de granitos ferrosos que pareciam ter sua ocorrência limitada a determinados grupos geocronológicos.

O segundo trabalho, submetido ao periódico *Near Surface Geophysics* trata das assinaturas gamaespectrométricas dos corpos estudados, comparando-as com aspectos de campo, processos deformacionais e petrológicos, e com dados de geoquímica de elementos traço e maiores em rocha total. O entendimento do comportamento das assinaturas radiométricas e tentativa de padronização em escala regional, pode servir em estudos futuros, em especial na identificação de novos corpos similares.

2 MATERIAIS E MÉTODOS

2.1 QUÍMICA MINERAL

A análise de química mineral de minerais máficos foi realizada com o intuito de aprimorar os dados petrográficos, tendo como maior objetivo investigar como processos geológicos modificam as composições minerais, bem como caracterizar grupos distintos nas suítes ferrosas.

Os dados foram obtidos através da utilização da Microssonda eletrônica do Instituto de Geociências da Universidade de São Paulo, modelo JEOL JXA-8600S, e da microssonda eletrônica do Intituto de Geociências da Universidade de Brasília, modelo JEOL JXA-8230. Parâmetros como voltagem e corrente de feixe foram específicados no artigo 1 (Capítulo 4).

2.2 GEOQUÍMICA EM ROCHA TOTAL

Análises em elementos maiores das intrusões estudadas foram obtidas por ICP-AES (*Inductively Coupled Plasma Emission Spectrometry*), enquanto concentrações delementos traços foram obtidas por ICP-MS (*Inductively Coupled Plasma Mass Spectrometry*) no Laboratório Acme, Canadá, a abertura das amostras foi realizada utilizando $LiBO_2$ (metaborato de lítio).

2.3 GEOLOGIA ISOTÓPICA

Geoquímica isotópica (Sm-Nd e Lu-Hf) se mostrou uma ferramenta essencial no entendimento das fontes que participaram da geração e evolução dos corpos graníticos estudados. Principalmente, porque a geração destes corpos é complexa, e usualmente envolve a participação de diversas fontes.

O sistema isotópico U-Pb agrega valor crono-estratigráfico ao estudo. Porém, além da idade de cristalização das intrusões estudadas, heranças trazem informações muito importantes, e colaboram com o entendimento das fontes envolvidas na gênese destes corpos.

2.3.1 Sm-Nd

Análises em rocha para o sistema isotópico Sm-Nd foram realizadas no Laboratório de Geocronologia da Universidade de Brasília, via TIMS (*Thermal Ionization Mass*

Spectrometry), utilizando o espectrômetro de massa modelo Finnigan MAT-262. Detalhes na extração de terras raras e isolamento do Sm e Nd são apresentados no artigo 1 (Capítulo 4).

2.3.2 Lu-Hf

Análises Lu-Hf em zircão foram realizadas na Universidade de Ouro Preto, e de acordo com os procedimentos de Matteini et al. (2010), em zircões com idade magmática bem definida, visto que idades diferentes apresentam coposições de Hf distintas (VERVOORT; KEMP, 2016). A partir dos dados foram calculadas idades modelo utilizando a constante de decaimento de Soderlund et al. (2004)

2.3.3 U-Pb

Idades U-Pb por LA-ICP-MS (*Laser Ablation - Inductively Coupled Plasma - Mass Spectrometer*) foram obtidas na Universidade Federal de Ouro Preto e Universidade de Brasília, enquanto análises por SHRIMP (*Sensitive High Resolution Ion Microprobe*) foram realizadas na Universidade de São Paulo e na *Australian National University*.

Cristais de zircão foram separados de acordo com as seguintes etapas:

- Britagem das amostras e peneiramento a úmido com peneiras de 0,500mm, 0,250mm e 0,125mm;

- Bateamento manual para separação e concentração das frações pesadas;

- Separação magnética 1, realizada com imã de mão, para separação de minerais altamente magnéticos e limalha resultante da britagem;

- Separação magnética 2 (FRANTZ inicial), a fração densa resultante dos procedimentos anteriores é submetida ao separador magnético FRANTZ, a condições específicas de inclinação e amperagem, com correntes variando de 0,7 - 1,0 A;

- Separação por líquidos densos, utilizando bromofórmio. Dentre os minerais com maior densidade que o líquido está o zircão, cuja densidade é 4,7 g/cm3;

- Separação magnética 3 (FRANTZ final), após a utilização de líquidos densos para eliminação de eventuais minerais magnéticos densos, como sulfetos, com correntes variando de 0,7 a 1,2 A;

- Separação óptica dos grãos com utilização de lupa e identificação de famílias com morfologia similar.

2.4 GAMAESPECTROMETRIA

Dados de gamaespectrometria foram gentilmente cedidos pela CPRM (Serviço Geológico do Brasil), projetos aerogeofísicos Borda leste do Planalto da Borborema e Pernambuco-Paraíba, realizados nos anos entre os anos de 2008 e 2010.

O espaçamento das linhas de voo são de 500m e com direção N-S, enquanto as linhas de controle têm espaçamento de 10km e direção E-W. Aquisição foi realizada utilizando o espectrômetro EXPLORANIUM GR-820 e Radiation Solutions Inc. modelo RS-500. O processamento dos dados foi realizado pela CPRM de acordo com as recomendações da IAEA (1991). Especificações a respeito dos intervalos energéticos e intervalo de amostragem são apresentados no artigo 2 (capítulo 5).

3 CONTEXTO GEOLÓGICO REGIONAL

A Província da Borborema (PB) é um sistema orogênico de longa história evolutiva, com eventos que começaram no Arqueano e culminaram no Neoproterozoico com o ciclo Brasiliano/Pan-Africano, com a colisão dos crátons São Francisco-Congo e São Luís-Oeste Africano (SCHMUS et al., 2008; SCHMUS et al., 1995; NEVES; SANTOS; SCHMUS, 2000; DANTAS et al., 1998).

Figura 1 - Representação esquemática da província borborema e suas intrusões (Rosa: suítes ferrosas; vermelho: suítes magnesianas). Abreviações: SN, Subprovíncia Norte; ST, Subprovíncia Transversal; SS, Subprovíncia Sul; CSF, Cráton São Francisco; BP, Bacia do Parnaíba.

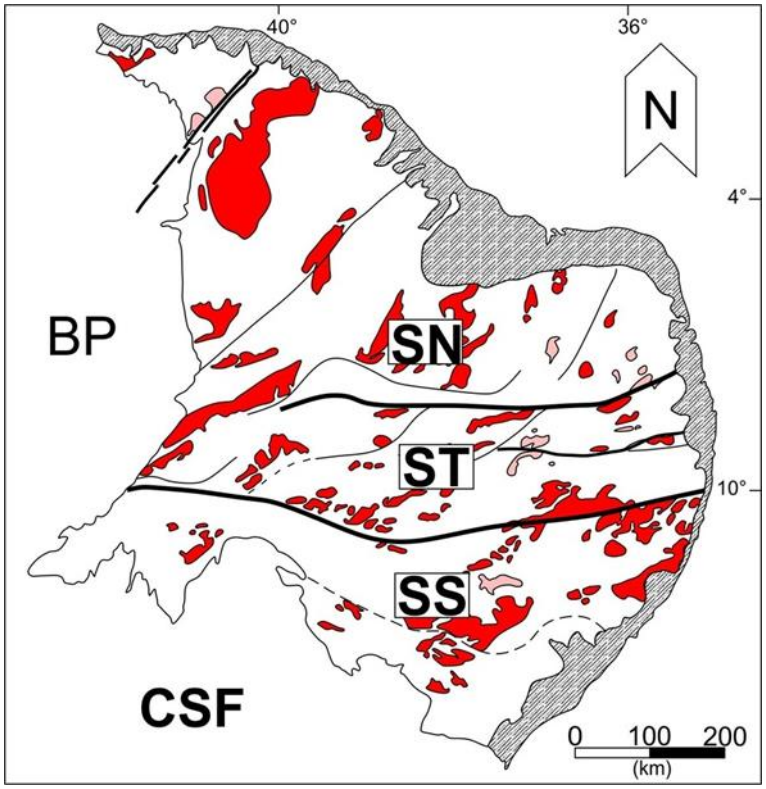

modificado de Hollanda et al. (2010)

É constituída de três subprovíncias (Figura 1), individualizadas por zonas de cisalhamento E-W dextrais (SCHMUS; KOZUCH; NEVES, 2011), em reconstruções pré-drift situa-se adjacente aos cinturões Pan-Africanos (WIT et al., 1998; TOTEU et al., 2001; NEVES; SANTOS; SCHMUS, 2000): 1) Subprovíncia Norte, fica a norte do sistema de cisalhamentos Patos; 2) subprovíncia Transversal fica a sul do cisalhamento Patos e ao norte da zona de cisalhamento Pernambuco; 3) subprovíncia Sul está situada entre o cisalhamento Pernambuco e o cráton São Francisco.

As unidades geológicas da subprovícia Transversal podem ser agrupadas em:

1) Rochas do embasamento dominantemente Paleoproterozoicas de afinidade TTG (SCHMUS et al., 1995; SCHMUS et al., 2008; SCHMUS; KOZUCH; NEVES, 2011; NEVES et al., 2006; SANTOS, 1995; SANTOS et al., 2015);

2) Ortognaisses anorogênicos e anortositos Mesoproterozoicos (ACCIOLY et al., 2000; SÁ et al., 2002);

3) Ortognaisses e sequências supracrustais Tonianos associados ao evento Cariris Velhos (SÁ et al., 1988; NEVES et al., 1995; NEVES et al., 2001; GUIMARAES et al., 2012; GUIMARÃES et al., 2016);

4) Sequências supracrustais Criogenianas a Ediacaranas que foram depositadas antes da colisão do evento Brasiliano (NEVES et al., 2006; NEVES, 2015);

5) Intrudidos por batólitos e *plutons* Ediacaranos (ALMEIDA; LEONARDOS JR.; VALENÇA, 1967; SIAL, 1986; NEVES et al., 2003; GUIMARÃES et al., 2004) e cortados por zonas de cisalhamento dextrais de orientação E-W e zonas de cisalhamento sinistrais de orientação NE-SW (VAUCHEZ et al., 1995; NEVES; VAUCHEZ; ARCHANJO, 1996; NEVES; VAUCHEZ; FERAUD, 2000).

A granitogênese ediacarana tem sido alvo de profundo estudo nas últimas décadas. Almeida et al. (1967) identificou quatro tipos petrográficos de *plutons*: 1) Tipo Conceição, suítes que compreendem rochas de composição tonalítica a granodiorítica; 2) tipo Itaporanga, granodioritos porfiríticos com megacristais de álcali-feldspato; 3) tipo Itapetim, biotita-granitos equigranulares finos associados aos granodioritos do tipo Itaporanga; 4) tipo Catingueira, granitos peralcalinos, sienitos e quartzo sienitos.

Sial (1986), utilizando critérios geoquímicos, caracterizou os plutons da faixa Cachoeirinha- Salgueiro e os correlacionou com os tipos petrográficos de Almeida et al., (1967): 1) *plutons* Cálcio-alcalinos (tipo Conceição) e de afinidade trondhjemítica (tipo Serrita); 2) *plutons* cálcio- alcalinos de alto potássio (tipo Itaporanga); e 3) *plutons* peralcalinos, ultrapotássicos e shoshoníticos (tipo Catingueira). Estas séries foram posteriormente subdivididas em suítes com epidoto magmático ou livres de epidoto magmático e em três intervalos geocronológicos: 1) 650-620Ma, *plutons* cálcio-alcalinos metaluminosos com ou

sem epidoto magmático e de afinidade trondhje- mítica; 2) 590-560 Ma, *plutons* cálcio-alcalinos peraluminosos, cálcio-alcalinos de alto postássio com ou sem epidoto magmático, shoshoníticos, peralcalinos e ultrapotássicos; 3) 550-510 Ma, *sets* de diques sieníticos peralcalinos (SIAL et al., 1998; FERREIRA et al., 1998; SIAL; FERREIRA, 2015).

Brito Neves et al. (2003) baseado em estudos prévios (Santos e Medeiros, 1999; Brito Neves et al., 2000), dividiu os granitoides brasilianos em três super suítes, de acordo com os conceitos de Pitcher (1993): 1) granitoides intrudidos entre 650-625Ma de fontes híbridas e crustais intrudidas no início do evento contracional, incluindo intrusões menos expressivas associadas a escape lateral; 2) granitoides intrudidos entre 580-570Ma derivados de manto enriquecido compreendendo intrusões sin a tardi-transcorrentes; 3) suítes híbridas, pequenos plutons e enxames de diques, alojados em eventos pós-colisionais, intrudidos entre 545-520Ma.

Combinando dados geocronológicos, geoquímicos e estruturais Guimarães et al. (2004) classificou os granitoides da porção leste da subprovíncia Central em quatro grupos: 1) rochas cálcio-alcalinas de médio a alto potássio, intrudidas entre 640-600 Ma, durante o pico de metamorfismo e desenvolvimento da foliação de baixo ângulo, devido a colisão dos crátons Congo – São Francisco e São Luís – Oeste Africano; 2) rochas cálcio-alcalinas de alto potássio e shoshoníticas, intrudidas de 590-581 Ma associadas a transição da colisão para o evento transcorrente; 3) granitos pós-colisionais intrudidos em aproximadamente 570 Ma, gerados por fusão parcial de crosta inferior granodiorítica, marcando o final da orogênese Brasiliana e o início do soerguimento, sincrônicas às rochas ultrapotássicas na faixa Cachoeirinha-Salgueiro e no Alto do Teixeira; 4) granitos tipo-A associados à eventos extensionais pós-orogênicos, com magmatismo bimodal subvulcânico e deposição de pequenas bacias de transição nas subprovíncias Norte e Transversal.

As suítes ferrosas, objeto de estudo deste volume, intrudem em intervalos geocronológicos equivalentes aos grupos 2, 3 e 4 de Guimarães et al. (2004). É importante salientar, que até então, magmatismo ferroso, intrudindo equivalente ao grupo 2, não havia sido bem caracterizado.

4 LATE NEOPROTEROZOIC FERROAN GRANITOIDS OF THE TRANSVERSAL SUBPROVINCE, BORBOREMA PROVINCE, NE BRAZIL: PETROGENESIS AND GEODYNAMIC IMPLICATIONS

Late-Neoproterozoic ferroan granitoids of the Transversal Subprovince, Borbo- rema Province, NE Brazil: Petrogenesis and Geodynamic implications

José Victor Antunes de Amorim[a]*, Ignez de Pinho Guimarães[a], Douglas José Silva Farias[a], Jefferson Valdemiro de Lima[a], Lucilene Santos[b], Vanessa Biondo Ribeiro[c],1, Caio Brainer[c]

[a] Programa de Pós-Graduação em Geociências, Universidade Federal de Pernambuco, Recife, Brasil; [b] Departamento de Geologia, Universidade Federal do Ceará, Fortaleza, Brasil; [c] Departamento de Geologia, Universidade Federal de Pernambuco, Recife, Brasil;

Av. da Arquitetura, s/n, sala 325, Centro de Tecnologia de Geociências, Departamento de Geologia, Cidade Universitária, 50740-550, Recife-PE, Brasil; e-mail: ; ORCID: https://orcid.org/0000-0002-1688-2218; telephone:+5581997588653*

Ignez de Pinho Guimarães, former full Professor at Universidade Federal de PernaMbuco, researcher at CNPq (Brazilian Research Council), e-mail: , Author ID (Scopus): 6603752311, address: Av. da Arquitetura, s/n, sala 520, Centro de Tecnologia de Geociências, Departamento de Geologia, Cidade Universitária, 50740-550, Recife-PE, Brasil; Douglas José da Silva Farias, Ph.D. student at the Programa de Pós-Graduação em Geociências, Universidade Federal de Pernambuco, e-mail: , ORCID: https://orcid.org/0000-0003-4505-9623, address: Av. da Arquitetura, s/n, sala 325, Centro de Tecnologia de Geociências, Departamento de Geologia, Cidade Universitária, 50740-550, Recife-PE, Brasil; Jefferson Valdemiro de Lima, Ph.D. student at the Programa de Pós-Graduação em Geociências, e-mail: , ORCID: https://orcid.org/0000-0002-7843-7312, ; Lucilene Santos, professor and researcher at Universidade Federal do Ceará, e-mail: , ORCID: http://orcid.org/0000-0002-8304-6869, Researcher ID: Q-5474-2017, adress: Rua Campus do Pici, Pici, 60440554, Fortaleza-CE, Brasil, telefone: +558533669867; Vanessa Biondo Ribeiro, researcher at CSIRO (Commmonwealth Scientific and Industrial Research Organisation), e-mail: , ORCID: https://orcid.org/0000-0002-4573-6893, address: 26 Dick Perry Ave, Kensington WA 6152, Australia; Caio Brainer, undergraduate student at Departamento de Geologia, Av. da Arquitetura, s/n, Centro de

Tecnologia de Geociências, Departamento de Geologia, Cidade Universitária, 50740-550, Recife-PE, Brasil

Late-Neoproterozoic ferroan granitoids of the Transversal Subprovince, Borborema Province, NE Brazil: Petrogenesis and Geodynamic implications

Ferroan granites have higher Fe-number than cordilleran granitoids, often emplaced in extensional settings, and are LILE and HFSE enriched. Ferroan granites (585 – 530 Ma) have been described in the Transversal subprovince of the Borborema Province (BP) and in Africa. They comprise two groups: G1 - slightly peraluminous to metaluminous, alkali-calcic rocks, with annite-poor mica and crystallized under intermediate fO_2 (Aroeiras Complex and Serra Branca – Coxixola dike swarms); G2 - metaluminous to slightly peraluminous, alkalic to alkali-calcic rocks, with annite rich mica and crystallized under low fO_2 (Queimadas and Prata intrusions). G1 marks the transition from collision to transcurrence (ca. 585 Ma), or from transcurrence to uplift and transtension (ca. 545 Ma). G2 represents the granitoids intruded during extensional tectonics in transcurrent setting (ca. 550 Ma), or coeval with deposition of transtensional intracratonic basins (ca. 530 Ma). Hf and Nd model ages are older than 2.0 Ga, suggesting that the ferroan granitoids involved partial melting of Paleoproterozoic rocks. Extension related gabbros (~582 Ma) occur in North Subprovince of the BP. The data presented in this paper show that the ferroan magmatism was widespread in the BP as well as its counterparts in Africa in pre-drift reconstructions.

Keywords: granite; ferroan; geochemistry; geochronology; extensional tectonics; Borborema Province

4.1 INTRODUCTION

The Borborema Province (Almeida et al., 1981) represents an orogenic belt with a complex tectonic history started in the Archean until late Neoproterozoic, culminating with the assembly of western Gondwana, due to the collision of major cratonic landmasses (São Franciso-Congo and São Luís-West Africa Cratons) along the Cryogenian-Ediacaran period, namely Brasiliano-Pan-African event (Van Schmus et al., 2008, references therein).

Succeeding the collisional events, the BP was influenced by strike-slip and extensional tectonics which lead to the intrusion of several post-collisional plutons, “anorogenic” granites

and dike swarms, as well as, development of sag-basins due to the collapse of orogenic chains and rupture of continental crust (Santos et al., 2008a).

Figura 2 - Figure 1. Sketch map of Brazil and its tectonic provinces with distribution of ferroan intrusions and their ages (modified from Dall'Agnol et al., 1999). Legend: I-II, Amazonian Craton; III, São Francisco Craton; IV, Tocantins Province; V, Borborema Province; VI, Mantiqueira Province. Abbreviations: AB, Amazonas Basin; PnB, Parnaíba Basin; PrB, Paraná Basin.

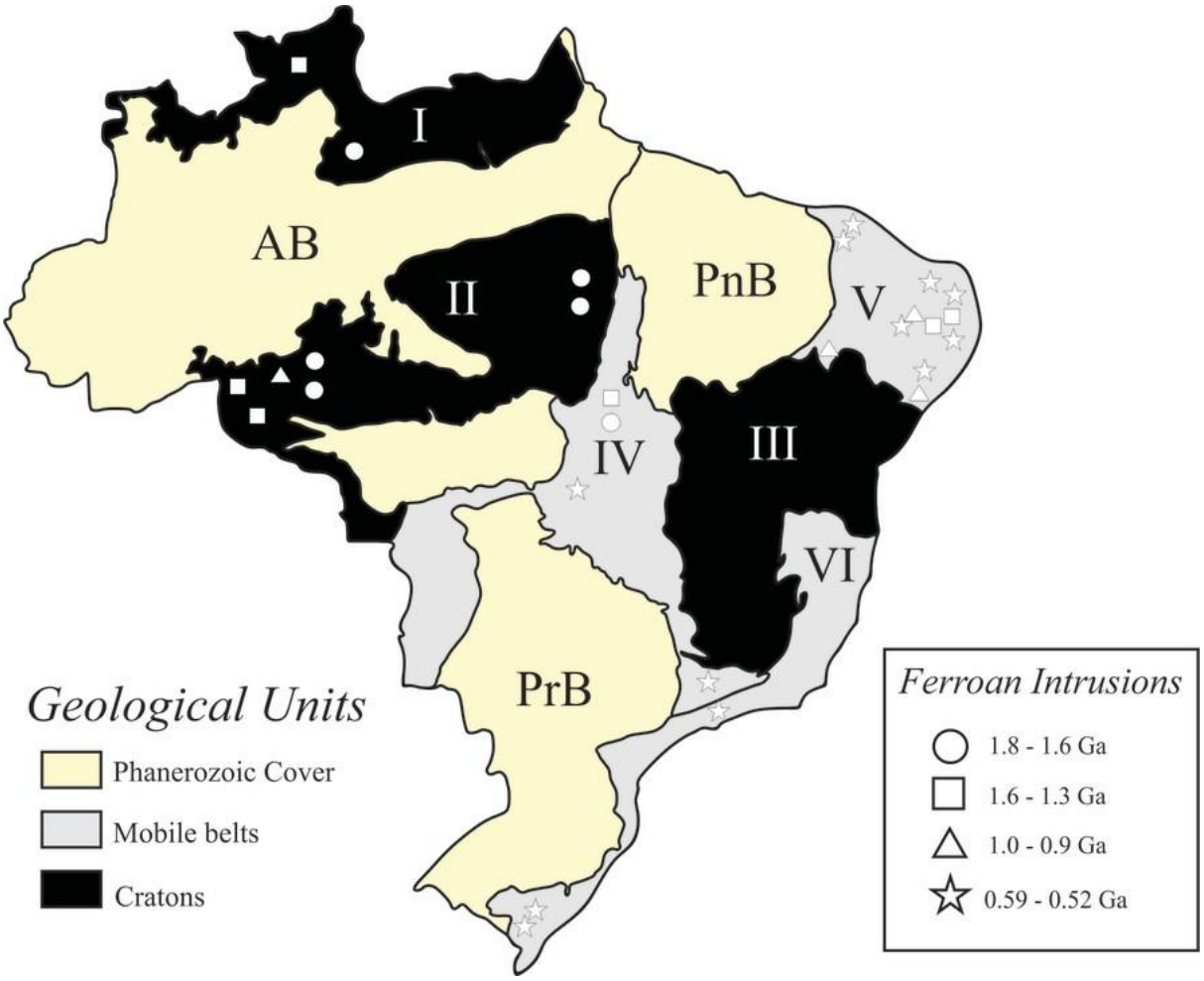

The endurance of such events is best controlled through the ages of its magmatic expressions, which can be characterized by plutons or dyke swarms. Over fifty years of studies, several magma associations were identified in the Borborema Province.

Almeida et al. (1967) recognized four types, on a petrographic basis: 1) Conceição-type comprises medium to fine grained tonalites and granodiorites; 2) Itaporanga-type, granodiorites with large K-feldspar crystals; 3) Itapetim-type, fine grained biotite granites related to the Itaporanga-type; 4) Catingueira-type peralkaline granites, syenites and quartz syenites.

Sial (1986), using geochemical data, characterized the granitoids from the Cachoeirinha- Salgueiro Fold Belt, and correlated with the petrographic types of Almeida et al. (1967): 1) Calc- alkalic (Conceição-type); 2) High-K Calc-alkalic (Itaporanga-type); 3)

Peralkalic, ultrapotassic and shoshonitic (Catingueira-type); 4) Trondhjemitic (Serrita-type). Some of these series were further divided into magmatic epidote-bearing or epidote-free associations (Sial et al., 1997; Ferreira et al., 1998; Sial and Ferreira, 2016).

Brito Neves et al. (2003) based on previous studies (Santos and Medeiros, 1999; Brito Neves et al., 2000) divided the brasiliano granitoids into three super suites, in agreement with the concept of Pitcher (1993): 1) ca. 650 – 625 Ma granitoids derived from hybrid and crustal sources (calc-alkaline, high-K calc-alkaline, trondhjemitic and peraluminous and peralkaline suites), pre- to syn-collision, including minor intrusions related to lateral extension; 2) ca. 580 – 570 Ma derived from enriched mantle (high-K calc-alkaline, shoshonitic, alkaline and ultrapotassic suites) comprising syn- to late-kinematic plutons akin to the strike-slip events; 3) ca. 545 – 520 Ma hybrid suites, small granitic intrusions and dike swarms connected to the post-collisional phases.

Using geochronological data from several plutons from the eastern part of the Transversal subprovince, Guimarães et al. (2004) identified four groups: 1) 640 – 600 Ma medium to high- K calc-alkaline granitoids intruded throughout the peak of high T, low-P metamorphism and development of the flat-lying foliation during the convergence of major cratonic landmasses (São Francisco-Congo Craton and São Luís-West Africa Craton); 2) 590 – 581 Ma high-K calc-alkaline and shoshonitic granitoids marking the transition between the flat-lying event and the transcurrent event; 3) ca. 570 Ma alkaline post-collision granites generated by partial melting of granodioritic lower crust marking the final stage of the Brasiliano – Pan-African orogeny and the beginning of the uplift, synchronous with the ultrapotassic intrusions in the Cachoeirinha-Salgueiro Belt and the Teixeira High; 4) ca. 540 – 510 Ma A-type post-orogenic extension-related associated with subvolcanic bimodal magmatism, coeval with the deposition of small basins from the North and Transversal subprovince.

This study is focused on new ocurrences of ferroan granitoids as sets of dikes and magmatic complex intruded along the Coxixola Shear Zone, respectively, and comparison with already known ferroan intrusions in the Transversal subprovince of the Borborema Province. We present new geochronological (U-Pb, LA-ICP-MS and SHRIMP), isotope (Lu-Hf and Sm-Nd) and geochemical data to discuss plausible sources and tectonic setting related to the intrusions and compare our data with contemporary geological records on a regional scale. The aim of this paper is to show that ferroan granitoids can occur in distinct tectonic environments

and are widespread in the Borborema Province and its counterparts in Africa, in pre-drift reconstructions.

4.2 GEOLOGY OF THE BORBOREMA PROVINCE

The Borborema Province has three subprovinces (Fig. 3a) which are subdivided into seven major domains (Van Schmus et al., 1995, 2008, 2011) and in pre-drift reconstructions lies adjacent to the Pan-African fold Belts (Fig. 2) (De Wit et al., 1988; Brito Neves et al., 2000; Toteu et al., 2001): 1) the North Subprovince lies north of the Patos shear zone and comprises the Médio Coreaú, Ceará Central and Rio Grande do Norte domains; 2) the Central Subprovince or Transversal subprovince occurs between the Pernambuco and Patos shear zone; 3) the South Subprovince stands between the Pernambuco shear zone and the São Francisco craton, and contains the Riacho do Pontal, Sergipano and Pernambuco-Alagoas domains.

Basement rocks consist dominantly of Paleoproterozoic orthogneisses with TTG affinities and ages within 2.5 – 2.0 Ga intervals (Santos, 1995; Van Schmus et al., 1995, 2008, 2011; Martins et al., 1998, 2009; Fetter, 1999; Brito Neves et al., 2001; Cavalcante et al., 2003; Neves et al., 2006a, 2015; Souza et al., 2007; Santos et al., 2015). Archean nuclei (3.4 – 2.7 Ga) have been reported in the North and South subprovinces (Dantas et al., 1998, 2004, 2013; Fetter, 1999; Fetter et al., 2000; Oliveira et al., 2010; Hollanda et al., 2015).

Orthogneisses, meta-anorthosites and supracrustal sequences represent the geological record of extensional events in the Sthaterian – Calymmian interval (1.8 – 1.52 Ga). Such rocks have been described specifically in the western sector of the North Subprovince (Sá et al., 1995; Santos et al., 2008b; Hollanda et al., 2011), and eastern belts from the Transversal subprovince (Van Schmus et al., 1995; Accioly et al., 2000; Sá et al., 2002; Santos et al., 2015).

Tonian orthogneisses (1.0 – 0.9 Ga) were first reported by Jardim de Sá et al. (1988) in the Riacho do Pontal domain, but the major expressions of early-Neoproterozoic events are from the ENE-trending belt named Cariris Velhos, in the central sector of the Transversal subprovince (Brito Neves et al., 1995; Santos, 1995). Petrotectonic associations comprehend granitic orthogneisses and bimodal volcanics, including pyroclastic, intercalated with metapelites, marbles and banded iron formations (Brito Neves et al., 2001; Kozuch, 2003; Guimarães et al., 2012, 2016). Coeval sequences and orthogneisses have also been reported

Figura 3 - Figure 2. Sketch map of a part of west Gondwana in pre-drift reconstructions modified from Van Schmus et al., (2008) (Legend: Br/PA, Brasiliano/Pan-African belts; PaleoPr, Paleoproterozoic crust. Subprovinces and domains: NSP, North subprovince; TSP, Transversal subprovince; SSP, South subprovince; PEAL, Pernambuco-Alagoas domain; SD, Sergipano domain; MK, Mayo Kebi terrane; NWCD, NW Cameroon domain; AYD, Adamawa-Yadé domain; YD, Yaoundé domain; OU, Oubanguides fold belt. Shear zones and faults: PaSZ, Patos shear zone; PeSZ, Pernambuco shear zone; TBL, Transbrasiliano Lineament; TBF, Tcholliré-Banyo fault; AF, Adamawa Fault. Cities: N, Natal; R, Recife; S, Salvador; D, Douala; G, Garoua; K, Kaduna area of Nigeria).

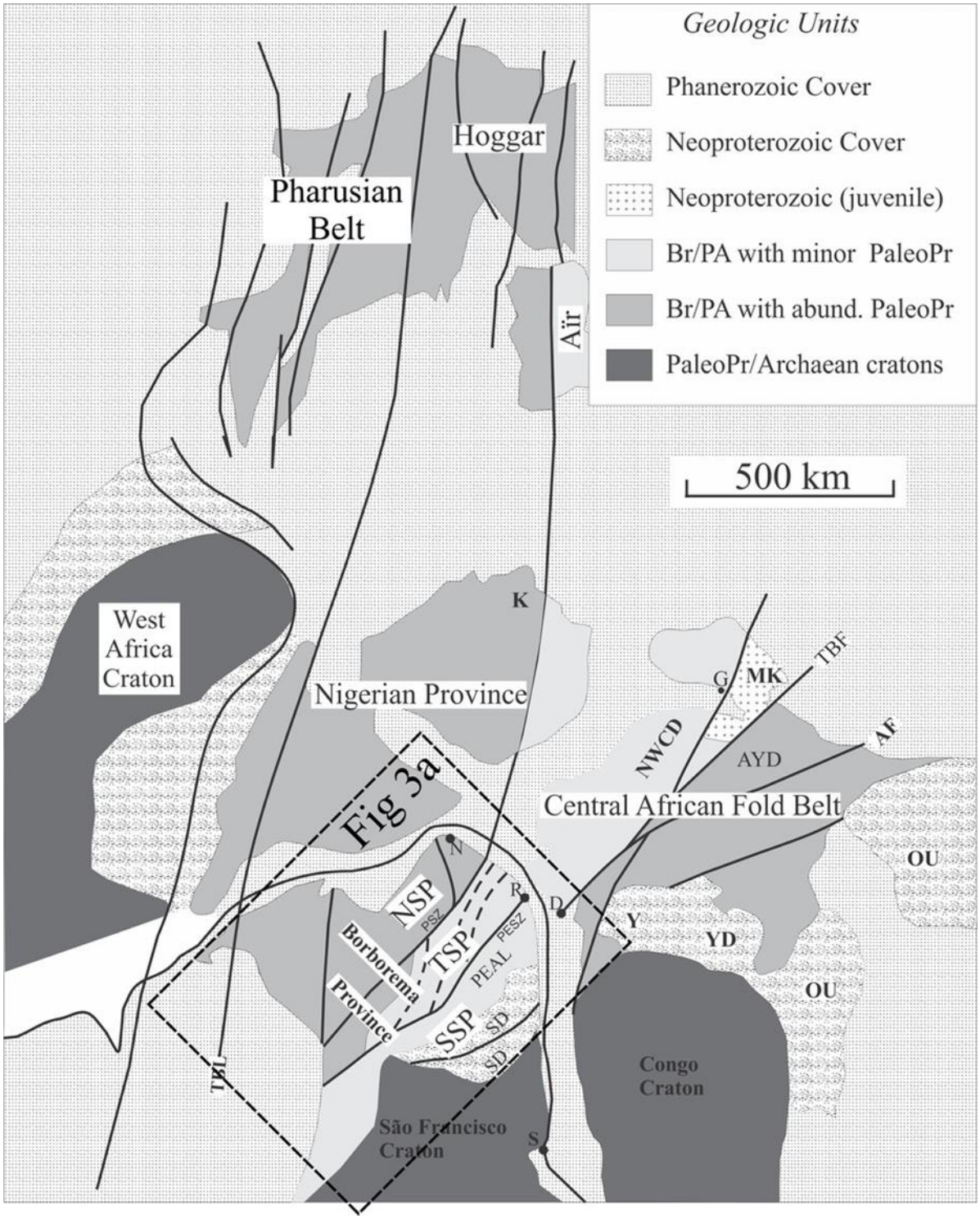

further east in the Transversal subprovince and South subprovince (Accioly et al., 2010; Carvalho, 2005; Brito et al., 2008; Cruz and Accioly, 2013; Caxito et al., 2014). So far, no

consensus has been reached regarding the tectonic setting of the Tonian granitoids and sequences. Some authors refer to a magmatic arc with possible back-arc association (Brito Neves et al., 2000; Kozuch, 2003; Santos et al., 2010; Oliveira et al., 2010; Van Schmus et al., 2011; Caxito et al., 2014a), other authors refer to rift related setting, with generation of A-type granites and bimodal volcanism (Guimarães et al., 2012, 2015; Cruz and Accioly, 2013).

The Brasiliano – Pan African event (650 – ca 550 Ma) is represented by supracrustal sequences with maximum deposition age between the Cryogenian-Ediacaran interval. The peak of regional metamorphism was mainly under amphibolite (high T, low P) conditions, and occurs between 630-610 Ma (Neves et al., 2006a), along with the development of flat-lying foliation and intrusion of several pre- to syn-orogenic plutons (Neves et al., 2006b; Ferreira et al., 2011; Sial et al., 2008; Guimarães et al., 2011, Silva Filho et al., 2016, Silva et al., 2016). Despite the numerous studies, there is no consensus on how the Brasiliano orogeny occurred. Models refer to collage of tectonostratigraphic terranes (Santos, 1995; Brito Neves et al., 2000), closure of large oceans between the Borborema and cratonic landmasses or subduction model (Oliveira et al., 2010; Araújo et al., 2014; Caxito et al., 2014b), and convergence of small continental blocks after extension of preexisting continent with minor consumption of oceanic lithosphere or intracontinental model (Neves, 2003, 2011, 2015).

According to Guimarães et al. (2004) and Silva Filho et al. (2010), the high-K calk-alkaline and shoshonitic granitoids with zircon ages between 590 – 581 Ma mark the transition between the flat-lying regime and the transcurrent event, the authors also propose that these plutons post-date an interval of migmatization related to the metamorphic peak. Vauchez et al., (1995) and Neves et al. (1996, 2000a) propose that such intrusions could nucleate shear zones, since incompletely solidified plutons represent rheological heterogeneities and induce strain localization.

Post-collisional plutons ca. 570 Ma are high-K calc-alkaline to alkaline (Guimarães et al., 2004) and syn- to late-transcurrent event. Emplacement is often assisted by synchronous movements of strike-slip shear zones setting up extensional spots (Guimarães et al., 2009; Santos et al., 2014; Lages et al., 2016; Lima et al., 2017). Synchronously, ultrapotassic intrusions occur in the Cachoeirinha belt and the Teixeira high (Sial and Ferreira, 1988; Ferreira et al., 1997, 1998).

Figura 4 - Figure 3. a) Sketch map of the Brasiliano intrusions in the Borborema Province. Abbreviations: PaSZ - Patos Shear Zone, PeSZ - Pernambuco Shear Zone; Ferroan intrusions: 6- Mucambo and Meruoca Plutons (Santos et al., 2008; Archanjo et al., 2009), 7- Acari Pluton (Archanjo et al., 2013; Nascimento et al., 2015), 8- Solânea and Dona Inês Plutons (Guimarães et al., 2009), and Riachão Mafic rocks (Guimarães et al., 2017), 9-Águas belas Pluton (Silva Filho et al., 2010), 10- Pilõezinhos Pluton (Lima et al., 2017); b) Studied Intrusions and associated shear zones of the Transversal subprovince. Abbreviations: AFSZ - Afogados da Ingazeira Shear Zone, TCSZ - Coxixola Shear Zone, CGSZ - Campina Grande Shear Zone, CSZ - Cabaceiras Shear Zone, PJSZ - Prata Shear Zone, BSZ - Batista Shear Zone, GBSZ - Gado Bravo Shear Zone. Ferroan intrusions: 1- Aroeiras Complex (this paper); 2- Queimadas Pluton (Almeida et al., 2002, this paper); 3- Prata Complex (Melo, 1997; Guimarães et al. 2005; Hollanda et al. 2010; this paper), 4- Bravo Pluton (Lages et al. 2016); 5- Serra Branca Pluton (Santos et al., 2014).

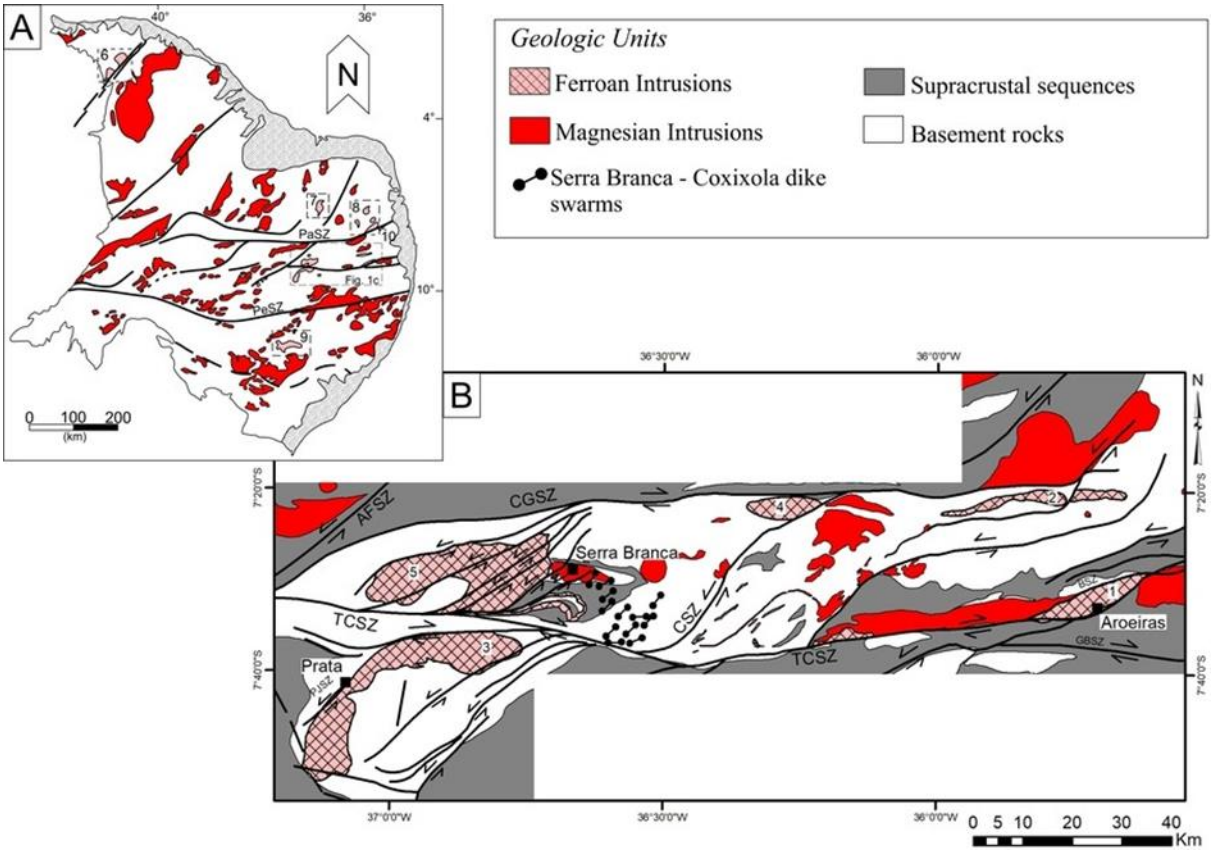

5The final stages of the Brasiliano orogeny (ca. 550 – 510 Ma) are marked by the intrusion of A-type granites and sub-volcanic bimodal magmatism, in the Transversal subprovince (Guimarães et al., 2004, 2005). Monié et al., (1997), in the North subprovince, demonstrated the swift uplift of the 2.7 Ga granulites of Granja Massif with $^{40}Ar/^{39}Ar$ biotite plateau ages of 558 ± 3 Ma, confirmed by Fetter (1999) with a precise Sm-Nd isochron (plagioclase-whole rock-garnet) of 557 ± 1 Ma.

Fetter (1999) and Guimarães et al., (2005) suggest that the late-Ediacaran and early-Cambrian magmatic records are coeval with the deposition of pull-apart basins in the North and Transversal subprovinces. However, Santos et al. (2008a) suggest that the Mucambo (532 ± 7 Ma) and Meruoca plutons are rift-related rather than post-tectonic products of the Brasiliano

orogeny. Hollanda et al., (2010) acquired U-Pb (SHRIMP) ages for the rock associations described by Guimarães et al. (2005), combined with anisotropy of magnetic susceptibility in plutons and sets of dikes, and $^{40}Ar/^{39}Ar$ plateau ages (amphibole, biotite and muscovite) for the Coxixola mylonites in the Transversal subprovince. The authors data show syn-transcurrent intrusions between 548 – 533 Ma and shear zone reactivation until 510 ± 5 Ma.

4.3 GEOLOGICAL SETTING OF FERROAN INTRUSIONS

4.3.1 Aroeiras Complex

The Aroeiras Complex (Fig. 3b - 1) intruded into a Neoproterozoic Pluton (Serra do Inácio Pereira), metapelites and marbles of the Surubim Complex, and Rhyacian orthogneisses and migmatites. It comprises several dikes, sheets, small dioritic bodies and a ENE-WSW trending main pluton, emplaced during synchronous movements of E-W trending dextral sense Coxixola shear zone and NE-SW trending sinistral sense Batista shear zone. Such structural context is propitious to the development of extensional sites and emplacement of granitic rocks (Guimarães et al., 2009; Santos et al., 2014; Lages et al., 2016; Lima et al., 2017).

The Aroeiras complex comprises porphyritic to equigranular biotite-hornblende monzogranite and biotite syenogranite (Fig. 4a), the main accessory phases are prismatic crystals of allanite and zircon, acicular apatite and ilmenite crystals mantled by sphene. Microgranular mafic enclaves (MME), composed of hornblende-biotite-diorite and quartz-diorite are common (Fig. 4b). Droplets of ovoid MME with crenulated borders, double enclave relations, granitic venules, and hybrid rocks with rapakivi texture are indicative of mingling and mixing processes that acted throughout the evolution of the Aroeiras granitoids.

4.3.2 Queimadas Pluton

The Queimadas Pluton (Fig. 3b - 2) intruded Rhyacian gneisses of tonalitic to granitic composition and comprises an E-W elongated 50km² body, showing S-C dextral foliation with C foliation plan parallel to the E-W trending branch of the Campina Grande Shear Zone. A 60Az trending late transcurrent dextral sense shear zone disrupts the body in a mega-boudin-like shape (Almeida et al., 2002).

Petrographically, it comprises porphyritic biotite ± amphibole granodiorites to monzogranites and the main accessory phases are large euhedral crystals of allanite, apatite,

prismatic or rounded crystals of zircon, subhedral crystals of ilmenite hosted by biotite or amphibole, and rare monazite crystals. Mafic phases (amphibole ± biotite) represent less than 10%. Quartz- monzonite and quartz-diorite occur close to the contact with the country rocks, and MME are locally observed in the porphyritic monzogranites and granodiorites (Almeida et al., 2002).

Almeida et al. (2002) suggest that the pluton was deformed under brittle-ductile conditions of the transcurrent event during the Brasiliano (=Pan-African) orogeny. Textural aspects of ductile deformation are represented by quartz ribbons and mosaic texture, kinks of biotite, disrupted sigmoidal porphyroclasts of plagioclase with patchy extinction, while necking, disruption and boudin-like shape of the Queimadas Pluton are result of the brittle system.

4.3.3 Serra Branca – Coxixola dike swarms

The Serra Branca – Coxixola dike swarms (Fig. 3c) intruded Paleoproterozoic orthogneis- ses, Neoproterozoic supracrustal sequences and magnesian alkali-calcic Ediacaran plutons of the Transversal subprovince. The main dike population trends NE-SW and crosscuts the flat-lying foliation of supracrustal sequences (Fig. 4c) and basement rocks. Close to the dextral sense E-W trending Coxixola Shear Zone, dike swarms are intruded concordant with the steeply-dipping mylonitic foliation, but evidences of deformational processes were nearly absent. The dike sets comprise porphyritic hornblende-biotite granite and equigranular biotite granite associated with subvolcanic mafic dikes (Fig. 4d).

4.3.4 Prata Complex

The Prata Complex (Fig. 3b - 3) intruded Siderian to Rhyacian orthogneisses and migmatites from the Transversal subprovince. It contains several granitic intrusions, as dikes and elongated stocks (Guimarães et al., 2005; Hollanda et al., 2010). Swarms of MME occur near the eastern boundary of the Complex and follow the NNE and E-W trend of basalt dikes. Solid state deformation is rare and restricted to the western boundary of the Prata Complex, where it is in contact with the Prata - Jabitacá Shear Zone (Fig. 3b).

Petrographically, biotite syenogranite and hornblende-biotite monzogranites are the main facies. The mafic petrographic facies comprise monzodiorite, quartz monzonitic, diorite and norite. Enclave swarms of norite showing evidences of magma mixing with felsic granites separates the Prata complex into north and south intrusions (Guimarães et al., 2005). The southern body, the Santa Catarina Pluton comprises biotite syenogranites, while the Sumé Pluton, crops out to the north, comprises hornblende-biotite monzogranites (Hollanda et al., 2010). The main accessory phases are allanite, rimmed by epidote, sphene, apatite and zircon. Several MME and syn-plutonic dikes are observed in the SE limit of the Sumé Pluton, displaying crenulated contacts and ovoid feldspar crystals mantled by plagioclase (rapakivi texture). Such characteristics are indicative of mingling and mixing processes between granitic and dioritic magmas (Guimarães et al., 2005).

Figura 5 - Figure 4. Field aspects of the studied ferroan intrusions. a) Mingling of hbl-diorite with bt syenogranite in the Aroeiras Complex; b) Petrographic granitic varieties, coexisting porphyritic and equigranular granites from the Aroeiras Complex; c) Leucocratic dike from the Serra Branca - Coxixola region cross-cutting flat-lying foliation of supracrustal sequences; d) Dikes from the Serra Branca - Coxixola swarms associated with subvolcanic mafic rocks.

4.4 ANALYTICAL PROCEDURES

4.4.1 Mineral Chemistry

Mineral compositions described in this paper include those from this work (Aroeiras and Serra Branca – Coxixola dike swarms) and from the literature ie. Queimadas Pluton (Almeida et al., 2002) and Prata Complex (Guimarães et al., 2005). Representative analyses of biotite are shown in Supplementary Table 1, while representative analyses of amphibole are in Supplementary Table 2.

New major element compositions for individual mineral phases were obtained by electron microprobe analyses and performed on C-coated thin sections using a JEOL JXA-8600S microprobe (University of São Paulo, Laboratório de Microssonda Eletrônica), under 15kv accelerating voltage and 20nA beam current, and a JEOL JXA-8230 microprobe from the University of Brasília, under 15kv accelerating voltage and 10nA beam current.

4.4.2 Whole-rock geochemistry

Major elements analyses of samples from the Aroeiras Pluton and the Serra Branca – Coxixola dike swarm were obtained by LiBO2 fusion ICP-AES (Inductively Coupled Plasma Emission Spectrometry) and trace elements concentrations by LiBO2 fusion ICP-MS (Inductively Coupled Plasma Mass Spectrometry) at Acme Laboratories Canada. Representative analyses and standards are shown in Supplementary Table 3, detection limits are available online in the Acme Laboratories brochure.

Whole-rock compositions of the Queimadas Pluton and Prata Complex included in this work have been collected from the literature, but trace element data has been recalculated to reasonable comparison (Almeida et al., 2002; Guimarães et al., 2005).

4.4.3 Sm-Nd Isotopes

Bulk rock Sm-Nd Isotopic analyses were carried out at the University of Brasília Geo-chronology Laboratory (Supplementary Table 4). First, REEs were separated as a group, using cation-exchange columns, afterwards Sm and Nd were isolated using columns loaded with HDEHP (di-2-ethylhexyl phosphoric acid) supported on Teflon powder (Richard et al., 1976). Sm and Nd samples were loaded onto Re filaments and the isotopic analyses were carried out

in a Finnigan MAT-262 mass spectrometer. Uncertainties on Sm/Nd and 143Nd/144Nd ratios were based on repeated analyses of international rock standards BCR-1 and BHVO-1. Supplementary data on procedures can be found in Goia and Pimentel (2000).

Data from the Queimadas pluton and Prata Complex have been compiled from literature (Almeida et al., 2002; Guimarães et al., 2005).

4.4.4 U-Pb Isotopes

Zircon grains were extracted using conventional techniques. Morphology of zircons was studied using BSE (back-scattered electron) and CL (cathodoluminescence) images.

In situ dating of the porphyritic hornblende-biotite granite (MA-50) from the Serra Branca - Coxixola dike swarm was performed using a Laser Ablation Inductively Coupled Plasma Mass Spectrometer (LA-ICP-MS) from the Federal University of Ouro Preto (UFOP), as a mylonitic sample from the Aroeiras Pluton (ARO-103) was analyzed at the LA-ICP-MS from the Brasilia University (Supplementary Table 5).

SHRIMP analyses were carried out at the University of São Paulo (biotite-syenogranite from the Aroeiras Pluton) and the Australian National University (monzogranite from the Queimadas Pluton). SHRIMP analyses are available on Supplementary Table 6.

4.4.5 Lu-Hf Isotopes

Lu-Hf isotope analyses (Supplementary Table 7) followed the procedures of Matteini et al. (2010). Hafnium model ages were calculated using a double staged evolution. Hf isotope data were obtained in zircon grain spots with well-defined magmatic crystallization age, since different age components will have different Hf isotope compositions (Vervoort and Kemp, 2016). The εHf(t) and the depleted model age were calculated using the (λ) decay constant of $1.867*10^{-11}$ (Söderlund et al., 2004). Chondritic values of $^{176}Hf/^{177}Hf = 0.0336$ and $^{176}Lu/^{177}Lu = 0.282785$ (Bouvier et al., 2008). Model depleted mantle with present day 176Hf/177Hf = 0.28325 and $^{176}Lu/^{177}Hf = 0.0388$ (Griffin et al., 2000; Andersen et al., 2009), mafic and felsic crust $^{176}Lu/^{177}Hf$ ratios from Pietranik et al. (2008) were used.

4.5 MAFIC MINERAL CHEMISTRY

4.5.1 Biotite

Biotite compositions in the studied granitoids range from annite poor to rich (Fig 5a). The biotites from the Aroeiras Complex and Serra Branca – Coxixola dike swarms are annite-poor, while the biotites from the Queimadas Pluton and Prata Complex are annite-rich.

Fe-number (Fetot/(Fetot+Mg)) vary from 0.69 to 0.77 in the Aroeiras granitoids, and from 0.60 to 0.65 in the granitoids from Serra Branca – Coxixola dike swarms. In contrast, the Fetot/(Fetot+Mg) ratios are > 0.8 for the biotites of the Queimadas Pluton and Prata Complex (Almeida et al., 2002; Guimarães et al., 2005).

In the FeO*-MgO-Al2O3 biotite discriminant diagram (Fig. 5b) (Abdel-Rhaman, 1994), the biotites from the Aroeiras Complex and Serra Branca – Coxixola dike swarms plot in the boundary of the calc alkaline and alkaline (Serra Branca – Coxixola dike swarms), and peraluminous and alkaline fields (Aroeiras). The biotites of the Prata Complex and Queimadas Pluton (Almeida et al., 2002; Guimarães et al., 2005) show a distinctly more iron enriched character for these rocks, plotting within the alkaline field.

4.5.2 Amphibole

Amphiboles from the Aroeiras Complex and Serra Branca – Coxixola dike swarms have been classified in accordance with the scheme proposed by Leake et al. (1997). Fe^{2+} and Fe^{3+} were calculated according to Holland and Blundy (1994), with Fe^{2+}/Fe^{3+} estimation assuming Σ13 cations.

Amphibole compositions in the studied granitoids range from Hastingsite, Fe-Edenite to Fe-Tschermakite.

Oxygen fugacity is believed to have a strong role on the chemistry of calcic amphiboles. With increasing oxygen fugacity amphiboles crystallizing from a magma become more enriched in Mg. Thus, amphiboles with high Fe-number ($Fe_{tot}/(Fe_{tot}+Mg)$) are considered to have formed under low oxygen fugacities (Wones, 1981; Anderson and Smith, 1995). In the Aroeiras Complex and Serra Branca – Coxixola dike swarms, the amphiboles have $Fe_{tot}/(Fe_{tot}+Mg)$ ratios ranging from 0.69 to 0.82, suggesting intermediate to low oxygen

fugacities, and in the Prata Complex and Queimadas Pluton the Fetot/(Fetot+Mg) ratios range between 0.82-0.93, indicating low fO2 conditions (Fig. 5c).

Figura 6 - Figure 5. a) Biotite compositions of Aroeiras Complex and Serra Branca Coxixola dike swarms compared to mineral compositions of the Queimadas Pluton and Prata Complex, QP - field of the Queimadas biotites, PC - field of the Prata biotites; b) Biotite compositions of the Aroeiras Complex and Serra Branca - Coxixola dike swarms compared to the Queimadas Pluton and Prata Complex samples, on the FeO-MgO-Al2O3 diagram with fields after Abdel-Rahman (1994). Abbreviations: A- alkaline biotites, C- calc-alkaline biotites, P- peraluminous biotites, QP - field of the Queimadas biotites, PC- field of the Prata biotites; c) composition of amphiboles from the Aroeiras Complex and Serra Branca - Coxixola dike swarms in terms of Fe/(Fe+Mg) versus AlIV. Fields of fO2 (Anderson and Smith, 1995) and composition of hornblende from Ediacaran and Cambrian ferroan granitoids of the Queimadas Pluton (Almeida et al., 2002) and Prata Complex (Guimarães et al., 2005) from the Transversal Subprovince, QP - field of the Queimadas amphiboles, PC - field of the Prata amphiboles.

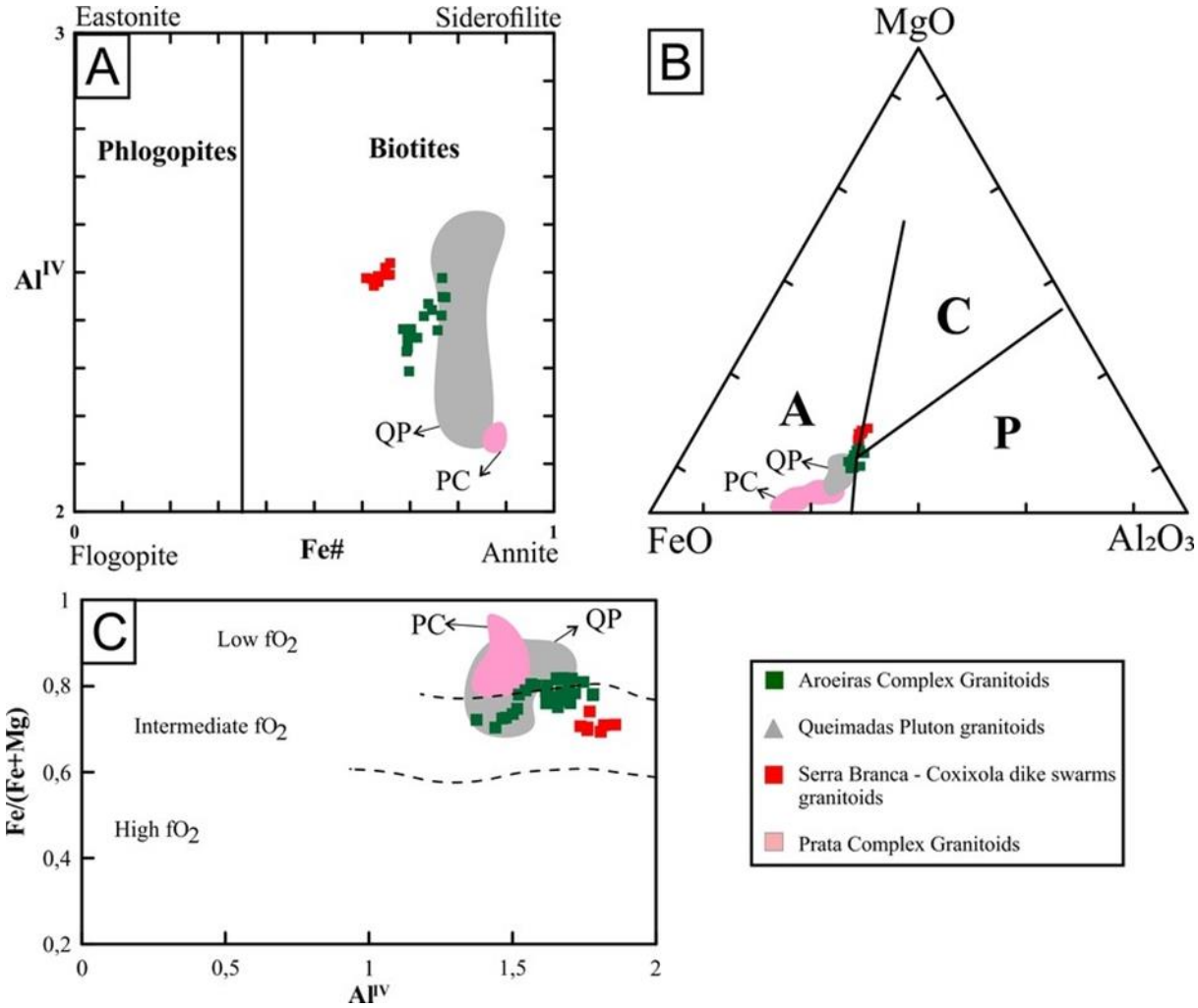

4.6 GEOCHEMISTRY

Most granitoids, over 60% of the analyzed samples, have SiO2 contents higher than 70%, exhibit high K2O contents (>4%), and K2O/Na2O ratios >1. According to Frost et al. (2001) geochemical classification (Fig 6), granitoids are ferroan, Fe* (FeOt/(FeOt+MgO)) > 0.81; metaluminous to peraluminous, alumina saturation index (ASI) ranging from 0.93 to 1.06;

displaying alkali-calcic to slightly alkalic character, modified alkali-lime index (MALI) between 4.86 and 8.8. Dioritic rocks of the Aroeiras Complex are ferroan Fe* > 0.81; metaluminous, ASI values between 0.79 – 0.87; and alkalic with MALI ranging from 1.08 to 2.94.

Figura 7 - Figure 6. Granitoids chemical classification after Frost et al. (2001). a) Studied suites in the FeOtot/(FeOtot+MgO) versus silica diagram; b) Studied suites in the Alumina Saturation Index diagram; c) Plot of the studied suites on the Modified alkali-lime index versus SiO2 diagram

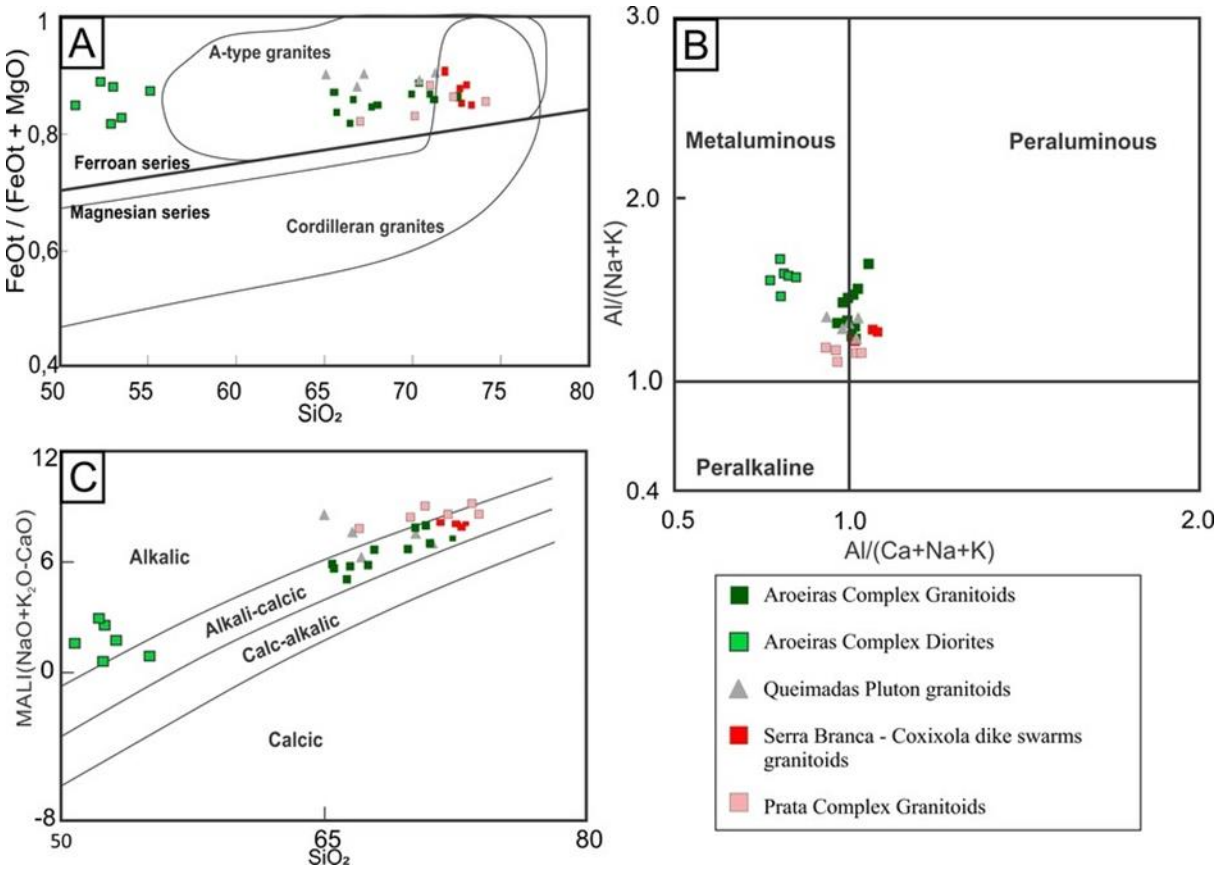

The chondrite normalized REE patterns (Fig. 7) (Nakamura, 1974) of the Aroeiras Complex granites are fractionated, with$(Ce/Yb)_N$ ratios ranging from 8.15 to 21.15, and exhibit negative Eu anomalies (Eu/Eu* = 0.45 to 0.68), while the diorites are less fractionated $(Ce/Yb)_N$ values between 6.9 and 8.56 and show small negative Eu anomalies (Eu/Eu*= 0.81-0.84). The granitoids of the Queimadas Pluton display negative Eu anomalies and $(Ce/Yb)_N$ ratios from 10.14 to 17.47. The Serra Branca – Coxixola samples exhibit significant negative Eu anomalies (Eu/Eu*= 0.23 to 0.34) and $(Ce/Yb)_N$ ratios ranging from 30.58 to 104.39. The REE patterns of granitoids from the Prata Complex rocks are fractionated, with $(Ce/Yb)_N$ ratios between 6.8 and 19.76 and characterized by negative Eu anomalies (Eu/Eu* = 0.21 – 0.65).

Figura 8 - Figure 7. Chondrite-normalized REE patterns (Nakamura, 1974) of the ferroan suites.

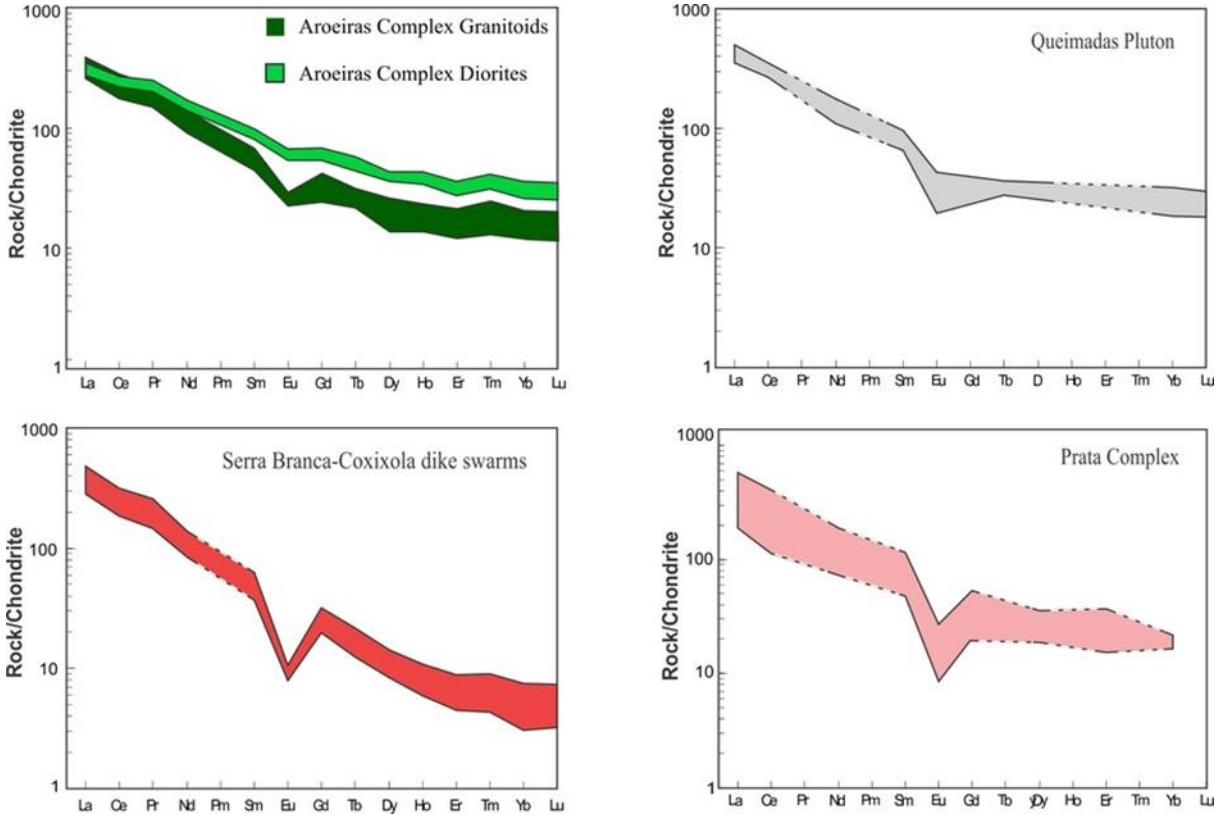

The incompatible element patterns (Fig. 8) of the studied granitoids normalized to the values suggested by Thompson (1982) display many affinities: variable troughs at Nb and Ta; deep troughs at Sr, P and Ti; and Ba troughs, except for the Aroeiras Complex granitoids. Diorites of the Aroeiras Complex exhibit troughs in Th, Sr and Ti and peaks in Ba, K and P.

Figura 9 – Figure 8. Trace elements abundance diagrams normalized to the values proposed by Sun and McDonough (1989).

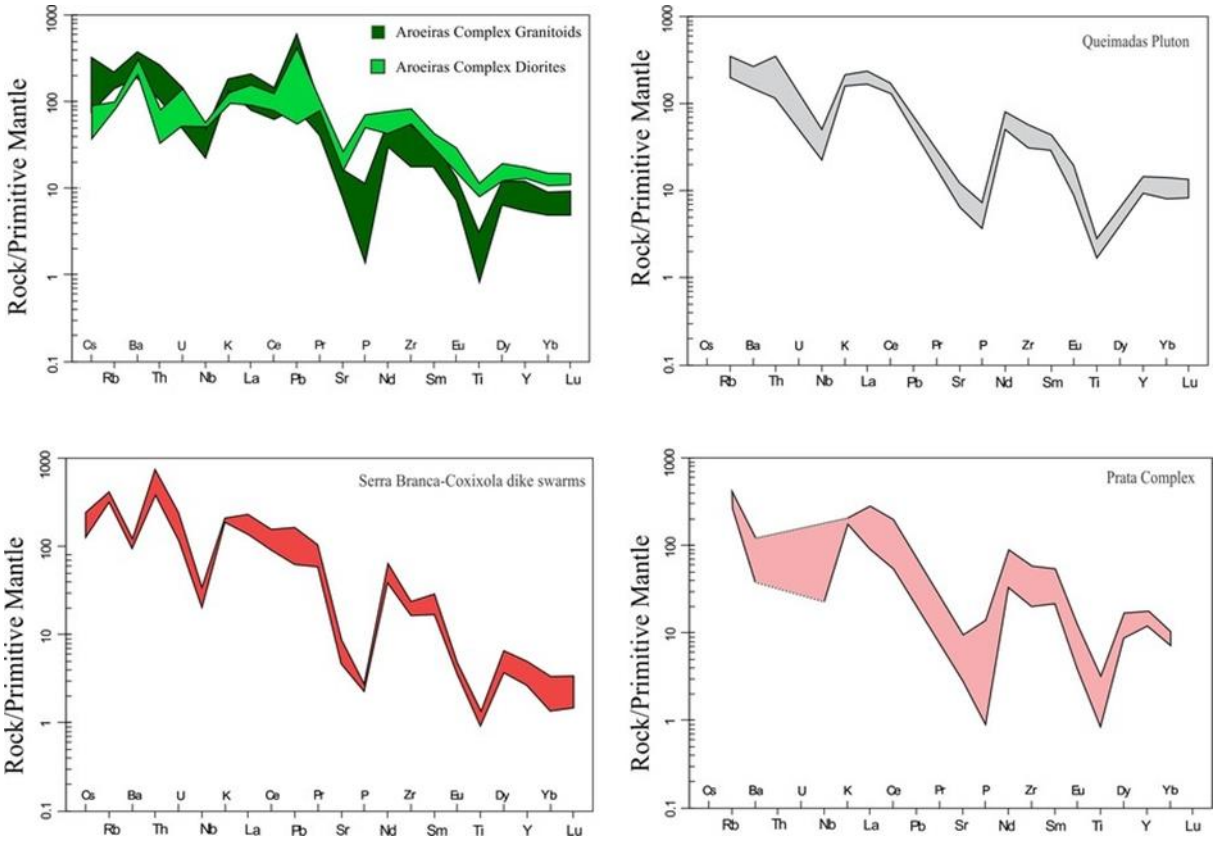

The studied granitoids (Fig. 9a) have high HSFE contents (Zr+Nb+Ce+Y > 350ppm), and plot on the A-Type granites field of Whalen et al. (1987). In the trace-element discrimination diagrams (Pearce et al., 1984; Pearce et al., 1996), most of the studied samples plot on the within-plate field and post-orogenic granites (Y+Nb > 50ppm) (Fig. 9b). Samples plotted on the A-Type (Whalen et al., 1987) and Within-Plate (Pearce et al., 1984) fields exhibit Y/Nb ratios > 1.2, equivalent to the A2-subtype (Eby, 1992).

Figura 10 - Figure 9. Studied granitoids plot in tectonic discriminant diagrams. a) FeO/MgO versus Zr+Nb+Ce+Y, fieldsafter Whalen et al. (1987); b) Nb versus Y, fields Pearce et al. (1984). Abbreviations: WPG - Within Plate Granites; VAG - Volcanic Arc Granites; ORG – Ocean Ridge Granites; COLG - Collisional Granites

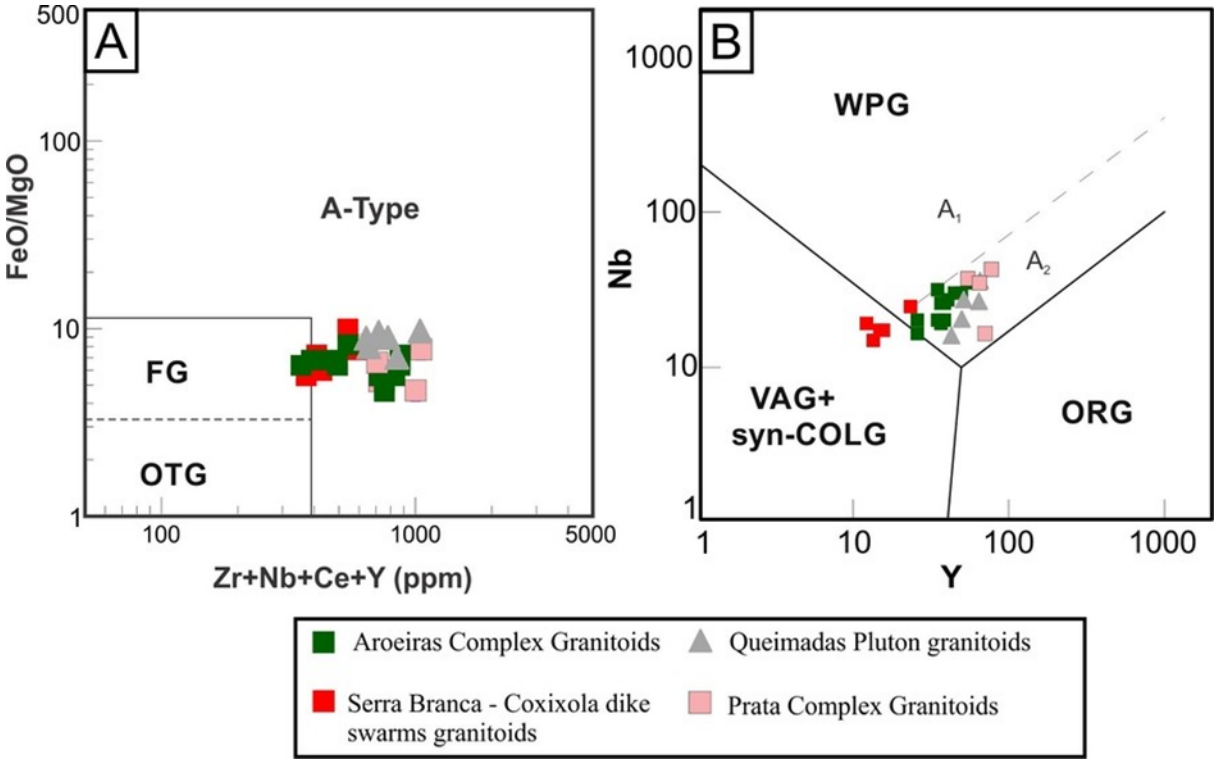

Zircon saturation temperatures of the ferroan studied granites were calculated according to Watson and Harrison (1983) and range from 795.2°C to 895.4°C.

4.7 U-PB GEOCHRONOLOGY

4.7.1 Aroeiras Complex

Two samples of the Aroeiras Complex were dated: 1) a sinistral sense monzogranitic mylonite sample (ARO-103) close to the contact with the country rocks (Serra do Inácio Pereira Pluton) exhibiting sigmoidal crystals of K-feldspar (Coordinates of this sample: 7°32’23”S and 35°46’11”W); and 2) a leucocratic biotite-syenogranite (ARO-1A) close to hybrid porphyritic hornblende-biotite-monzogranites and microgranular mafic enclaves of dioritic composition (Coordinates of this sample: 7°32’37”S and 35°44’03”W).

4.7.1.1 ARO – 103

The LA-ICP-MS (Laser Ablation Inductive Coupled Plasma Mass Spetrometer) from the Universidade de Brasília was used to date this sample. Zircon grains distinguish two populations (Fig. 10): 1) rounded grains with xenocrystic cores, oscillatory zoning, mostly

inherited from Rhyacian and Sthaterian orthogneisses from the basement (2.0 – 1.7 Ga); 2) prismatic elongated, length/width ratios from 5:1 to 4:1, showing oscillatory zoning and xenocrystic cores. Two intercepts yield the ages of 603 ± 5 Ma (MSWD = 0.16; Probability of concordance = 0.69), and 585 ± 5.6 Ma (MSWD = 1.4; Probability of concordance = 0.24). The age of 585 Ma is interpreted as the crystallization age due to be coherent with the geochemical nature of this magmatic complex, since plutons older than 600 Ma are tonalitic to granodioritic, calc-alkaline and related to the Brasiliano compressional event of the Borborema Province.

Figura 11 - Figure 10. Left: Concordia Diagram of sample ARO-103; Right: full concordia diagram with emphasis on showing inherited Paleoproterozoic zircons and cathodoluminescence images of zircons. Sample localities and details are provided in the text.

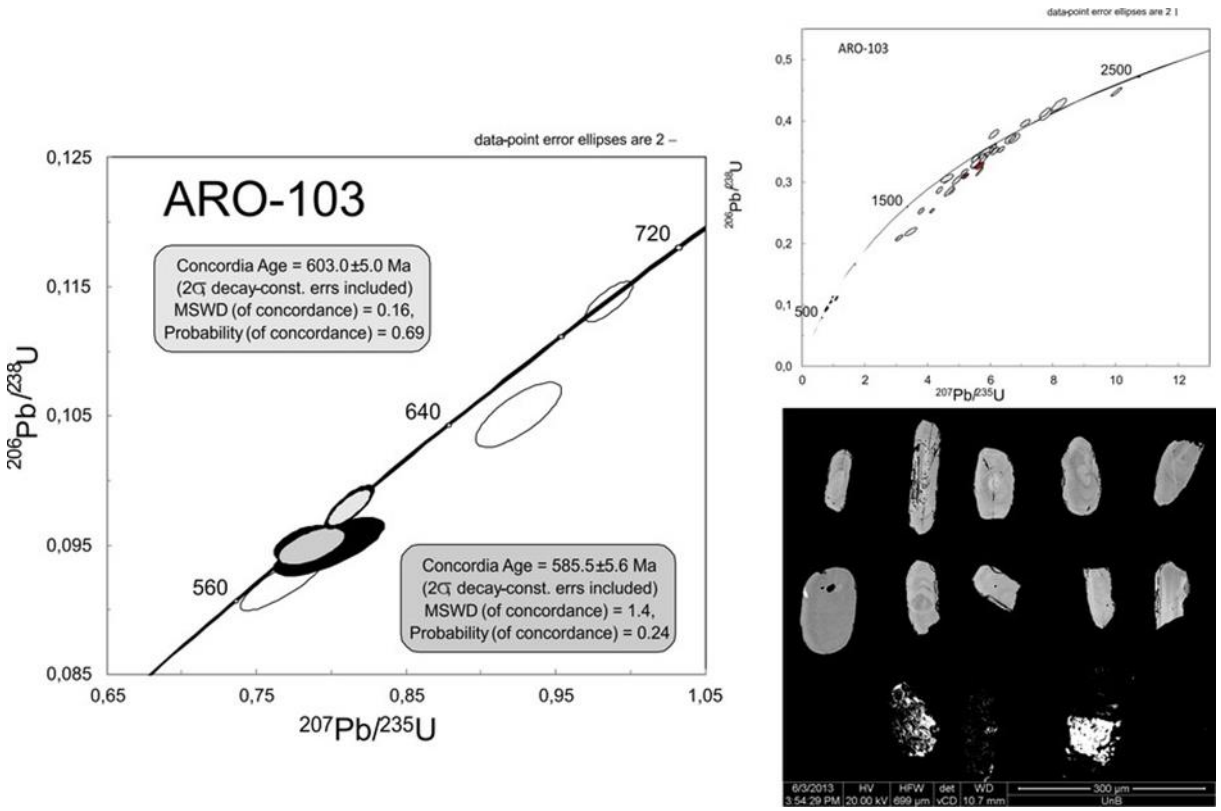

4.7.1.2 ARO – 01

The SHRIMP (Sensitive High Resolution Ion Microprobe) from the Universidade de São Paulo was used to date this sample. Zircon grains display variable contents of U (some grains ~2000ppm). Some crystals exhibit high contents of common Pb, increasing the analytical error, hence making difficult to obtain a precise age. Zircon grains (Fig. 11) are euhedral to subhedral (length/width ratios from 5:1 to 5:3), show oscillatory zoning, and some crystals have xenocrystic cores inherited from Mesoproterozoic sources (~1.58 Ga). Twenty spots were analyzed. An age of 567 ± 12 Ma was recorded in the superior intercept when forced

to zero (MSWD = 0.5). However, a Concordia age of 545 ± 3.5 Ma (MSWD = 9.6), with 100% of probability of concordance, we interpreted as the crystallization age, based on the smaller error and the geology.

Figura 12 - Figure 11. Left: Concordia Diagram of sample ARO-01; Right: full concordia diagram with emphasis on showing inherited Mesoproterozoic zircons and BSE images of zircons. Sample localities and details are provided in the text.

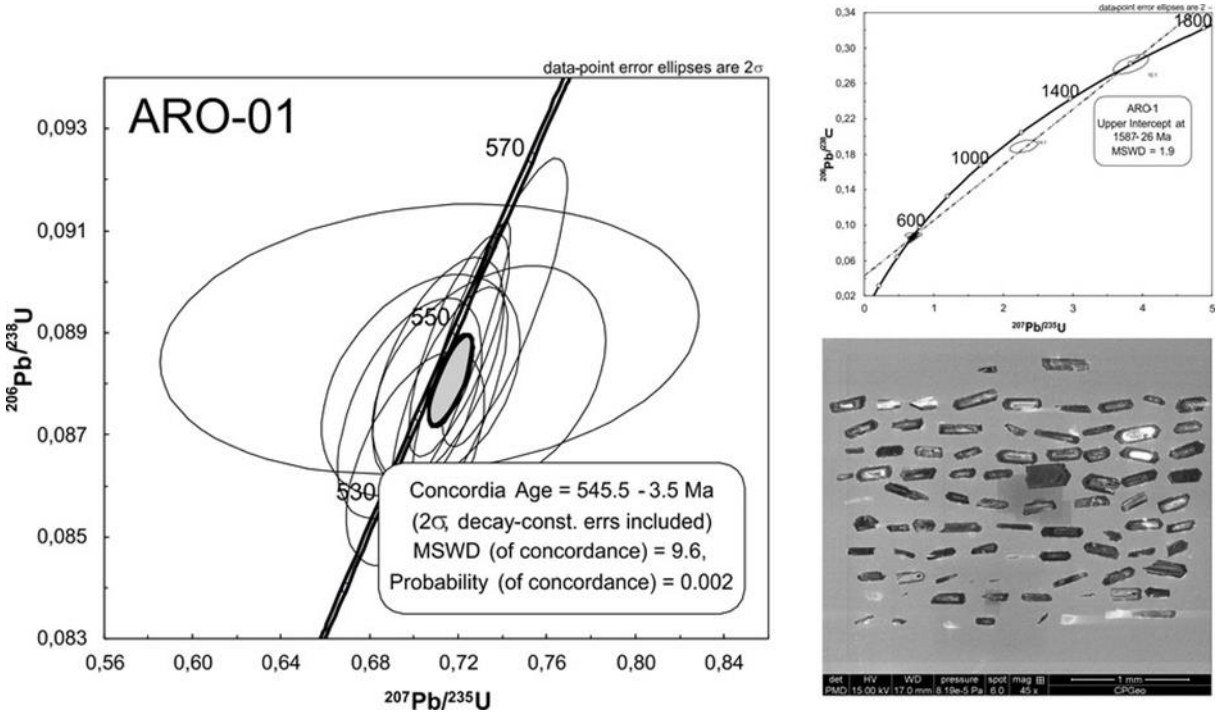

4.7.2 Queimadas Pluton

Zircons from the Queimadas Pluton were collected from the same sample that Almeida et al., (2002) dated using ID-TIMS, a monzogranite located at 7°20’30”S and 35°52’30”W.

4.7.2.1 NA-97

The SHRIMP RG from the Australian National University was used to date this sample. Zircon grains (Fig. 12) are euhedral to subhedral (length/width ratios from 5:1 to 2:1), prismatic and exhibit oscillatory zoning, some crystals have xenocrystic cores. A cluster of 16 grains show a concordia age of 550 ± 5.5 Ma (MSWD = 0.81; Probability of concordance = 0.848).

Figura 13 - Figure 12. Left: Concordia Diagram of sample NA-97; Right: BSE images of zircons. Sample localities and details are provided in the text.

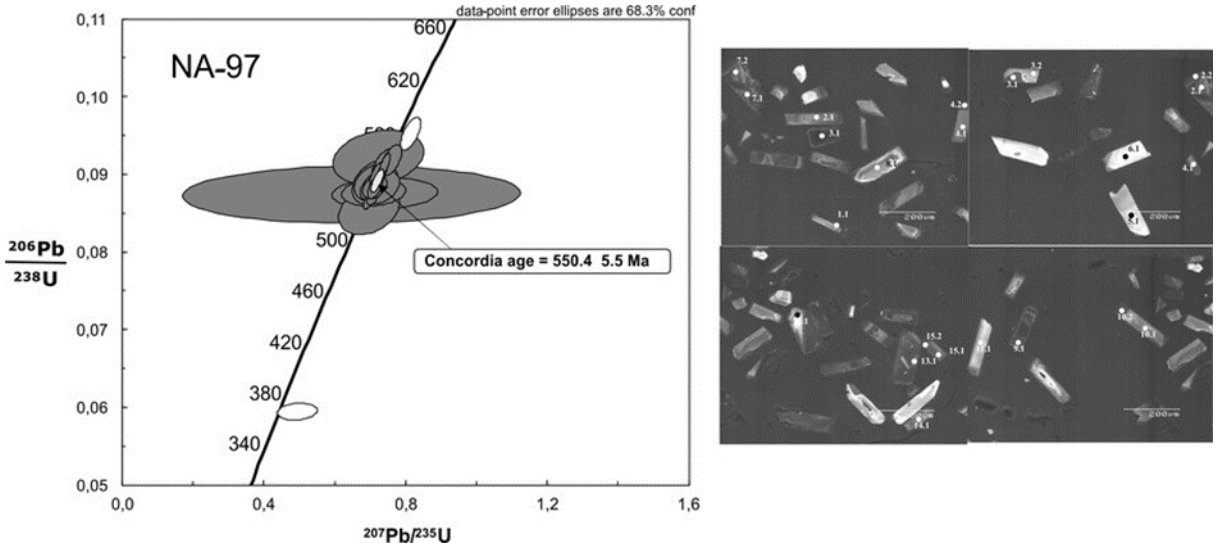

4.7.3 Serra Branca – Coxixola dike swarms

A northeast trending porphyritic hornblende-biotite granitic dike with dioritic enclaves and mafic clots was used to date this sample located at 7°30’42”S and 36°38’51”W.

4.7.3.1 MA-50

The LA-ICP-MS from the Universidade Federal de Ouro Preto was used to date this sample. Zircon grains (Fig. 13) are prismatic and exhibit oscillatory zoning, some crystals have fractures and display evidences of magmatic resorption. Fifty-eight zircon spots were analyzed in this sample, but 19 spots give a nice cluster of data, defining a concordia age of 545.2 ± 3.4 Ma (MSWD = 1.01; Probability of concordance = 0.44).

Figura 14 - Figure 13. Left: Concordia Diagram of sample MA-50; Right: CL images of zircon crystals. Sample localities and details are provided in the text.

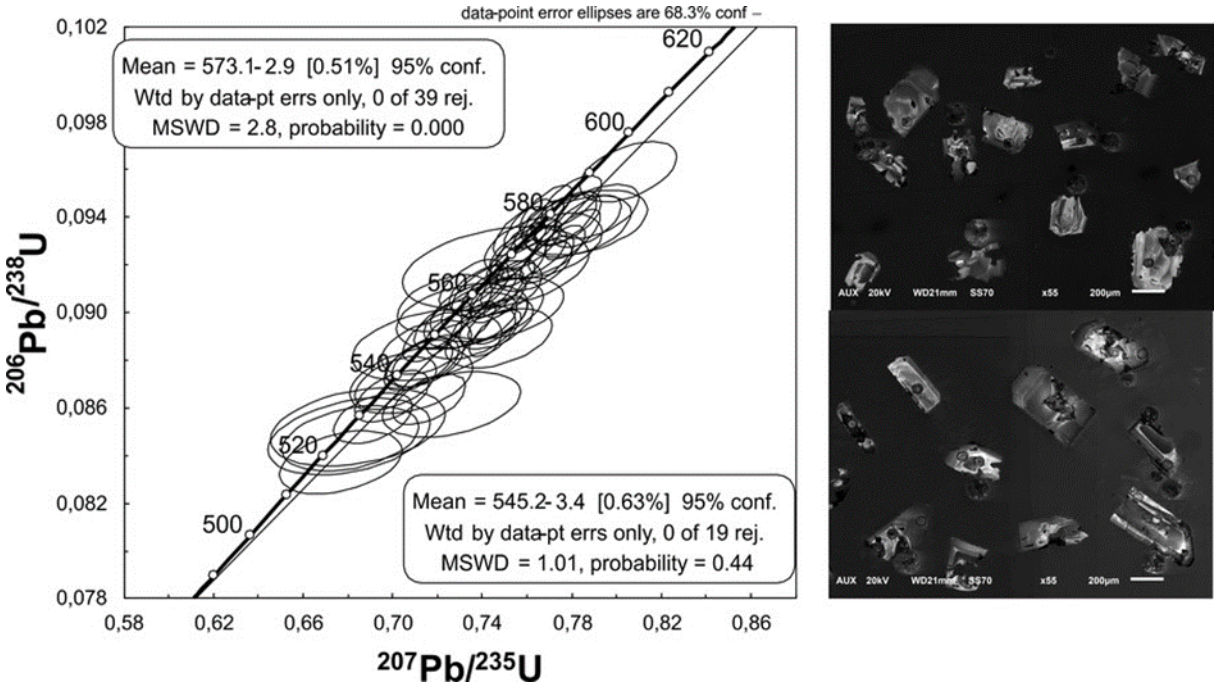

4.8 ISOTOPE GEOCHEMISTRY (SM-ND AND LU-HF)

4.8.1 Lu-Hf in zircon

Eighteen of the 19 spots from the sample MA-50 were used to define the Lu-Hf compositions, the results are presented in Fig. 14a. Relatively uniform initial $^{176}Hf/^{177}Hf$ ratios have been observed, ranging from 0.281730 to 0.281789. Samples exhibit very negative εHf values, between -21.6 and -24.8, and Hf TDM model ages are exclusively Paleoproterozoic, varying between 1.97 Ga and 2.12 Ga.

4.8.2 Sm-Nd

Sm-Nd data were obtained in 03 samples of the Aroeiras Complex, and data from 7 samples of the Queimadas Pluton and Prata Complex were compiled from Almeida et al., (2002) and Guimarães et al., (2005), results are shown in Figure 14b. The Aroeiras Complex samples have TDM model ages in the 2.04 – 2.15 Ga range, and display very negative εNd(585 Ma) values ranging from -11.68 to -14.15. The Queimadas Pluton granitoids have TDM model ages older than those recorded in the Aroeiras Complex (2.07 to 2.2 Ga), and εNd(550 Ma) values more negative, varying from -16.37 to -17.13. The Prata Complex samples show the oldest TDM model ages, ranging from 2.06 to 2.44 Ga, and remarkably negative εNd(530 Ma) values (-17.67 and -19.85).

Figura 15 - Figure 14.a) εHf plot for zircon grains of the Serra Branca-Coxixola granites; b) Nd isotopic composition of the studied ferroan suites.

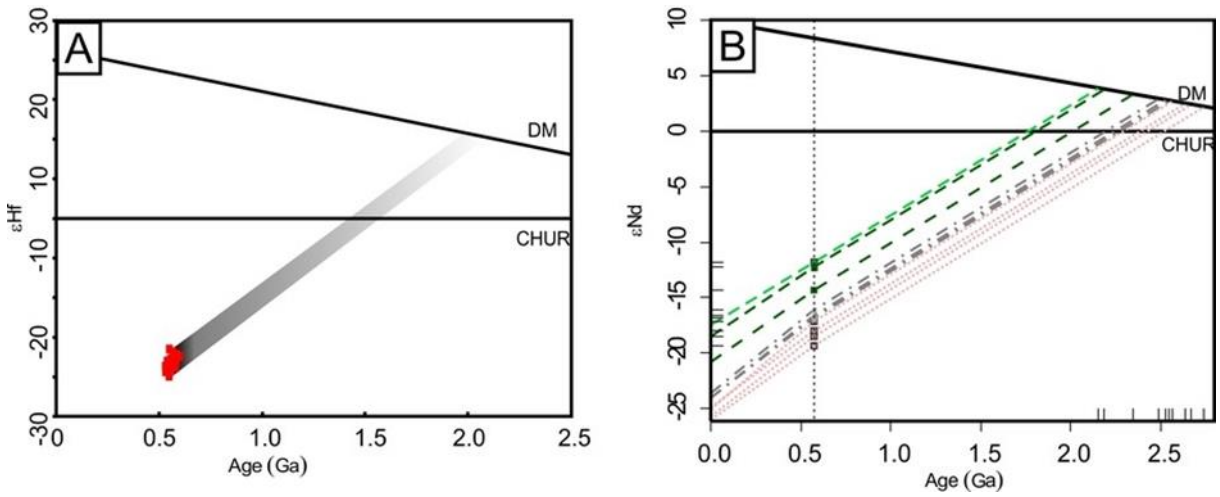

4.9 DISCUSSION

4.9.1 Sources of the ferroan intrusions

Ferroan granitic rocks are those with higher FeOt/(FeOt+MgO) ratios than subduction-related Cordilleran granitoids. Such rocks are correspondingly more reduced (Frost et al., 2001). Most of the ferroan granitoids are referred to as “A-type” granites, but the term has become confusing to the wide spectrum of chemical compositions with diverse petrogenesis (Bonin, 2007; Frost and Frost, 2011).

The Transversal subprovince ferroan granites distinguish two groups: 1) slightly peralumi- nous to slightly metaluminous, alkali-calcic rocks, with annite-poor mica and crystallized under intermediate oxygen fugacity (Aroeiras Complex and Serra Branca – Coxixola dike swarm); 2) metaluminous to slightly peraluminous, alkalic to alkali-calcic rocks, with annite-rich mica and crystallized under low oxygen fugacity conditions (Queimadas Pluton and Prata Complex).

Except for the Queimadas Pluton, the other studied granitoids exhibit expressive relationships between felsic and mafic rocks, this could either be related to fractionation from mafic melts, or incomplete mixing between crustal and mantle melts. Field evidences of mingling and mixing between dioritic or grabbroic magmas with granitic rocks favor the second model.

Frost and Frost (2011) summarized three main modes to produce ferroan granitic com- positions: 1) Partial melting of quartzfeldspathic crust; 2) differentiation of basaltic magma; 3)

partial melting of quartzfeldspathic crust or assimilation and fractional crystallization of basaltic magma.

4.9.1.1 Sources of the Queimadas Pluton

The generation of the Queimadas granitoids would be better explained by the partial melting of quartzfeldspathic crust, due to the lack of microgranular mafic enclaves or other signs of mantle conection.

Patiño Douce (1997) undertook dehydration melting experiments on magnesian tonalites and granodiorites at 950°C at 4 and 8 kbar, at lower pressures the produced melts tend to be calc-alkaline and ferroan, but at higher pressures, melts tend to be magnesian and peraluminous, these experiments suggest that metaluminous ferroan compositions can only be achieved by dehydration melting, if it takes place in the shallow crust. This experiment does not provide a plausible explanation to the generation of the Queimadas granitoids, due to their calculated temperatures lower than 900°C, and its alkali-calcic character.

Bogaerts et al. (2006) performed 4 kbar vapor-excess melting on ferroan granodiorites. The first melts are ferroan and slightly peraluminous. The increasing degree of melting favor compositions more magnesian and metaluminous. Such conditions are unlikely to have generated the Queimadas granitioids, due to the lack of ferroan granodiorites as the country rocks (Neves et al., 2015), mineral chemistry suggesting low H_2O activities and alkali-calcic character.

Skjerlie and Johnston (1993) performed dehydration melting experiments on magnesian tonalite gneiss containing ∼20% biotite and ∼2% hornblende. Melts produced at 10 kbar are strongly ferroan, at 6 kbar are slightly ferroan, and with greater degrees of melting the melts tend to reach the ferroan magnesian boundary composition. This experiment is the only to approach alkali-calcic compositions. The temperature required to the generation of the Queimadas grani- toids could be achieved by high geothermal gradient caused by crustal extension in a thickened crust, explaining also the lack of MME, TDM model ages between 2.07 – 2.2 Ga suggest the 2.05 – 2.2Ga calc-alkalic TTG suites described by Neves et al. (2015a) as a reasonable source, the alkali-calcic character would be favored by K_2O enriched nature of some source rocks.

4.9.1.2 Sources of the Aroeiras and Prata Complexes

The Aroeiras and Prata granitoids genesis requires a more elaborate model than the other studied granitoids, because of the strong interaction between mafic and felsic rocks, favoring partial melting and assimilation of quartzfeldspathic crust coupled with incomplete mixing of mantle derived rocks.

Diorites of both complexes are LILE enriched, and show Paleoproterozoic TDM model ages (2.04 – 2.1 Ga) and strongly negative εNd. Dolerites from the Prata Complex also exhibit TDM model ages ca. 2.25 Ga (Guimarães et al., 2005). These characteristics have been recognized in many plutons of the Borborema Province, several authors attribute these aspects to a metasomatized by previous orogenic events lithospheric mantle (Silva Filho et al., 1993; Ferreira et al., 1997; Neves and Mariano, 1997, 2004; Neves et al., 2000b; Mariano et al., 2001; Hollanda et al., 2003; Guimarães et al., 2005), ca. 2.04 Ga model ages are consistent with the peak of a metamorphic event dated at c. 2.06 – 2.04 Ga in the basement rocks (Neves et al., 2015) which the Aroeiras Complex intrudes.

Noritic rocks from the Prata Complex, however, show positive εNd, and are less LILE-enriched. We suggest, in this case, crustal extension buildup to the rise of astenospheric mantle. Since norites display the same interactions with felsic melts of the Prata Complex as dolerites and diorites, the Nd signature of these rocks cannot reflect homogenization with enclosing granites (Guimarães et al., 2005), in addition, interaction between mafic and felsic rocks favors heat, fluids and LILE diffusion from mafic to felsic rocks, resulting in chemical quenching of the mafic members (Pistone et al., 2016). Therefore, the isotopic signature of MME in the Aroeiras and Prata Complexes, should express the mantle composition beneath the Borborema Province.

The Aroeiras granitoids exhibit ca. 2.15 Ga TDM model ages, as well as, Meso to Paleoproterozoic inherited zircons. We suggest that generation of these rocks involved partial melting of basement TTG rocks, as those described by Neves et al. (2015). Mesoproterozoic zircon grains must have been assimilated as the Aroeiras granitoids rose through the crust. Sá et al. (2002) reported ca. 1.5 Ga ferroan orthogneisses further south in Transversal subprovince.

Assimilation processes probably shifted granitoid compostitions from metaluminous to slightly peraluminous. The Aroeiras granitoids could not be generated by simple fractiona- tion processes directly from a dioritic magma. Fractionation from alkalic diorites would lead to

strongly alkalic granitic compositions. Since alkali-calcic character is hardly achieved by partial melting of quartzfelspathic rocks, it likely that besides partial melting from TTG rocks, interactions between intermediate and felsic melts favored diffusion of LILE from diorites to granites.

A similar model of generation for the Prata granitoids was proposed by Guimarães et al. (2005). Santos et al. (2015) identified a 2.44 Ga TTG association, as the basement of this region, they provide a logical source for these granitoids and could explain the identical and oldest TDM model age found in ferroan granites of the Transversal subprovince.

4.9.1.3 Sources of the Serra Branca – Coxixola dike swarms

The granitoids of the Serra Branca – Coxixola dikes are silica-rich SiO2> 70%, alkali-calcic and peraluminous. Rocks with analogous compositions were described in collisional settings (Pichavant, et al., 1988; Visona and Lombardo, 2002), and anorogenic settings (Kleeman and Twist, 1989; Hildreth et al., 1991; Hill et al., 1996). Frost et al. (2016), compiling petrogenetic models, suggest that in collisional settings such compositions can be reached by partial melting of pelitic rocks, and in anorogenic settings by partial melting and/or differentiation of tholeiite.

However, the studied granitoids neither display typical peraluminous assemblages with tourmaline and two-mica granites nor metaluminous granites associated. Thus, the processes involved in their generation should differ from other silica-rich, alkali-calcic, peraluminous granites.

Hafnium model ages point to Paleoproterozoic sources to these rocks (1.9 – 2.12 Ga). Lithospheric stretching leads to crustal thinning and increases the geothermal gradient (McKenzie, 1978), providing the necessary heat to promote limited melting of Rhyacian tonalitic to granodioritic rocks with assimilation of metasedimentary components during their ascent. Small percentages of melts could explain the alkali-calcic nature and assimilation of pelitic sedimentary rocks would contribute to achieve peraluminous compositions.

4.10 CONCLUSION

Ferroan granites in the Transversal subprovince distinguish two geochemical groups in different stages of the Brasiliano Orogeny (Fig. 15):

(1) slightly peraluminous to slightly metaluminous, alkali-calcic rocks, with

annite-poor mica and amphiboles crystallized under intermediate oxygen fugacity. This group marks shifts in geotectonic settings. For instance, the Aroeiras Complex marks the transition from collisional to strike-slip tectonics (ca. 585 Ma); and the Serra Branca – Coxixola and late leucocratic dikes of the Aroeiras Complex, marks the transition from strike-slip to uplift and transtensional tectonics with development of intracratonic basins (ca. 545 Ma);

(2) metaluminous to slightly peraluminous, alkalic to alkali-calcic rocks, with annite- rich mica and low oxygen fugacity crystallization of amphibole (Queimadas Pluton and Prata Complex). This group is related with fully developed extensional environments. The Queimadas Pluton granitoids are related to heterogenous thinning of previously thickened lithosphere, in post-collisional environments associated with strike-slip shear zones between 570-550 Ma; and the Prata Complex granitoids are associated with transtension contemporary with deposition in the intracratonic basins and the latest ferroan intrusions the Borborema Province.

Generation of ferroan granites in the Transversal subprovince involve largely partial melting of the TTG rocks of Paleoproterozoic age in the basement of the Borborema Province, and country rocks assimilation, to some extent. The presence of mafic rocks is related to heat transfer, and/or intertwined with geochemical deviations of the granite compositions.

Ferroan granitoids can occur at any of the deformational stages of the Brasiliano-Pan- African orogenic cycle, since extensional sites can develop in any tectonic setting.

Figura 16 - Figure 15. Summary diagram of the tectonomagmatic evolution of the Transversal Subprovince, Borborema Province as discussed in this study. The focus on the post-collisional phases and their relatioships with ferroan intrusions, ages of Magnesian calc-alkalic and alkali-calcic granitoids are those described in Guimarães et al. (2004), as age intervals of Ferroan intrusions are the ones described in this paper. 590 - 580 Ma marks the transition from collision to strike-slip tectonics, and early extensional sites; 570 - 550 Ma marks extensional events and heterogenous crustal thinning related to the transcurrent event; 545 - 520 Ma marks the uplift and onset of transtensional tectonics in the Transversal subprovince.

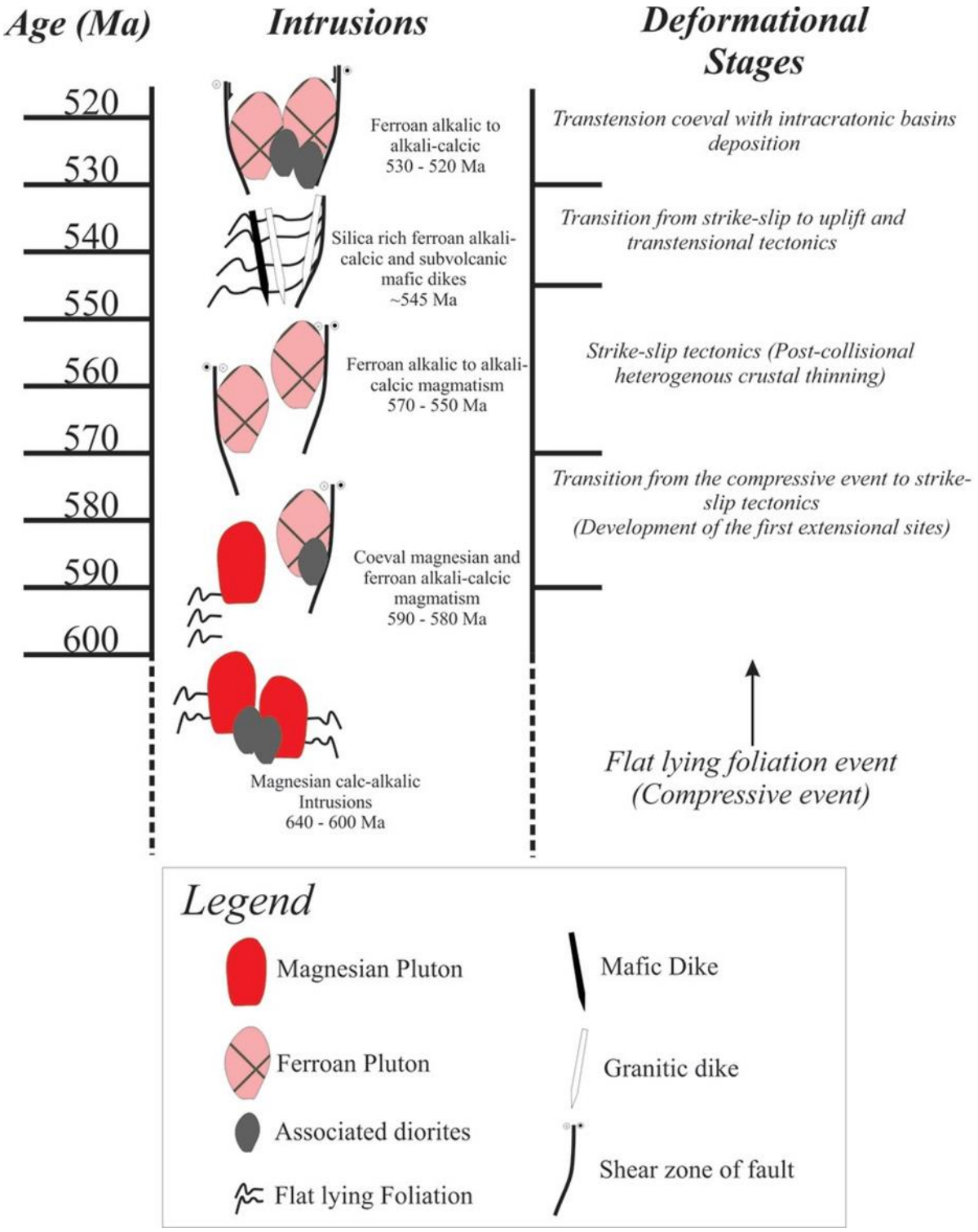

4.11 ACKNOWLEDGEMENTS

This work was supported by Fundação de Amparo à Ciência e Tecnologia do estado de Pernambuco (FACEPE); under grant [IBPG-1074-1.07/15].

4.12 REFERENCES

Archanjo, C.J., Viegas, L.G.F., Hollanda, M.H.B.M., Souza, L.C., Liu, D., 2013, Timing of the HT/LP transpression in the Neoproterozoic Seridó Belt (Borborema Province, Brazil): Constraints from UPb (SHRIMP) geochronology and implications for the connections between NE Brazil and West Africa: Gondwana Research, v. 23 (2), p. 701-714.

Attoh, K., Corfu, F., Nude, P.M., 2007, U-Pb zircon age of deformed carbonatite and alkaline rocks in the Pan-African Dahomeyide suture zone, West Africa: Precambrian Res. v. 155, p. 251-260.

Azzouni-Sekkal, A., Liégeois, J.P., Bechiri-Benmerzoug, F., Belaidi-Zinet, S., Bonin, B., 2003, The “Taourirt” magmatic province, a marker of the closing stage of the Pan-African orogeny in the Touareg Shield: review of available data and Sr–Nd isotope evidence: Journal of African Earth Sciences, v. 37, p. 331–350.

Bogaerts, M., Scaillet, B., Vander Auwera, J., 2006, Phase equilibria of the Lyngdal granodiorite (Norway): Implications for the origin of metaluminous ferroan granitoids: Journal of Petrology, v.47, p. 2405-2431.

Bonin, B., 2007, A-type granites and related rocks: evolution of a concept, problems and prospects: Lithos, v. 97, p. 1-29.

Bouvier, A., Vervoort, J.D., Patchett, P.J., 2008. The Lu-Hf and Sm-Nd isotopic composition of CHUR: constraints from unequilibrated chondrites and implications for the bulk composition of terrestrial planets: Earth and Planet Science Letters, v. 273, p. 48-57.

Brito Neves, B.B., Van Schmus, W.R., Santos, E.J., Campos Neto, M.C., Kozuch, M., 1995, O evento Cariris Velhos na Província Borborema: integração de dados, implicações e perspectivas: Revista Brasileira de Geociências, v. 25, p. 279-296.

Brito Neves, B.B., Santos, E.J., Van Schmus, W.R., 2000, Tectonic History of the Borborema Province. in Cordani, U.G., Milani, E.J., Thomaz Filho, A., Campos, D.A., eds., Tectonic evolution of South America, Rio de Janeiro, p. 151-182.

Brito Neves, B.B., Campos Neto, M.C., Van Schmus, W.R., Santos, E.J., 2001, O "Sistema Pajeú-Paraíba" e o "Maciço" Sao José do Campestre no leste da Borborema: Revista Brasileira de Geociências, v. 31 (2), p. 173–184.

Brito Neves, B.B., Basei, M.A.S., Passarelli, C.R., Santos, E.J., 2003, Idades U Pb em zircao de alguns granitos clássicos da Província Borborema, Revista do Instituto de Geociências da Universidade de São Paulo, v. 3, p. 25-38.

Brito, M.F.L., Mendes, V.A., Paiva, I.P., 2008, Metagranitoide Serra das Flores: magma- tismo Toniano (tipo-A) no Domínio Pernambuco-Alagoas, Nordeste do Brasil, 44º Brazilian Geological Congress, Curitiba, Abstract in CD-ROM.

Carvalho, M.J., 2005, Tectonic Evolution of the Maranco-Poço Redondo Domain: Records of the Cariris Velhos and Brasiliano Orogenesis in the Sergipano Belt, NE Brazil [DoctoralArchanjo, C.J., Viegas, L.G.F., Hollanda, M.H.B.M., Souza, L.C., Liu, D., 2013, Timing of the HT/LP transpression in the Neoproterozoic Seridó Belt (Borborema Province, Brazil): Constraints from UPb (SHRIMP) geochronology and implications for the connections between NE Brazil and West Africa: Gondwana Research, v. 23 (2), p. 701-714.

Attoh, K., Corfu, F., Nude, P.M., 2007, U-Pb zircon age of deformed carbonatite and alkaline rocks in the Pan-African Dahomeyide suture zone, West Africa: Precambrian Res. v. 155, p. 251-260.

Azzouni-Sekkal, A., Liégeois, J.P., Bechiri-Benmerzoug, F., Belaidi-Zinet, S., Bonin, B., 2003, The "Taourirt" magmatic province, a marker of the closing stage of the Pan-African orogeny in the Touareg Shield: review of available data and Sr–Nd isotope evidence: Journal of African Earth Sciences, v. 37, p. 331–350.

Bogaerts, M., Scaillet, B., Vander Auwera, J., 2006, Phase equilibria of the Lyngdal granodiorite (Norway): Implications for the origin of metaluminous ferroan granitoids: Journal of Petrology, v.47, p. 2405-2431.

Bonin, B., 2007, A-type granites and related rocks: evolution of a concept, problems and prospects: Lithos, v. 97, p. 1-29.

Bouvier, A., Vervoort, J.D., Patchett, P.J., 2008. The Lu-Hf and Sm-Nd isotopic composition of CHUR: constraints from unequilibrated chondrites and implications for the bulk composition of terrestrial planets: Earth and Planet Science Letters, v. 273, p. 48-57.

Brito Neves, B.B., Van Schmus, W.R., Santos, E.J., Campos Neto, M.C., Kozuch, M., 1995, O evento Cariris Velhos na Província Borborema: integração de dados, implicações e perspectivas: Revista Brasileira de Geociências, v. 25, p. 279-296.

Brito Neves, B.B., Santos, E.J., Van Schmus, W.R., 2000, Tectonic History of the Borborema Province. in Cordani, U.G., Milani, E.J., Thomaz Filho, A., Campos, D.A., eds., Tectonic evolution of South America, Rio de Janeiro, p. 151-182.

Brito Neves, B.B., Campos Neto, M.C., Van Schmus, W.R., Santos, E.J., 2001, O "Sistema Pajeú-Paraíba" e o "Maciço" Sao José do Campestre no leste da Borborema: Revista Brasileira de Geociências, v. 31 (2), p. 173–184.

Brito Neves, B.B., Basei, M.A.S., Passarelli, C.R., Santos, E.J., 2003, Idades U Pb em zircao de alguns granitos clássicos da Província Borborema, Revista do Instituto de Geociências da Universidade de São Paulo, v. 3, p. 25-38.

Brito, M.F.L., Mendes, V.A., Paiva, I.P., 2008, Metagranitoide Serra das Flores: magma- tismo Toniano (tipo-A) no Domínio Pernambuco-Alagoas, Nordeste do Brasil, 44º Brazilian Geological Congress, Curitiba, Abstract in CD-ROM.

Carvalho, M.J., 2005, Tectonic Evolution of the Maranco-Poço Redondo Domain: Records of the Cariris Velhos and Brasiliano Orogenesis in the Sergipano Belt, NE Brazil [Doctoral thesis]: Campinas University, 202 p.

Cavalcante, J.C., Vasconcelos, A.M., Medeiros, M.F., Paiva, I.P., Gomes, F.E.M., Caval- cante, S.N., Cavalcante, J.E., Melo, A.C.R., Duarte Neto, V.C., Benevides, H.C., 2003, Mapa Geologico do Estado do Ceará: Ministerio das Minas e Energia/Companhia de Pesquisa de Recursos Minerais, Fortaleza, scale 1:500 000.

Caxito, F.A., Uhlein, A., Dantas, E.L., 2014a, The Afeição augen-gneiss Suite and the record of the Cariris Velhos Orogeny (1000-960 Ma) within the Riacho do Pontal fold belt, NE Brazil: Journal of South American Earth Sciences, v. 51, p. 12-27.

Caxito, F.A., Uhlein, A., Stevenson, R., Uhlein, G.J., 2014b, Neoproterozoic oceanic crust remnants in northeast Brazil: Geology, v. 42, p. 387-390.

Cruz, R.F., Acciolly, A.C.A., 2013, Petrografia, geoquímica e idade U/Pb do Ortognaisse Rocinha, no Domínio Pernambuco-Alagoas W da Província Borborema, Estudos Geologicos, v. 23 (2), p. 1-27.

Dall'Agnoll, R., Costi, H.T., Leite, A.A.S., Magalhães, M.S., Teixeira, N.P., 1999, Rapakivi granites from Brazil and adjacent areas, Precambrian Research v. 95(1), p. 9-39.

Dantas, E.L., Hackspacher, P.C., Van Schmus, W.R., Neves, B.B.B., 1998, Archean accretion in the Sao Jose do Campestre Massif, Borborema Province, Northeast Brazil: Revista Brasileira de Geociências, v. 28 (2), p. 221-228.

Dantas, E.L., Souza, Z.S., Wernicke, E., Hackspacher, Martin, H., Xiaodong, L., 2013, Crustal growth in the 3.4 to 2.7 Ga Sao Jose de Campestre Massif, Borborema Province, NE Brazil: Precambrian Research, v. 227, p. 120-156.

Dantas, E.L., Van Schmus, W.R., Hackspacher, P.C., Fetter, A., Brito Neves, B.B., Cordani, U.G., Nutman, A.P., Williams, I.S., 2004, The 3.4-3.5 Ga Sao Jose do Campestre massif, NE Brazil: remnants of the oldest crust in South America: Precambrian Research, v. 130, p. 113-137.

De Wit, M.J., Jeffery, M., Bergh, H., Nicolaysen, L., 1998, Geological Map of Sectors of Gondwana, Reconstructed to Their Disposition 150 Ma: American Association of Petroleum Geologists, Tulsa, USA, scale 1:10 000 000

Eby, G.N., 1992, Chemical subdivision of the A-type granitoids: petrogenetic and tectonic implications: Geology, v. 20, p. 641-644.

Ferré, E., Caby, R., Peucat, J.J., Capdevila, R., Monié, P., 1998, PanAfrican, post-collisional, ferro-potassic granite and quartz–monzonite plutons of Eastern Nigeria: Lithos, v. 45, p. 255–279.

Ferreira, V.P., Sial, A.N., Long, L.E., Pin, C., 1997, Isotopic signatures of Neoproterozoic to Cambrian ultrapotassic syenitic magmas, northeastern Brazil: implications for enriched mantle source: International Geology Review, v. 39, p. 660-669.

Ferreira, V.P., Sial, A.N., Jardim de Sa, E.F., 1998, Geochemical and isotopic signatures of proterozoic granitoids in terranes of Borborema structural province, northeast Brazil. Journal of South America Earth Sciences, v. 11, p. 439-455.

Ferreira, V.P., Sial, A.N., Pimentel, M.M., Armstrong, R., Spicuzza, M., Guimaraes, I.P., Silva Filho, A.F., 2011, Contrasting sources and P-T crystallization conditions of epidote-bearing granitic rocks, Northeastern Brazil: O, Sr and Nd isotopes: Lithos, v. 121, p. 189-201.

Fetter, A.H., 1999, U-Pb and Sm-Nd Geochronological Constraints on the Crustal Framework and Geologic History of Ceara State, NW Borborema Province, NE Brazil: Implications for the Assembly of Gondwana [Ph.D. Thesis]: Kansas University, 164 p.

Fetter, A.H., Van Schmus, W.R., Santos, T.J.S., Nogueira Neto, J.A., Arthaud, M.H., 2000, U-Pb and Sm-Nd geochronological constraints on the crustal evolution of basement architecture of Ceara state, NW Borborema province, NE Brazil: implications for the existence of the Paleoproterozoic supercontinent ‘Atlantica’: Revista Brasileira de Geociências, v. 30, p. 102-106.

Frost, B.R., Barnes, C., Collins, W., Arculus, R, Ellis D., Frost, C., 2001, A chemical classification for granitic rocks: Journal of Petrology, v. 42, p. 2033-2048.

Frost C.D., Frost B.R., 2011, On Ferroan (A-type) Granitoids: their Compositional Variability and Modes of Origin: Journal of Petrology, v. 52, p. 39-53.

Frost, C.D., Frost, B.R., Beard, J.S., 2016, On silica-rich granitoids and their eruptive equivalentes: American Mineralogist, v. 101, p. 1268-1284.

Gioia, S.M.C.L., Pimentel, M.M., 2000, The Sm-Nd isotopic method in the geochronology laboratory of the university of Brasília: Anais da Academia Brasileira de Ciências v. 72 (2), p. 219-245.

Goodenough, K.M., Lusty, P.A.J., Roberts, N.M.W., Key, R.M., Garba, A., 2014, Postcol- lisional Pan-African granitoids and rare-metal pegmatites in western Nigeria: age, petrogenesis and the pegmatite conundrum: Lithos, v. 200, p. 22-34.

Griffin, W.L., Pearson, N.J., Belousova, E., Jackson, S.E., Van Achterbergh, E., O'Reilly, S.Y., Shee, S.R., 2000, The Hf isotope composition of cratonic mantle: LAM-MC-ICPMS analysis of zircon megacrysts in kimberlites: Geochimica et Cosmochimica Acta, v. 64, p. 133-147.

Guimarães, I.P., Silva Filho, A.F., Almeida, C.N., Van Schmus, W.R., Araújo, J.M.M., Melo, S.C., Melo, E.B., 2004, Brasiliano (Pan-African) granitic magmatism in the Pajeú-Paraíba belt, Northeast Brazil: an isotopic and geochronological approach: Precambrian Research, v. 135, p. 23–53.

Guimarães, I.P., Silva Filho, A.F., Melo, S.C., Macambira, M.B., 2005, Petrogenesis of A-type granitoids from Alto Moxotó and Alto Pajeú terranes of the Borborema Province, NE Brazil: constraints from geochemistry and isotopic compositions: Gondwana Research, v. 8, p. 347–362.

Guimaraes, I.P., da Silva Filho, A.F., de Araújo, D.B., de Almeida, C.N., Dantas, E., 2009, Trans-alkaline magmatism in the Serrinha-Pedro Velho complex, Borborema province, NE Brazil and its correlations with the magmatism in eastern Nigeria: Gondwana Research, v. 15, p. 98-110.

Guimarães, I.P., Silva Filho, A.F., Almeida, C.N., Macambira, M., Armstrong, R.A., 2011, U-Pb SHRIMP data constraints on calc-alkaline granitoids with 1.3-1.6 Ga Nd TDM model ages from the central domain of the Borborema province, NE Brazil: Journal of South America Earth Sciences, v. 31, p. 383-396.

Guimaraes, I.P., Van Schmus, W.R., Brito Neves, B.B., Bittar, S.M., Silva Filho, A.F., Armstrong, R., 2012, U-Pb zircon ages of orthogneisses and supracrustal rocks of the Cariris Velhos belt: onset of Neoproterozoic rifting in the Borborema Province, NE Brazil: Precambrian Research, 192-v. 195, p. 52-77

Guimarães, I.P., Brito, M.F.L., Lages, G.A., Silva Filho, A.F., Santos, L., Brasilino, R.G., 2016, Tonian granitic magmatism of the Borborema Province: A review: Journal of South American Earth Sciences, v. 68, p. 97-112.

Guimarães, I.P., Silva Filho, A.F., Armstrong, R., 2017, Origin and age of coeval gabbros and leucogranites in the northern supbrovince of the Borborema Province, NE Brazil: Journal of South America Earth Sciences, v. 76, p. 71-93.

Hagen-Peter, G., Cottle, J.M., 2016, Synchronous alkaline and subalkaline magmatism during the late Neoproterozoic–early Paleozoic Ross orogeny, Antarctica: Insights into magmatic sources and processes within a continental arc: Lithos, v. 262, p. 677-698.

Hildreth, W., Halliday, A.N., Christiansen, R.L., 1991, Isotopic and chemical evidence concerning the genesis and contamination of basaltic and rhyolitic magma beneath the Yellowstone plateau volcanic field: Journal of Petrology, v. 32, p. 63–138.

Hill, M., Barker, F., Hunter, D., Knight, R., 1996, Geochemical characteristics and origin of the Lebowa granite suite, Bushveld Complex: International Geology Review, v. 38, p. 195–227.

Holland, T., Blundy, J., 1994, Non-ideal interactions in calcic amphiboles and their bearing on amphibole-plagioclase thermometry. Contribibutions to Mineralogy and Petrology, v. 116, p. 433-447.

Hollanda, M.H.B., Pimentel, M.M., Jardim de Sá, E.F., 2003, Paleoproterozoic subduction- related metasomatic signatures in the lithospheric mantle beneath NE Brazil: inferences from trace element and Sr–Nd–Pb isotopic compositions of Neoproterozoic high-K igneous rocks.: Journal of South American Earth Sciences, v. 15, p. 885–900.

Hollanda, M.H.B.M., Archanjo, C.J., Souza, L.C., Armstrong, R., Vasconscelos, P.M., 2010, Cambrian mafic o felsic magmatism and its connections with transcurrent shear zones of the Borborema Province (NE Brazil): Implications for the late assembly of West Gondwana: Precambrian Research, v. 178 , p. 1-14.

Hollanda, M.H.B.M., Archanjo, C.J., Souza, L.C., Dunyi, L., Armstrong, R.A., 2011, Long lived Paleoproterozoic granitic magmatism in the Serido-Jaguaribe domain, Borborema Province NE Brazil: Journa of South America Earth Sciences, v. 32, p. 287-300.

Hollanda, M.H.B.M., Archanjo, C.J., Bautista, J.R., Souza, L.C., 2015, Detrital zircon ages and Nd isotope compositions of the Serido and Lavras da Mangabeira basins (Borborema Province, NE Brazil): evidence for exhumation and recycling associated with a major shift in sedimentary provenance. Precambrian Research, v. 258, p. 186-207.

Jardim de Sa, E.F., Macedo, M.H.F., Torres, H.H.F., Kawashita, K., 1988, Geochronology of metaplutonics and the evolution of supracrustal belts in the Borborema province: VII Latino- americano Geological Congress, Extended Abstract, p. 49-62.

King P.L., White A.J.R., Chapell B.W., Allen C.M., 1997, Characterization and origin of aluminous A-type granites from the Lachlan Fold Belt, Southeastern Australia: Journal of Petrology, v. 38, p. 371-391

Kisters, A.F.M., Belcher, R.W., Scheepers, R., Rozendaal, A., Jordaan, L.S., Armstrong, R., 2002, Timing and kinematics of the Colenso Fault: The Early Paleozoic shift from collisional to extensional tectonics in the Pan-African Saldania Belt, South Africa: South African Journal of Geology, v. 105, p. 257-270.

Kleeman, G.J., and Twist, D., 1989, The compositionally zoned sheet-like granite pluton of the Bushveld Complex: Evidence bearing on the nature of A-type magmatism: Journal of Petrology, v. 30, p. 1383–1414.

Kozuch, M., 2003, Isotopic and Trace Element Geochemistry of Early Neoproterozoic Gneissic and Metavolcanic Rocks in the Cariris Velhos Orogen of the Borborema Province, Brazil and Their Bearing Tectonic Setting [Ph.D. thesis]: Kansas University, 199p.

Lages, G.A., Marinho, M.S., Nascimento, M.A.L., Medeiros, V.C., Dantas, E.L., 2016, Geocronologia e aspectos estruturais e petrologicos do Pluton Bravo, Domínio Central da Província Borborema, Nordeste do Brasil: um granito transalcalino precoce no estágio pos-colisional da Orogenese Brasiliana: Brazilian Journal of Geology, v. 46 (1), p. 41-61.

Leake, B.E., Woolley, A.R., Arps, C.E.S., Birch, W.D., Gilbert, M.C., Grice, J.D., Hawthorne, C. & Kato, A., 1997, Nomenclature of amphiboles: Report of the subcommittee on amphiboles of the International Mineralogical Association, Commission on new minerals and mineral names: American Mineralogist, v. 82, p. 1019-1037.

Liégeois, J.P., Black, R., 1984, Pétrographie et géochronologie Rb–Sr de la transition calco-alcaline–alcaline fini-Panafricaine dans l'Adrar des Iforas (Mali): Accrétion crustale au Précambrien supérieur, in Klerkx, J., Michot, J., eds., Géologie africaine — African geology, Volume en hommage à L. Cahen, Tervuren, p. 115–145.

Lima, J.V., Guimarães, I.P., Santos, L., Amorim, J.V.A., Farias, D.J.S., 2017, Geochemi- cal and isotopic characterization of the granitic magmatism along the Remígio-Pocinhos shear zone, Borborema Province, NE Brazil: Journal of South America Earth Sciences, v. 75, p. 116- 133.

Mariano, G., Neves, S.P., Da Silva Filho, A.F., Guimarães, I.P., 2001, Diorites of the high- K calc-alkalic Association: geochemistry and Sm–Nd data and Implications for the evolution of the Borborema Province, Northeast Brazil: International Geology Review v. 43, p. 921–929.

Martins, G., Oliveira, E.P., Lafon, J.-M., 2009, The Algodões amphibolite-tonalite gneiss sequence, Borborema Province, NE Brazil: Geochemical and geochronological evidence for Palaeoproterozoic accretion of oceanic plateau/back-arc basalts and adakitic plutons: Gondwana Research, v. 15, p. 71-85.

Martins, G., Oliveira, E.P., Souza Filho, C.R., Lafon, J.M., 1998, Geochemistry and geochronology of the Algodões sequence, Ceará, NE Brazil: a paleoproterozoic magmatic arc in the Central Ceará domain of the Borborema Province: 40 Congresso. Brasileiro de Geologia, Anais, p. 28.

Matteini, M., Dantas, E.L., Pimentel, M.M., Bühn, B., 2010,Combined U-Pb and Lu-Hf isotope analyses by laser ablation MC-ICP-MS: methodology and applications, Anais da Academia Brasileira de Ciências, v. 82 (2), p. 479-491.

McKenzie, D., 1978, Some remarks on the development of sedimentary basins: Earth and Planetary Science Letters, v. 40(1), p. 25-32.

Monié, P., Caby, R., Arthaud, M.H., 1997, The Neoproterozoic Brasiliano Orogeny in Northeast Brazil: 40Ar/39Ar and petrostructural data from Ceará: Precambrian Research v. 81, p. 241–264.

Nakamura, N., 1974, Determination of REE, Ba, Fe, Mg, Na, and K in carbonaceous and ordinary chondrites: Geochimica et Cosmochimica Acta, v. 38, p. 757-775.

Nascimento, M.A.L., Galindo, A.C., Medeiros, V.C., 2015, Ediacaran to Cambrian magmatic suites in the Rio Grande do Norte domain, extreme Northeastern Borborema Province (NE of Brazil): Current knowledge: Journal of South American Earth Sciences, v. 58, p. 281-299.

Neves, S.P., Vauchez, A., Archanjo, C.J., 1996, Shear zone-controlled magma emplacement or magma-assisted nucleation of shear zones? Insights from northeast Brazil: Tectonophysics, v. 262, p. 349-364.

Neves, S.P., Mariano, G., 1997, High-K calc-alkalic plutons in Northeast Brazil: origin of the biotite diorite/quartz monzonite to granite association and implications for the evolution of the Borborema Province: International Geologic Review, v. 39, p. 621–638.

Neves, S.P., Vauchez, A., Feraud, G., 2000a, Tectono-thermal evolution, magma emplacement, and shear zone development in the Caruaru area (Borborema Province, NE Brazil): Precambrian Research, v. 99, p. 1–32.

Neves, S.P., Mariano,G., Guimarães, I.P., SilvaFilho, A.F., Melo, S.C., 2000b, Intralithospheric differentiation and crustal growth: evidence from the Borborema province, northeas- tern Brazil: Geology, v. 28, p. 519–522.

Neves, S.P., 2003, Proterozoic history of the Borborema Province (NE Brazil): correlations with neighboring cratons and Pan-African belts, and implications for the evolution of western Gondwana: Tectonics, v. 22, p. 1031.

Neves, S.P., Mariano, G., 2004, Heat-producing elements-enriched continental mantle lithosphere and Proterozoic intracontinental orogens: insights from Brasiliano/PanAfrican Belts: Gondwana Research, v. 7 (2), p. 427–436.

Neves, S.P., Bruguier, O., Vauchez, A., Bosch, D., Silva, J.M.R., Mariano, G., 2006a, Timing of crust formation, deposition of supracrustal sequences, and Transamazonian and Brasi- liano metamorphism in the East Pernambuco belt (Borborema Province, NE Brazil): implications for western Gondwana assembly: Precambrian Research, v. 149, p. 197-216.

Neves, S.P., Mariano, G., Correia, P.B., Silva, J.M.R., 2006b, 70 m.y. of synorogenic plutonism in eastern Borborema Province (NE Brazil): temporal and kinematic constraints on the Brasiliano Orogeny: Geodinamica Acta, v. 19, p. 213-237.

Neves, S.P., 2011, Atlantica revisited: new data and thoughts on the formation and evolution of a long-lived continente: International Geologic Review, v. 53, p. 1377-1391.

Neves, S.P., 2015, Constraints from zircon geochronology on the tectonic evolution of the Borborema Province (NE Brazil): widespread intracontinental Neoproterozoic reworking of a Paleoproterozoic accreationary orogeny: Journal of South America Earth Sciences, v. 58, p. 150-164.

Neves, S.P., Lages, G.A., Brasilino, R.G., Miranda, A.W.A., 2015, Paleoproterozoic accretionary and collisional processes and the build-up of the Borborema Province (NE Brazil): Geochronological and geochemical evidence from the Central Domain: Journal of South America Earth Sciences, v. 58, p. 165-187.

Oliveira, D.C., Mohriak, W.U., 2003, Jaibaras trough: an important element in the early tectonic evolution of the Parnaíba interior sag basin, Northern Brazil: Marine and Petroleum Geology, v. 20, p. 351-383.

Oliveira, E.P., Windley, B.F., Araújo, D.B., 2010, The Neoproterozoic Sergipano orogenic belt, NE Brazil: a complete plate tectonic cycle in western Gondwana: Precambrian Research, v. 181, p. 64-84

Ordóñez-Casado, B., 1998, Geochronological studies of the Pre-Mesozoic basement of the Iberian Massif: The Ossa Morena Zone and the Allochthonous Complexes within the Central Iberian Zone [Ph. D. Thesis]: Geology, Swiss Federal Institute of Technology Zurich, ETH, p. 1-207.

Patiño Douce, A., 1997, Generation of metaluminous A-type granites by low pressure melting of calc-alkaline granitoids. Geology: v. 25, p. 743–746.

Pearce, J., Harris, N.B.W., Tindle, A.D., 1984, Trace element discrimination diagrams for the tectonic interpretation of granitic rocks: Journal of Petrology, v. 25, p. 956-983.

Pearce, J., 1996, Sources and setting of granitic rocks: Episodes, v. 19 (4), p. 120-125.

Pedrosa Jr., N.C., Vidotti, R.M., Fuck, R.A., Oliveira, K.M.L., Branco, R.M.G.C., 2015, Structural framework of the Jaibaras Rift, Brasil, based on geophysical data: Journal of South America Earth Sciences, v. 58, p. 318-334.

Pereira, M.F., Chichorro, M., Solá, A.R., Silva, J.B., Sanchez-García, T., Bellido, F., 2011, Tracing the Cadomian magmatism with detrital/inherited zircon ages by in-situ U–Pb SHRIMP geochronology (Ossa-Morena Zone, SW Iberian Massif): Lithos, v. 123, p. 204-217.

Pichavant, M., Kontak, D.J., Briqueu, L., Valencia Herrera, J., and Clark, A.H., 1988, The Miocene-Pliocene Macsani Volcanics, SE Peru II. Geochemistry and origin of a felsic peraluminous magma: Contributions to Mineralogy and Petrology, v. 100, p. 325–338.

Pietranik, A.B., Hawkesworth, C.J., Storey, C.D., Kemp, A.I.S., Sircombe, K.N., Whitehouse, M.J., Bleeker, W., 2008, Episodic, mafic crust formation from 4.5 to 2.8 Ga: new evidence from detrital zircons, Slave craton, Canada: Geology, v. 36 (11), p. 875-878.

Pistone, M., Blundy, J.D., Brooker, R.A., EIMF, 2015, Textural and chemical consequences of interactions between hydrous mafic and felsic magmas: an experimental study: Contribution to Mineralogy and Petrology, v. 171, p. 8.

Pitcher, W.S., 1993, The nature and origin of granite: Blackie Academ. Profess., 321 p.

Richard, P., Shimizu, N., Allegre, C.J., 1976, 143Nd/144Nd, a natural tracer: an application to oceanic basalts: Earth Planet Science Letters, v. 31, p. 269-278.

Sá, J.M., McReath, I., Leterrier, J., 1995, Petrology, geochemistry and tectonic setting of Proterozoic Igneous suites of the Orós fold belt (Borborema Province, Northeast Brazil): Journal of South American Earth Sciences, v. 8, p. 299-314.

Sa, J.M., Bertrand, J.M., Leterrier, J., Macedo, M.H.F., 2002, Geochemistry and geochronology of pre-Brasiliano rocks from the Transversal Zone, Borborema Province, Northeast Brazil: Journal of South America Earth Sciences, v. 14, p. 851-866.

Santos, E.J., 1995, O complexo granítico Lagoa das Pedras: Acresção e colisão na região de Floresta (Pernambuco) Província da Borborema [Doctor Thesis]: Universidade de Sao Paulo, 220 p.

Santos, E. J.; Medeiros, W.C., 1999, Constraints from granitic plutonism on Proterozoic crustal growth of the Transverse Zone, Borborema Province, NE Brazil: Revista Brasileira de Geociências, v. 29(1), p. 73-84.

Santos, T.J.S., Fetter, A.H., Hackspacher, P.C., Van Schmus, W.R., Nogueira Neto, J.A., 2008a, Neoproterozoic tectonic and magmatic episodes in the NW sector of Borborema Province, NE Brazil, during assembly of Western Gondwana: Journal of South American Earth Sciences, v. 25, p. 271–284.

Santos, T.J.S., Fetter, A.H., Nogueira Neto, J.A., 2008b, Comparisons between the northwestern Borborema Province, NE Brazil, and the southwestern Pharusian-Dahomey Belt, SW Central Africa: Geological Society of London Spececial Publications v. 294, p. 101-119.

Santos, L., Guimarães, I.P., Silva Filho, A.F., Farias, D.J.S., Lima, J.V., Antunes, J.V., 2014, Magmatismo Ediacarano extensional na Província Borborema, NE Brasil: Pluton Serra Branca: Comunicações Geológicas, v. 101, Especial I, p. 199-203.

Santos, L.C.M.L., Dantas, E.L., Santos, E.J., Santos, R.V., Lima, H.M., 2015, Early to late Paleoproterozoic magmatism in NE Brazil: the Alto Moxoto Terrane and its tectonic implications for the pre-Western Gondwana assembly: Journal of South America Earth Sciences, v. 58, p. 188-209.

Sial, A.N., 1986, Granite-types of Northeast Brazil: current knowledge. Revista Brasileira de Geociencias, v. 16, p. 54-72.

Sial, A.N., Ferreira, V.P., 1988, Brasiliano age peralkalic plutonic rocks of the Cen- tral Structural Domain, Northeast Brazil: RENDICONTI DELLA SOCJETA ITAUANA DJ MINERALOGIA E PETROLOGIA, v. 43, p. 307-342.

Sial, A.N., Ferreira, V.P., Santos, E.J., 1997, Magmatic Epidote-bearing Granitoids and Ultrapotassic Magmatism of the Borborema Province, NE Brazil, in Second International Symposium on Granites and Associated Mineralizations (ISGAM), Field Trip Guide, pp. 33e54. Salvador, Bahia, Brazil.

Sial, A.N., Vasconcelos, P.M., Ferreira, V.P., Pessoa, R.R., Brasilino, R.G., Morais Neto, J.M., 2008, Geochronological and mineralogical constraints on depth of emplacement and ascension rates of epidote-bearing magmas from northeastern Brazil: Lithos, v. 105, p. 225-238.

Sial, A.N., Ferreira, V.P., 2015, Magma associations in ediacaran granitoids of the Cachoeirinha-Salgueiro and Alto Pajeú terranes, northeastern Brazil: Forty years of studies:Journal of South America Earth Sciences,Special Issue: Granite Magmatism in Brazil, v. 68, p. 113-133.

Silva Filho, A.F., Guimaraes, I.P., Thompson, R.N., 1993, Shoshonitic and ultrapotassic Proterozoic suites in the Cachoeirinha –Salgueiro fold Belt, NE Brazil: a transition from collisional to post-collisional magmatism, Precambrian Research., v. 62, p. 323–342.

Silva Filho, A.F., Guimarães, I.P., Ferreira, V.P., Armstrong, R.A., Sial, A.N., 2010, Ediacaran Aguas Belas pluton, Northeastern Brazil: evidence on age, emplacement and magma sources during Gondwana amalgamation. Gondwana Research, v. 17, p. 676-687.

Silva Filho, A.F., Guimarães, I.P., Santos, L., Armstrong, R., Van Schmus, W.R., 2016, Geochemistry, U-Pb geochronology, Sm-Nd and O isotopes of ca. 50my long Ediacaran High-K Syn-Collisional magmatism in the Pernambuco-Alagoas Domain, Borborema Province, NE Brazil: Journal of South America Earth Sciences, v. 68, p. 134-154.

Silva, T.R., Ferreia, V.P., Lima, M.M.C., Sial, A.N., 2016, Two-stage mantle derived granitic rocks and the onset of the Brasiliano orogeny: Evidence from Sr, Nd, and O isotopes: Lithos, v. 264, p. 189-200.

Skjerlie, K.P., Johnston, A.D., 1993, Fluid-absent melting behavior of an F-rich tonalitic gneiss at mid-crustal pressures: Implications for the generation of anorogenic granites: Journal of Petrology, v. 34, p. 785-815.

Soderlund, U., Patchett, J.P., Vervoort, J.D., Isachsen, C.E., 2004, The 176Lu decay constant determined by Lu-Hf and U-Pb isotope systematics of Precambrian mafic intrusions: Earth Planet: Science Letters, v. 219, p. 311-324.

Souza, Z.S., Martin, H., Peucat, J.J., Jardim de Sa, E.F., Macedo, M.H.F., 2007, Calc-alkaline magmatism at the Archean-Proterozoic Transition: the Caico complex basement (NE Brazil): Journal of Petrology, v. 48, p. 2149-2185.

Tagne-Kamga, G., 2003, Petrogenesis of the Neoproterozoic Ngondo Plutonic complex (Cameroon, west central Africa): a case of late-collisional ferro-potassic magmatism. Journal of African Earth Sciences, v. 36, p. 149-171.

Thompson, R.N., 1982, Magmatism of the british tertiary volcanic province. Scottish Journal of Geology, v. 18, p. 50-107.

Toteu, S.F., Van Schmus, W.R., Penaye, J., Michard, A., 2001, New U–Pb and Sm–Nd data from north-central Cameroon and its bearing on pre-Pan African history of central Africa: Precambrian Research, v. 108, p. 45–73.

Van Schmus, W.R., Brito Neves, B.B., Hackspacher, P.C., Babinski, M., 1995, U/Pb and Sm/Nd geochronologic studies of Eastern Borborema Province, northeastern Brazil: initial conclusions: Journal of South America Earth Sciences, v. 8, p. 267-288.

Van Schmus, W.R., Oliveira, E.P., Silva Filho, A.F., Toteu, S.F., Penaye, J., Guimaraes, I.P., 2008, Proterozoic links between the Borborema province, NE Brazil, and the central African fold belt: Geological Society of London, Special Publication, v. 294, p. 69-99.

Van Schmus, W.R., Kozuch, M., Brito Neves, B.B., 2011, Precambrian history of the Zona transversal of the Borborema province, NE Brazil: insights from Sm/Nd and U/Pb geochronology, Journal of South America Earth Sciences, v. 31, p. 227-252.

Vauchez, A., Neves, S.P., Caby, R., Corsini, M., Egydio-Silva, M., Arthaud, M.H., Amaro, V., 1995, The Borborema shear zone system, NE Brazil: Journal of South America Earth Sciences, v. 8, p. 247–266.

Vervoort, J.D., Kemp, A.I.S., 2016, Clarifying the zircon Hf isotope record of crust-mantle evolution, Chemical Geology, v. 425, p. 65-75.

Visona, D., and Lombardo, B., 2002, Two-mica and tourmaline leucogranites from the Everest-Makalu region (Nepal-Tibet). Himalayan leucogranite genesis by isobaric heating: Lithos, v. 62, p. 125–150.

Watson, E.B., Harrison, T.M., 1983, Zircon saturation revisited: temperature and composition effects in a variety of crustal magma types: Earth Planet Science Letters, v. 64, p. 295-304.

Whalen, J.B., Currie, K.L., Chappell, B.W., 1987, A-types granites: geochemical charac- teristics, discrimination and petrogenesis: Contributions Mineralogy Petrology, v. 95, p. 407-419.

Wones, D.R., 1981, Mafic silicates as indicators of intensive variables in granitic magmas: Mining Geology, v. 31, p. 191-212.

Wones, D.R., 1989, Significance of the assemblage titanite+magnetite+quartz in Granitic rocks: American Mineralogist, v. 74, p. 744-749.

5 AIRBORNE GAMMA-RAY CHARACTERIZATION OF THE FERROAN MAGMATISM IN THE TRANSVERSAL SUBPROVINCE OF THE BORBOREMA PROVINCE, NE BRAZIL

Airborne gamma-ray characterization of the Ferroan magmatism in the Transver- sal Subprovince of the Borborema Province, NE Brazil

José Victor Antunes de Amorim[a]*, Vanessa Biondo Ribeiro[b],[1], Ignez de Pinho Guimarães[a], Douglas José Silva Farias[a], Jefferson Valdemiro de Lima[a].

[a] Programa de Pós-Graduação em Geociências, Universidade Federal de Pernambuco, Recife, Brasil; bDepartamento de Geologia, Universidade Federal de Pernambuco, Recife, Brasil.

Av. da Arquitetura, s/n, sala 325, Centro de Tecnologia de Geociências, Departamento de Geologia, Cidade Universitária, 50740-550, Recife-PE, Brasil; e-mail: ; ORCID: https://orcid.org/0000-0002-1688-2218; telephone:*

Ignez de Pinho Guimarães, former full Professor at Universidade Federal de Pernambuco, researcher at CNPq (Brazilian Research Council), e-mail: , Author ID (Scopus): 6603752311, address: Av. da Arquitetura, s/n, sala 520, Centro de Tecnologia de Geociências, Departamento de Geologia, Cidade Universitária, 50740-550, Recife-PE, Brasil ;. Douglas José da Silva Farias, Ph.D. student at the Programa de Pós-Graduação em Geociências, Universidade Federal de Pernambuco, e-mail: , ORCID: https://orcid.org/0000-0003-45 05-9623, address: Av. da Arquitetura, s/n, sala 325, Centro de Tecnologia de Geociências, Departamento de Geologia, Cidade Universitária, 50740-550, Recife-PE, Brasil; Jefferson Valdemiro de Lima, Ph.D. student at the Programa de Pós-Graduação em Geociências, e-mail: , ORCID: https://orcid.org/0000-0002-7843-7312, ; Vanessa Biondo Ribeiro, researcher at CSIRO (Commmonwealth Scientific and Industrial Research Organisation), e-mail: , ORCID: https://orcid.org/0000-0002-4573-6893, address: 26 Dick Perry Ave, Kensington WA 6152, Australia.

Abreviated title: Gamma-ray characterization of ferroan magmatism

Abstract

Ferroan granites have higher Fe-number than cordilleran granitoids, often emplaced in extensional settings, and are LILE and HFSE enriched. Ferroan granites (585 – 530 Ma) have been described in the Transversal subprovince of the Borborema Province (BP). They comprise

two groups: G1 - slightly peraluminous to metaluminous, alkali-calcic rocks (Aroeiras Complex and Serra Branca – Coxixola dike swarms); G2 metaluminous to slightly peraluminous, alkalic to alkali-calcic rocks, (Queimadas and Prata intrusions). G1 marks the transition from collision to transcurrence (ca. 585 Ma), or from transcurrence to uplift and transtension (ca. 545 Ma). G2 represents the granitoids intruded during extensional tectonics in transcurrent setting (ca. 550 Ma), or coeval with deposition of transtensional intracratonic basins (ca. 530 Ma). These granitoids pre-date mineralized pegmatites and skarns of NE Brazil. The LILE and HFSE enriched nature of these granitoids, as expected, is recognizable in gamma spectrometric maps of regional scale, highest values of K(%), eTh (ppm) and eU (ppm) contrasts significantly with country rocks and magnesian granites. Some of the ferroan granitoids are associated with coeval diorites and gabbros, comprising heterogeneous rock associations. In gamma spectrometric maps it is possible to identify these heterogeneities and link to geological processes (mingling, shear zone deformation), geochemistry, as well as, petrography. Diorites and gabbros show low to medium values of K (1 – 3%), eTh (5 – 20ppm) and eU (0.2 – 2ppm), contrasting with the high values of regions with dominance of ferroan granitoids (K, 3 – 6%; eTh, 15 – 60ppm; eU, 2 – 4ppm).

Keywords: granitoids; ferroan; gamma spectrometry; Borborema province; geochemistry

5.1 INTRODUCTION

Ferroan (A-type) granites have higher FeOt/ FeOt+MgO ratios than cordilleran granites and are rich in incompatible trace elements, as large-ion lithophile elements (LILE) and high field strength elements (HFSE), but low in compatible trace elements in mafic silicates and feldspars (Loiselle and Wones, 1979; Whalen et al., 1987; Eby, 1992; Bonin, 2007; Frost and Frost, 2011). In this regard, gammaspectrometry is an important tool for the identification of these intrusions, since it uses natural decay of U and Th (both HSFE) and K (LILE) elements as parameters for differentiation of geological lithotypes.

In the Transversal subprovince of Borborema Province ferroan suites mark major shifts of tectonic regime, latest stages of the Brasiliano (Pan-African) orogeny (Guimarães et al., 2004, 2005), pre-date and occasionally occur close to mineralized granitic pegmatites and skarns (Baumgartner et al., 2006; Hollanda et al., 2017). They also exhibit distinct geochemical patterns and intrude in different geochronological intervals. For instance, Aroeiras Complex (Figure 1b) is the earliest intrusion (ca. 585 Ma) and marks the transition between the contractional and transcurrent event. Queimadas Pluton (Figure 1b) is related to post-collisional

and heterogeneous crustal thinning during the strike-slip event, was dated ca. 550 Ma. The Serra Branca – Coxixola dike swarms (Figure 1b) mark the transition from strike-slip tectonics to uplift and transtension, around 545 Ma. The Prata Complex (Figure 1b) is the youngest intrusion (ca. 530 Ma), coeval with deposition of intracratonic sedimentary basins in a transtensional setting (Amorim et al., in preparation).

Magmatic differentiation, tectonic environment and geochemical events (e.g. hydrothermal fluids action, chemical erosion and metamorphism) can affect radioelements concentration observed for a specific intrusion through the dissolution of the radioelements increasing their mobility, replacement of the elements in the rock matrix as observed in apatite where U can substitute Ca or be responsible for the radioelements removal from the system. Therefore, the difference observed in these suites geochemical pattern and their geological history has a direct influence over their gammaspectrometry signature.

In fact, several authors have been using radioelements ratios to characterize granites suites around the world. Pagel (1982) describes ranges of 0.5% of UO2 in the cores of the granites of the Vosges, in France, with a marked enrichment in the borders (up to 3.5% of UO2). Johan and Johan (1994) studied granites intrusions in Cinovec (Zinnwald), Czech Republic. In these granites, the zircon shows a magmatic zonation in both the hydrothermal dome and main granite body, and high content of H2O (up to 18.5% in weight) and F (up to 2.41%) partly replaced by monazite and xenotime. In general, hydration and fluoridation encourage the ingress of rare earth elements (REE), U and Th in zircons by substitution reaction (ETR, Y, Sc)3++ P5+ Zr4+ + Si4+ (Johan and Johan, 2005). According to Johan and Johan (2005), the monazites in granites rich in Li have a positive correlation between Th content and Ca+Si, suggesting two types of substitution: Th4+ + Si4+ (ETR)3+ + P5+ and Ca2+ + Th4+ (ETR)3+. Allanite appears in several types of granites, especially in metaluminous and peralkaline, either as primary mineral with higher levels of ThO2 (0.5-3%) than UO2 (0.3%), or as secondary mineral (Pagel 1982, Bea 1996).

Uranium becomes soluble in supergene conditions, unlike thorium which has the lowest geochemical mobility of the three elements. This phenomenon is known as the antagonism between thorium and potassium described by Ostrovsky (1975). This geochemical behavior can be used not only to characterize differentiated granites intrusions (Ulbrich et al., 2009, Ribeiro et al., 2013) but also to identify possible new targets for exploration associated with hydrothermal process (Ribeiro and Mantovani, 2016). In this paper we focus on the study of the four distinct ferroan intrusions of the Transversal subprovince and identify their common

gammaspectrometric features and differences. The better knowledge of their radiometric signature and its correlation with the geotectonic events recognized for the Borborema Province will significantly contribute to the comprehension of the ferroan granites and their role in the Borborema Province geological evolution.

5.2 REGIONAL GEOLOGY

The Borborema Province (Figure 1a) (Almeida et al., 1981) represents an orogenic belt with complex tectonic history started in the Archean until late Neoproterozoic, culminating with the assembly of western Gondwana, due to collision of major cratonic landmasses (São Franciso-Congo and São Luís-West Africa Cratons) along the Cryogenian-Ediacaran period, namely Brasiliano-Pan-African Orogeny (Van Schmus et al., 2008, references therein).

Figura 17 - Fig. 1. a) Sketch map of the Brasiliano intrusions in the Borborema Province. Abbreviations: PaSZ - Patos Shear Zone, PeSZ - Pernambuco Shear Zone; Ferroan intrusions: 6- Mucambo and Meruoca Plutons (Santos et al., 2008; Archanjo et al., 2009), 7- Acari Pluton (Archanjo et al., 2013; Nascimento et al., 2015), 8- Solânea and Dona Inês Plutons (Guimarães et al., 2009), and Riachão Mafic rocks (Guimarães et al., 2017), 9-Águas belas Pluton (Silva Filho et al., 2010), 10- Pilõezinhos Pluton (Lima et al., 2017); b) Studied Intrusions and associated shear zones of the Transversal subprovince. Abbreviations: AFSZ - Afogados da Ingazeira Shear Zone, TCSZ - Coxixola Shear Zone, CGSZ - Campina Grande Shear Zone, CSZ - Cabaceiras Shear Zone, PJSZ - Prata Shear Zone, BSZ - Batista Shear Zone, GBSZ - Gado Bravo Shear Zone. Ferroan intrusions: 1- Aroeiras Complex (this paper); 2- Queimadas Pluton (Almeida et al., 2002, this paper); 3- Prata Complex (Melo, 1997; Guimarães et al. 2005; Hollanda et al. 2010; this paper), 4- Bravo Pluton (Lages et al. 2016); 5- Serra Branca Pluton (Santos et al., 2014).

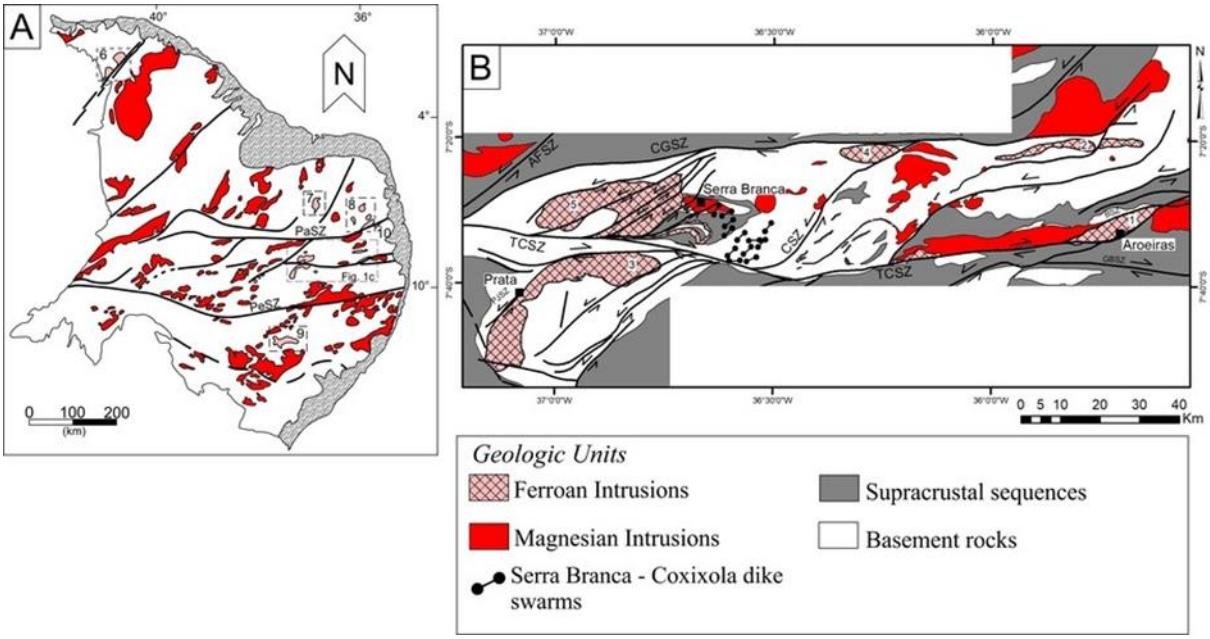

It has three subprovinces individualized by a branching system of strike-slip shear zones, subdivided into seven domains (Van Schmus et al., 1995, 2008, 2011) and in pre-drift reconstructions lies adjacent to the Pan-African fold Belts (Figure 2) (De Wit et al., 1988; Brito Neves et al., 2000; Toteu et al., 2001) (Figure 2): 1) the Northern subprovince lies north of the Patos shear zone and comprises the Médio Coreaú, Ceará Central and Rio Grande do Norte

domains; 2) the Central Subprovince or Transversal subprovince (Figure 1a) occurs between the Pernambuco and Patos shear zone; 3) the Southern subprovince stands between the Pernambuco shear zone and the São Francisco craton, and contains the Riacho do Pontal, Sergipano and Pernambuco-Alagoas domains.

The Transversal subprovince geological units can be grouped into: 1) basement rocks mostly Paleoproterozoic (2.5 – 2.0 Ga) orthogneisses with TTG affinities, although Archean rocks have been reported recently (Santos, 1995; Van Schmus et al., 1995, 2008, 2011; Neves et al., 2006, 2015; Santos et al., 2015, 2017); 2) Mesoproterozoic (ca. 1.5 Ga) anorogenic orthogneisses and anorthosites (Sá et al, 2002; Accioly et al., 2000); 3) Tonian orthogneisses and supracrustal sequences of the Cariris Velhos event (Jardim de Sá et al., 1988; Brito Neves et al., 1995, 2001; Santos, 1995; Kozuch, 2003; Guimarães et al., 2012, 2016); 4) Cryogenian to Ediacaran supracrustal sequences deposited prior to the main collisional event (Neves et al., 2006; Neves, 2015); 3) all of these intruded by brasiliano plutons (Figure 1b) (Almeida et al., 1967; Sial, 1986; Brito Neves et al., 2003; Guimarães et al., 2004) and cut by strike-slip E-W trending dextral sense and NE-SW trending sinistral sense shear zones (Vauchez et al., 1995; Neves et al., 1996, 2000).

Ediacaran - Cambrian granitogenesis in the Transversal subprovince has been extensively studied. First studies by Almeida et al. (1967) recognized four petrographic types of granites: 1) Conceição-type comprises medium to fine grained tonalites and granodiorites; 2) Itaporanga-type, granodiorites with large K-feldspar crystals; 3) Itapetim-type, fine grained biotite granites related to the Itaporanga-type; 4) Catingueira-type peralkaline granites, syenites and quartz syenites.

Sial (1986), using geochemical data, characterized the granitoids from the Cachoeirinha- Salgueiro Fold Belt, and correlated with the petrographic types of Almeida et al. (1967): 1) Calc- alkalic (Conceição-type); 2) High-K Calc-alkalic (Itaporanga-type); 3) Peralkalic, ultrapotassic and shoshonitic (Catingueira-type); 4) Trondhjemitic (Serrita-type).

Brito Neves et al. (2003) divided the brasiliano granitoids into three super suites: 1) ca. 650 – 625 Ma granitoids derived from hybrid and crustal sources (calc-alkaline, high-K calc-alkaline, trondhjemitic and peraluminous and peralkaline suites) intruded at the start of contractional event including minor intrusions related to lateral extension; 2) ca. 580 – 570 Ma derived from enriched mantle (high-K calc-alkaline, shoshonitic, alkaline and ultrapotassic suites) comprising syn to late-kinematic plutons akin to the strike-slip events; 3) ca. 545 – 520

Ma hybrid suites, small granitic intrusions and dike swarms connected to the post-collisional phases.

Figura 18 - Fig 2. Sketch map of a part of west Gondwana in pre-drift reconstructions modified from Van Schmus et al., (2008) (Legend: Br/PA, Brasiliano/Pan-African belts; PaleoPr, Paleoproterozoic crust. Subprovinces and domains: NSP, North subprovince; TSP, Transversal subprovince; SSP, South subprovince; PEAL, Pernambuco-Alagoas domain; SD, Sergipano domain; MK, Mayo Kebi terrane; NWCD, NW Cameroon domain; AYD, Adamawa-Yadé domain; YD, Yaoundé domain; OU, Oubanguides fold belt. Shear zones and faults: PaSZ, Patos shear zone; PeSZ, Pernambuco shear zone; TBL, Transbrasiliano Lineament; TBF, Tcholliré-Banyo fault; AF, Adamawa Fault. Cities: N, Natal; R, Recife; S, Salvador; D, Douala; G, Garoua; K, Kaduna area of Nigeria)

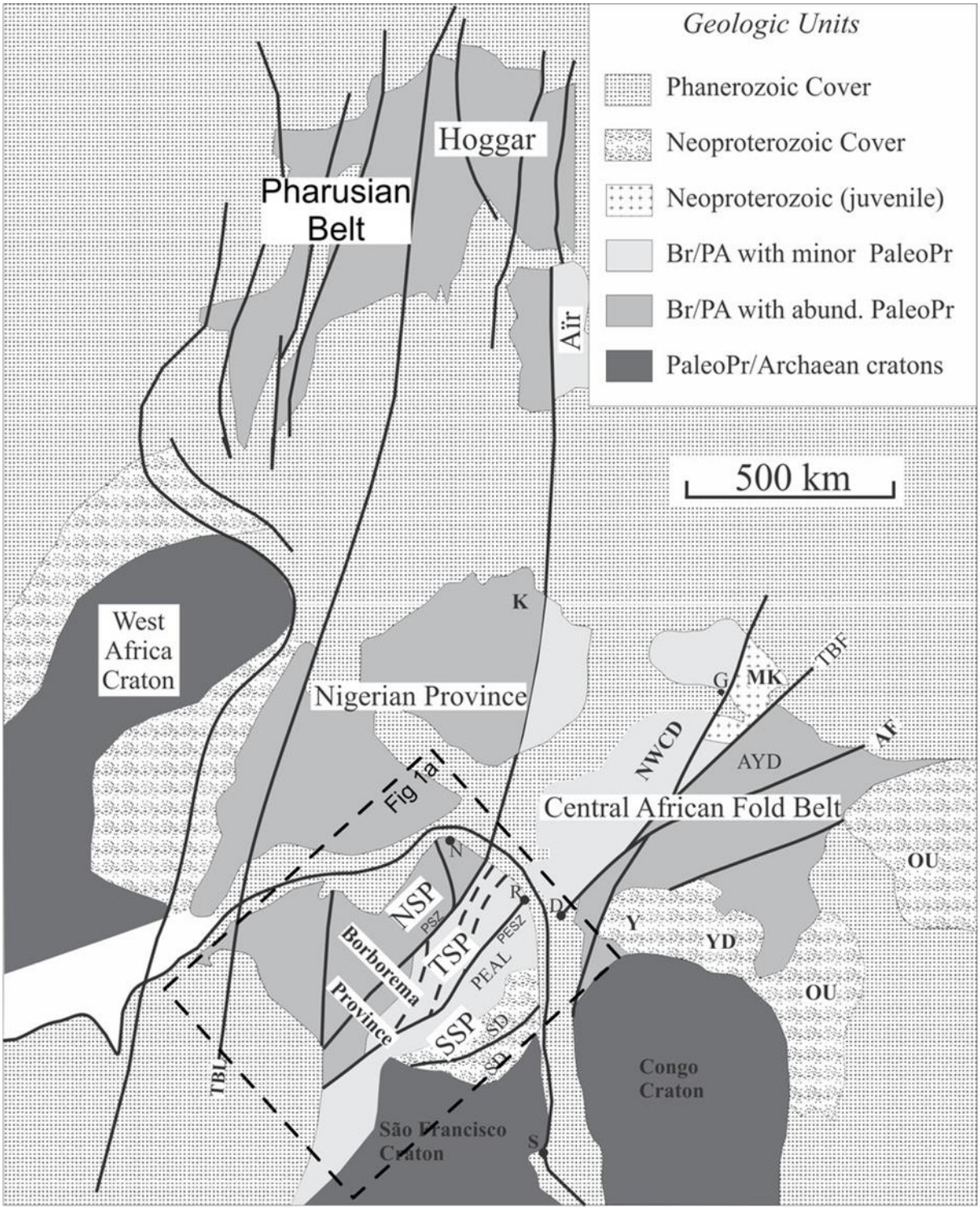

Guimarães et al. (2004) identified four groups: 1) 640 – 600 Ma medium to high-K calc-alkaline granitoids intruded throughout the peak of metamorphism and development of the flat-lying foliation; 2) 590 – 581 Ma high-K calc-alkaline and shoshonitic granitoids marking the transition between the flat-lying event and the transcurrent event; 3) ca. 570 Ma alkaline post-collision granites generated by partial melting of granodioritic lower crust marking the final stage of the Brasiliano – Pan-African orogeny and the beginning of the uplift, synchronous with the ultrapotassic intrusions in the Cachoeirinha-Salgueiro Belt and the Teixeira High; 4) ca. 540 – 510 Ma A-type post-orogenic extension-related associated with subvolcanic bimodal magmatism, coeval with the deposition of small basins from the North and Transversal subprovince. Ferroan intrusions have been identified coeval with the last three groups of Guimarães et al. (2004).

5.3 GEOLOGICAL SETTING OF THE STUDIED FERROAN INTRUSIONS

5.3.1 Aroeiras Complex

The Aroeiras Complex (Figure 1b) intruded into an older Ediacaran pluton (Serra do Inácio Pereira), Cryogenian supracrustal sequences of the Surubim Complex, and Rhyacian orthogneisses and migmatites. Its bimodal character, typical of extensional environments, is proffered by granitic dikes and sheets associated small dioritic bodies. The main granitic pluton intrudes ENE-WSW trending, emplaced during synchronous movements of E-W trending dextral Coxixola shear zone and NE-SW trending sinistral Batista shear zone.

It encompasses equigranular and/or porphyritic hornblende-biotite-monzogranite and biotite-sienogranite. Accessory phases are prismatic crystals of allanite and zircon, acicular apatite, texture typical of interaction between magmas with contrasting temperatures, and ilmenite crystals mantled by sphene, related to deformational processes in solid state. Microgranular mafic enclaves (MME) are hornblende-biotite diorites or quartz diorites usually found near to Aroeiras city. Droplets of ovoid MME with crenulated borders, double enclave relations, granitic venules, and hybrid rocks with rapakivi texture are indicative of mingling and mixing processes that acted throughout the evolution of the pluton.

5.3.2 Queimadas Pluton

Queimadas Pluton (Figure 1b) intruded Rhyacian gneisses and holds an E-W elongated 50km² body, showing S-C dextral foliation with C foliation plan parallel to the E-W trending branch of the Campina Grande Shear Zone. A late transcurrent dextral shear zone 60Az trending disrupts the body in a mega-boudin-like shape (Almeida et al., 2002).

Petrographically, it comprises leucocratic (less than 10% of mafic phases) porphyritic biotite-amphibole granodiorites to monzogranites. Accessory phases are euhedral crystals of allanite, apatite, prismatic or rounded crystals of zircon, subhedral crystals of ilmenite hosted by biotite or amphibole, and rare monazite crystals. Quartz-monzonitic and quartz-dioritic bodies occur close to the contact with country rocks, and microgranular mafic enclaves are locally observed in the porphyritic monzogranites and granodiorites (Almeida et al., 2002).

Almeida et al. (2002) suggest that the pluton was deformed under brittle-ductile conditions of the transcurrent event during the Brasiliano (Pan-African) orogeny. Textural aspects of ductile deformation are represented by quartz ribbons and mosaic texture, kinks of biotite, disrupted sigmoidal porphyroclasts of plagioclase with patchy extinction, while necking, disruption and boudin-like shape of the Queimadas Pluton are result of the brittle system.

5.3.3 Serra Branca – Coxixola dike swarms

The Serra Branca – Coxixola dike swarm (SBCDS) (Figure 1b) intruded Paleoproterozoic orthogneisses, Neoproterozoic supracrustal sequences and magnesian alkali-calcic Ediacaran plutons of the Transversal Subprovince. The main population of dikes trends NE-SW and cross-cuts the flat-lying foliation of supracrustal sequences and basement rocks. Closer to the dextral E-W trending Coxixola Shear Zone, dikes intruded concordant with the steeply-dipping mylonitic foliation, but evidences of deformational processes were nearly absent.

Dike sets mineral assemblage is monotonous and comprise porphyritic hornblende-biotite granite and equigranular biotite granite. Accessory phases are more abundant in hornblende- biotite granites, and comprise prismatic crystals of zircon, allanite and subhedral crystals of ilmenite.

5.3.4 Prata Complex

The Prata Complex (Figure 1b) intruded Siderian to Rhyacian orthogneisses and migmatites. It contains several granitic intrusions, as dikes and elongated stocks (Melo, 1997; Guimarães et al., 2005; Hollanda et al., 2010). Swarms of MME occur near the eastern boundary of the Complex and follow the NNE and E-W trend of basalt dikes. Solid state deformation is rare and restricted to the western boundary of the Prata Complex, where it is in contact with the Prata Shear Zone.

Petrographically, biotite syenogranite and hornblende-biotite monzogranites are the main facies, but the complex comprises intermediate to mafic rocks, such as monzodioritic to

quartz monzonitic, as well as, dioritic and noritic rocks. Enclave swarms of norite separates the Prata complex into two main granitic plutons (Guimarães et al., 2005). The southern body, Santa Catarina Pluton, comprises biotite syenogranites, and the Sumé Pluton, crops out to the north, and comprises hornblende-biotite monzogranites (Hollanda et al., 2010). The main accessory phases are allanite rimmed by epidote, sphene, apatite and zircon. Several MME and syn-plutonic dikes are observed in the SE limit of the Sumé Pluton, displaying crenulated contacts and ovoid feldspar crystals mantled by plagioclase (rapakivi texture). Such characteristics are indicative of mingling and mixing processes between granitic and dioritic magmas (Mello, 1997; Guimarães et al., 2005).

5.4 ANALYTICAL METHODS

5.4.1 Whole-rock geochemistry

Major elements analysis of 18 granitic samples from the Aroeiras Pluton and the Serra Branca – Coxixola dike swarm were obtained by LiBO2 fusion ICP-AES (Inductively Coupled Plasma Emission Spectrometry) and trace elements concentrations by LiBO2 fusion ICP-MA (Inductively Coupled Plasma Mass Spectrometry) at Acme Laboratories Canada. Representative analyses are shown in table 1.

Whole-rock compositions of the Queimadas Pluton and Prata Complex included in this work have been collected from the literature, but trace element data has been recalculated to reasonable comparison (Almeida et al., 2002; Mello, 1997; Guimarães et al., 2005).

5.4.2 Geophysical Data

Airborne gamma-ray data were acquired from two projects of the CPRM (Brazilian Geological Survey). Acquisition parameters were nearly the same for both surveys and are shown in table 2. Gamma-ray spectrometer used were the EXPLORANIUM model GR-820 and Radiation Solutions Inc. model RS-500.

Tabela 3 – Table 2. Technical specifications of each airborne survey (CPRM, 2008, 2010).

Project	Borda Leste do Planalto da Borborema	Pernambuco-Paraíba
Year	2007-2008	2009
Flight line spacing	500 m	500 m
Flight nominal height	100 m	100 m
Flight line direction	N-S	N-S
Control line direction	E-W	E-W
Control line spacing	10 km	10 km
Sampling time	1.0 s	1.0 s

Gamma spectrometric data was collected considering, simultaneously, four energetic intervals. Since 238U and 232Th do not emit gamma radiation, the products of their decay are used for gamma-ray quantification: 214Bi and 208Tl, respectively. The energy windows for each element were: 40K (1.37 – 1.57 MeV), eTh (1.66 – 1.86 MeV), eU (2.41 – 2.81 MeV) and total count (0.41 – 2.81 MeV). Gamma spectrometric data processing was done by the Brazilian Geological survey and respected recommendations of IAEA (1991). Available data were already corrected for Compton effect, flight effective height, cosmic background removal from the airplane, atmospheric Radon and altimetric correction. Parallax effect was not identified therefore such correction was not necessary.

5.5 GEOCHEMISTRY OF THE FERROAN INTRUSIONS

Rocks are ferroan, Fe* (FeOtFeOt+MgO) > 0.81; metaluminous to peraluminous, alumina saturation index (ASI) ranging from 0.93 to 1.06; displaying alkali-calcic to slightly alkalic character, modified alkali-lime index (MALI) between 4.86 and 8.8. Dioritic rocks of the Aroeiras Complex are ferroan Fe* > 0.81; metaluminous, ASI values between 0.79 – 0.87; and alkalic with MALI ranging from 1.08 to 2.94 (Figure 3).

Figura 19 - Fig. 3. Granitoids chemical classification after Frost et al. (2001). a) Studied suites in the FeOtot/(FeOtot+MgO) versus silica diagram; b) Studied suites in the Alumina Saturation index

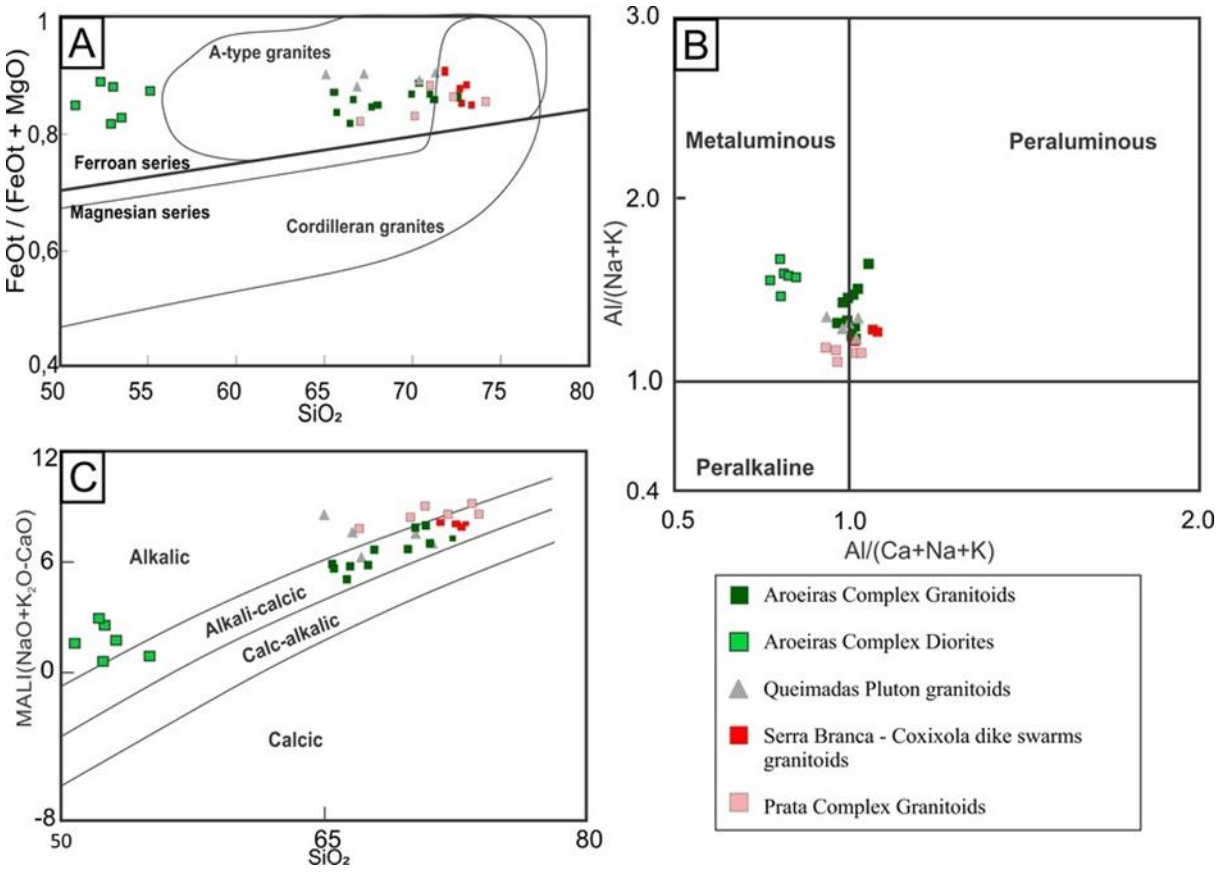

The chondrite normalized REE patterns (Figure 4) (Nakamura, 1974) of the Aroeiras Complex granites are fractionated, with (Ce/Yb)N ratios ranging from 8.15 to 21.15, and exhibit negative Eu anomalies (Eu/Eu* = 0.45 to 0.68). The granitoids of the Queimadas Pluton display negative Eu anomalies and (Ce/Yb)N ratios from 10.14 to 17.47. The Serra Branca – Coxixola samples exhibit significant negative Eu anomalies (Eu/Eu*= 0.23 to 0.34) and (Ce/Yb)N ratios ranging from 30.58 to 104.39. The REE patterns of granitoids from the Prata Complex rocks are fractionated, with (Ce/Yb)N ratios between 6.8 and 19.76 and characterized by negative Eu anomalies (Eu/Eu* = 0.21 – 0.65).

Figura 20 - Fig 4. Chondrite-normalized REE patterns (Nakamura, 1974) of the ferroan suítes.

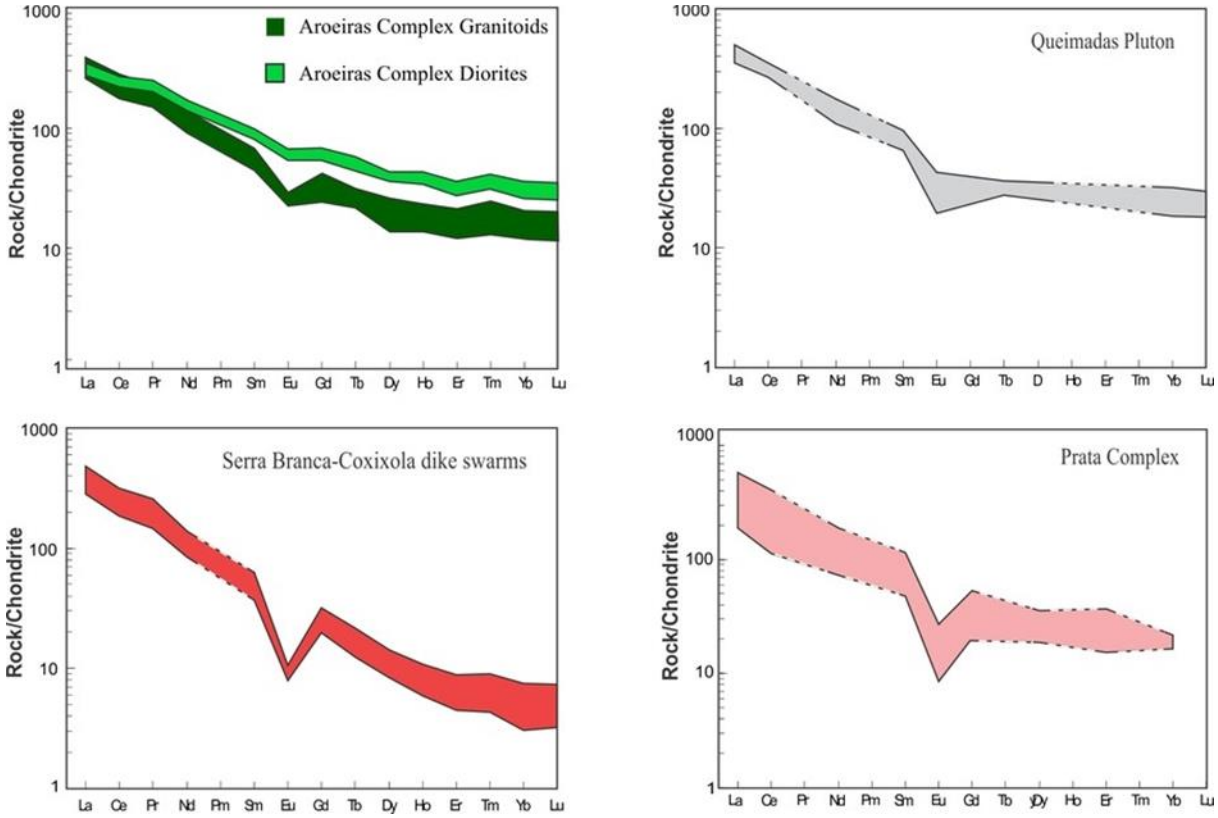

The incompatible element patterns (Figure 5) of the studied granitoids normalized to the values suggested by McDonough and Sun (1989) display many affinities: peaks in Th and U, variable troughs at Nb and Ta; deep troughs at Sr, P and Ti; and Ba troughs (except in the Aroeiras granitoids). Aroeiras Complex diorites exhibit peaks in Ba, lowest contents of K, and small troughs in Th, U, Sr and Ti.

Figura 21 - Fig. 5. Trace elements abundance diagrams normalized to the values proposed by Sun and McDonough (1989).

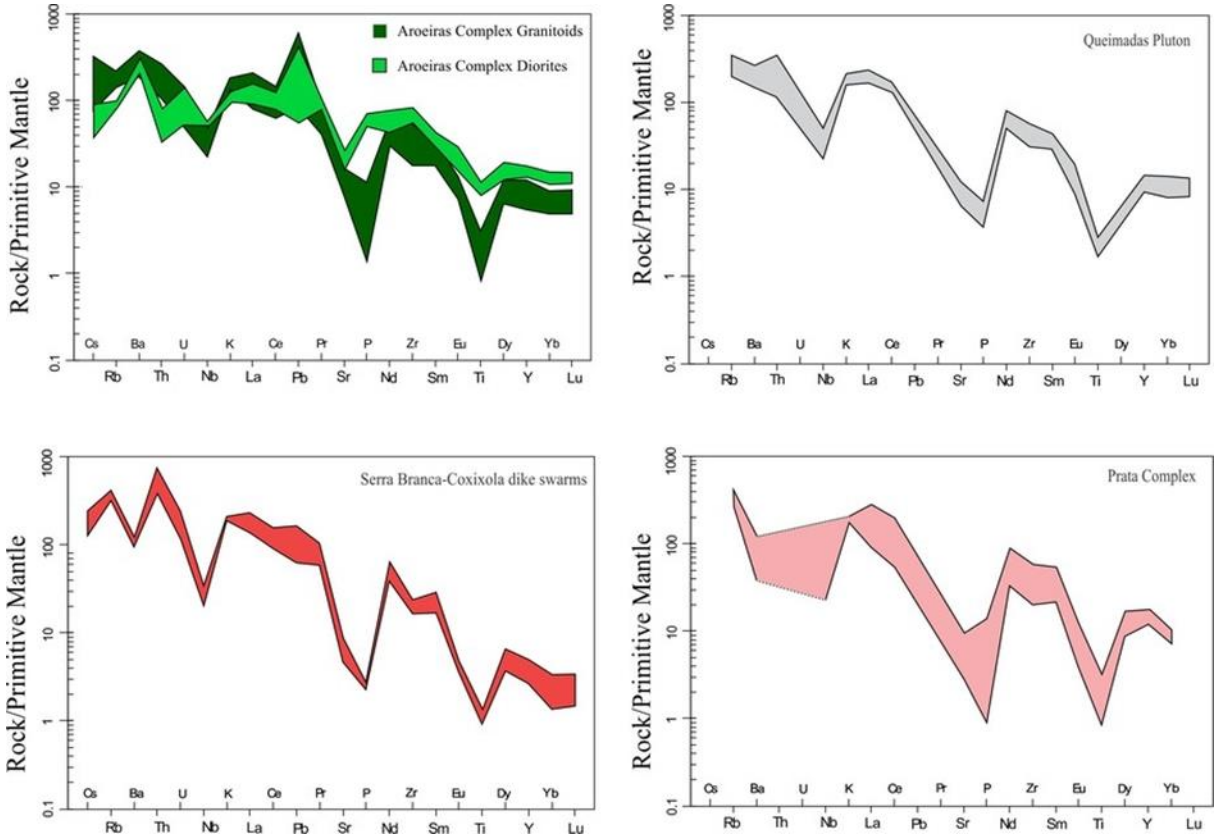

The studied granitoids have high HSFE content (Zr+Nb+Ce+Y > 350ppm), and plot on the A-Type granites field of Whalen et al. (1987) (Figure 6a). In the trace-element discrimination diagrams (Pearce et al., 1984), most of the studied samples plot on the within-plate field (Figure 6b) and post-orogenic granites (Y+Nb > 50ppm).

Figura 22 - Fig. 6. Studied granitoids plot in tectonic discriminant diagrams. a) FeO/MgO versus Zr+Nb+Ce+Y, fieldsafter Whalen et al. (1987); b) Nb versus Y, fields Pearce et al. (1984).

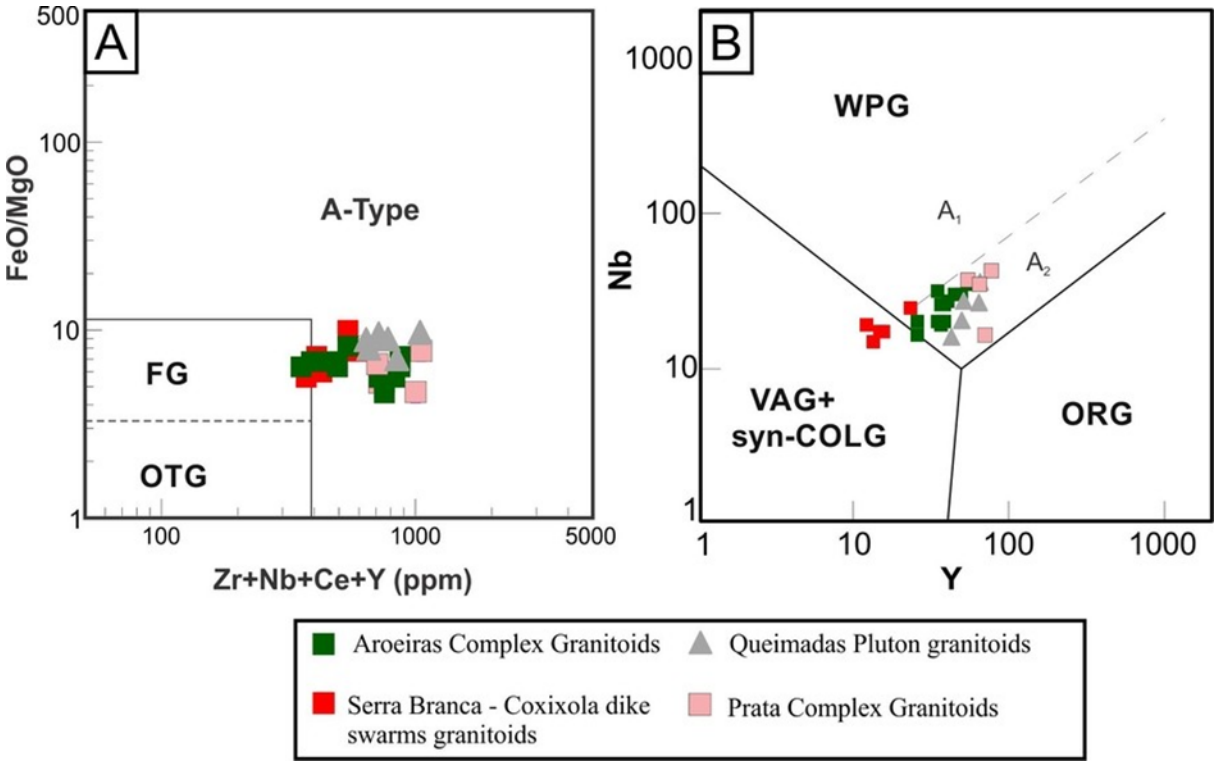

5.6 GAMMAESPECTROMETRIC ATTRIBUTES OF THE FERROAN INTRUSIONS

On a regional scale it is possible to identify the main ferroan intrusions already described in the Transversal subprovince (Figure 7). Regions mapped as ferroan intrusions exhibit in the ternary image higher abundances of radioelements compared to the country rocks, or other granitic intrusions, due to greater amounts of LILE and HFSE.

Figura 23 – Fig. 7. Gamma-ray spectrometric map from a section of the Transversal subprovince with the studied granitoids and other Ferroan intrusions (RGB ternary image). TCSZ - Coxixola

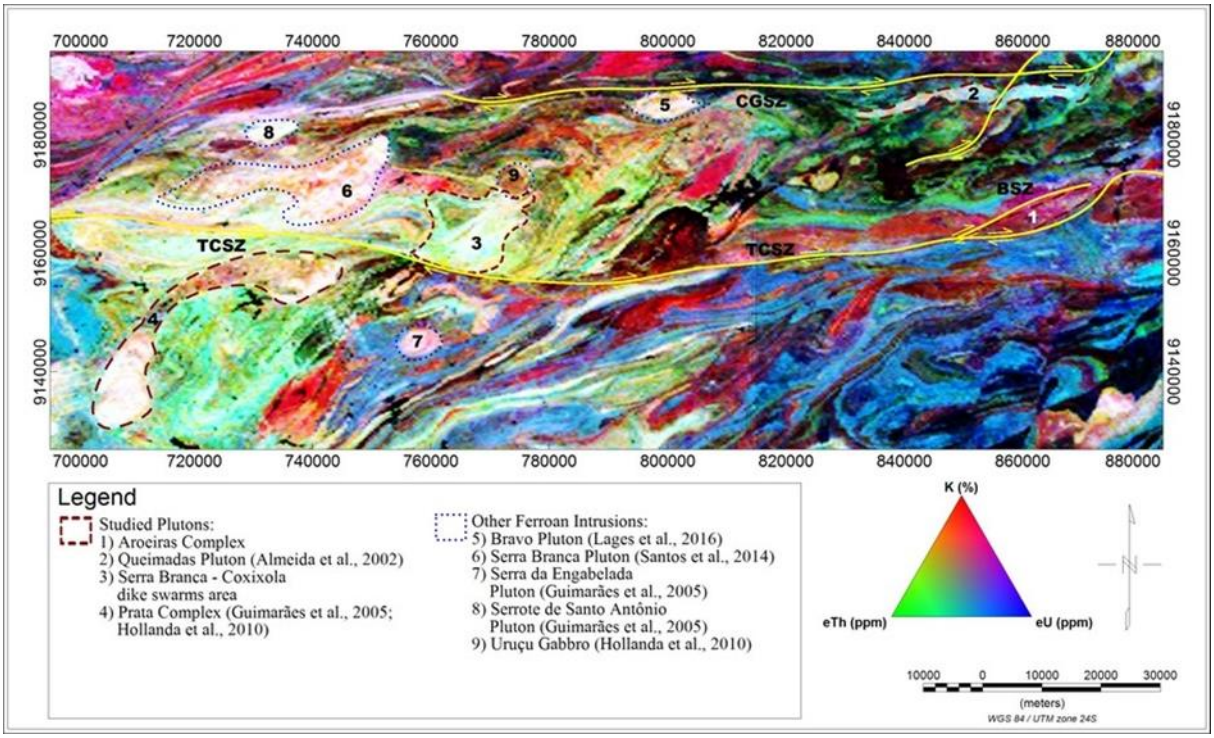

5.6.1 Aroeiras Complex

From the ternary radioelements distribution (Figure 8a), it is possible to identify three distinct zones within the Aroeiras Complex: northeastern sector with high contents of the three elements (K%> 3%; eTh, 15 – 20ppm; eU, 2 – 3ppm), southwestern and central sector with intermediate to low values of K (1.5 - 2.13%) and eU (0.5 - 1.5ppm) and low values of eTh (5 - 9ppm) (Figure 8b,c,d) and, a diffuse pattern of elements distribution surrounding those sectors.

Figura 24 - Figure 8. Gamma-ray spectrometric maps of the Aroeiras complex: a) Ternary (RGB), b) K(%), c) eTh (ppm), d) eU (ppm)

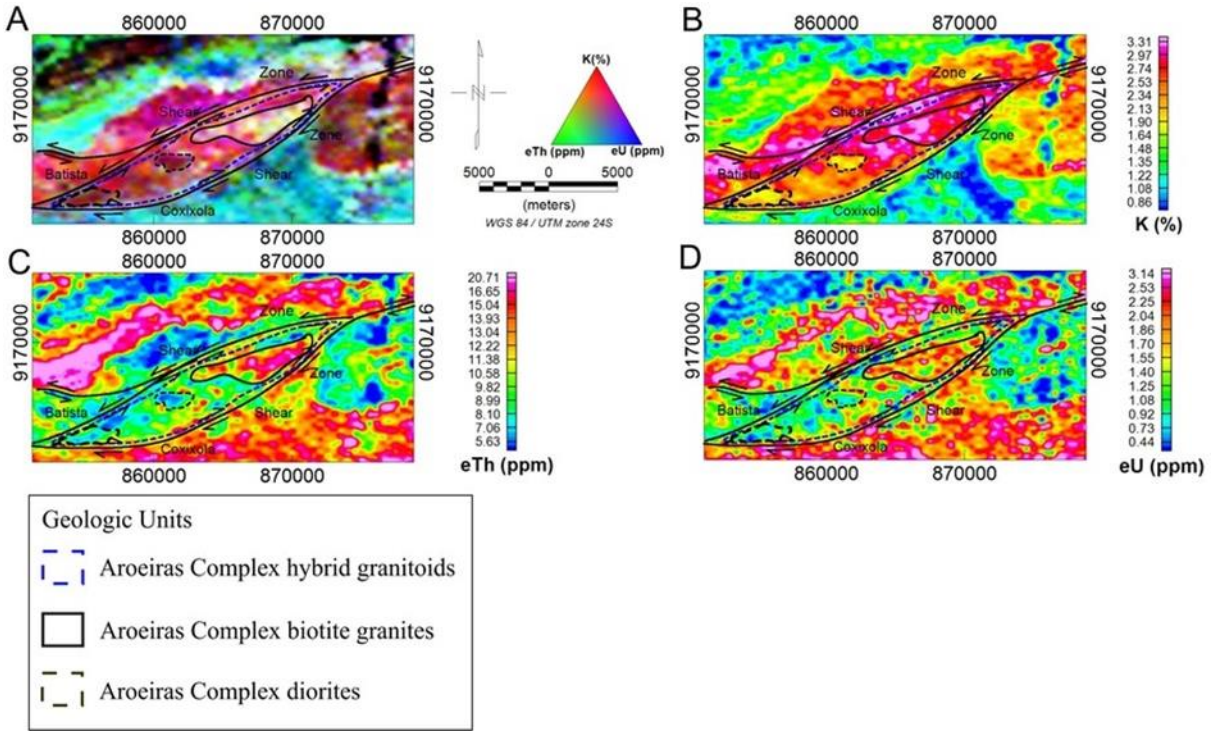

In the northeastern zone, leucocratic ferroan alkali-calcic biotite syenogranites are abundant, the presence of apatite, allanite and zircon, up to 1% of the rocks volume, would explain the high values of U and Th, since these minerals are responsible for carrying almost all the contents of these elements in rocks.

The southwestern and central sector of the Aroeiras Complex (Figure 8) is marked by the presence of alkalic hornblende-biotite dioritic bodies. Despite their alkalic character, K2O weight percentages in dioritic rocks are lower (2-3%) than in granitic rocks (4-5%), close to those observed in gamma spectrometric maps. This justifies the low to intermediate values of K, when compared to the northwest sector which is dominated by biotite syenogranites.

Surrounding those sectors, the Aroeiras Complex comprises a heterogenous rock association, mostly hybrid porphyritic rocks enclosing dioritic enclaves and leucocratic equigranular biotite granites. Mingling and processes between granitic and dioritic rocks are often chaotic (Flinders and Clemens, 1996), thus no clear gamma spectrometric signature related to this process is visible in this sector of the Aroeiras Complex.

5.6.2 Queimadas Pluton

The ternary image of Queimadas Pluton (Figure 9a) contrasts with country rocks due to elevated values of K (values higher than 3%), eTh (19 – 30ppm) and eU (2 – 3.3ppm). Nevertheless, the east intrusion seems to be more enriched in eTh and eU than the west body. This signature is evidenced on the individual counting maps (Figure 9b,c,d).

Figura 25 - Figure 9. Gamma-ray spectrometric maps of the Queimadas Pluton: a) Ternary (RGB), b) K(%), c) eTh (ppm), d) eU (ppm)

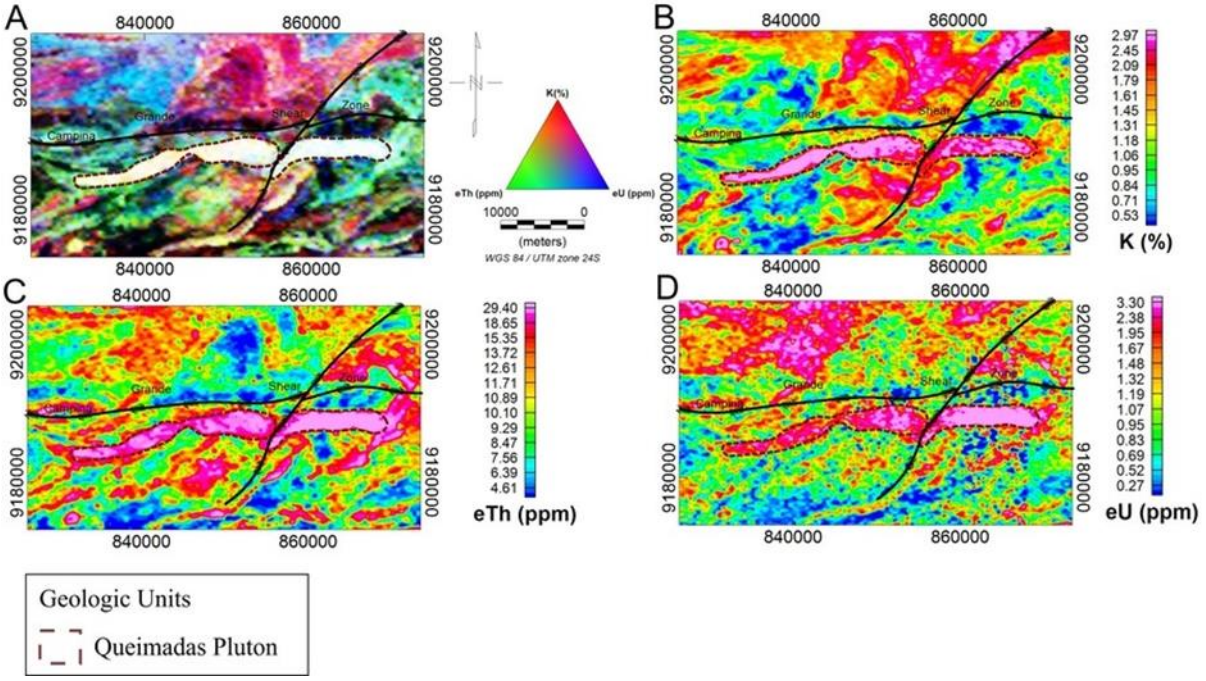

The alkalic to alkali-calcic nature of the granitoids explain the high values of K related to the intrusion. As the presence of zircon, allanite and monazite, described by Almeida et al. (2002), minerals that have high contents of radiogenic elements in their structure, are related to the high values of eU and eTh observed in the pluton, this assemblage should occur in higher amounts in the west body.

Deformational processes and textures described by (Almeida et al., 2002) did not lead to K and U enrichment. In fact, lower values of K (~1.8%) are found closer to the shear zone that disrupts this pluton (Figure 9b). Deformation processes in brittle-ductile conditions, as those described by Almeida et al. (2002), lead to perthite formation and albite replacement in K-feldspar (Pryer and Robin, 1995), subsequently Na increase and decrease in K values, explain the decreasing on this element counts.

5.6.3 Serra Branca – Coxixola dike swarms

In the Serra Branca – Coxixola dike swarms region, the ternary distribution (Figure 10a) does not provide much information apart from high contents of K (4.3 – 5%), eTh (~40ppm)

and eU (>3ppm).

Instead, individual channels (Fig. 10b,c,d) were used to trace the main population of dikes, since they are too small for the flight line spacing (Table 2). In these maps, positive contrasts with NE-SW trends in the K and eU counts, often coincide with outcrops of dike swarms (black dots in Figure 10). It is not possible to make any further connections with magmatic processes occurring in these dykes due to their outcrop scale.

Figura 26 - Figure 10. Gamma-ray spectrometric maps of the Serra Branca - Coxixola dike swarms region: a) Ternary (RGB), b) K(%), c) eTh (ppm), d) eU (ppm)

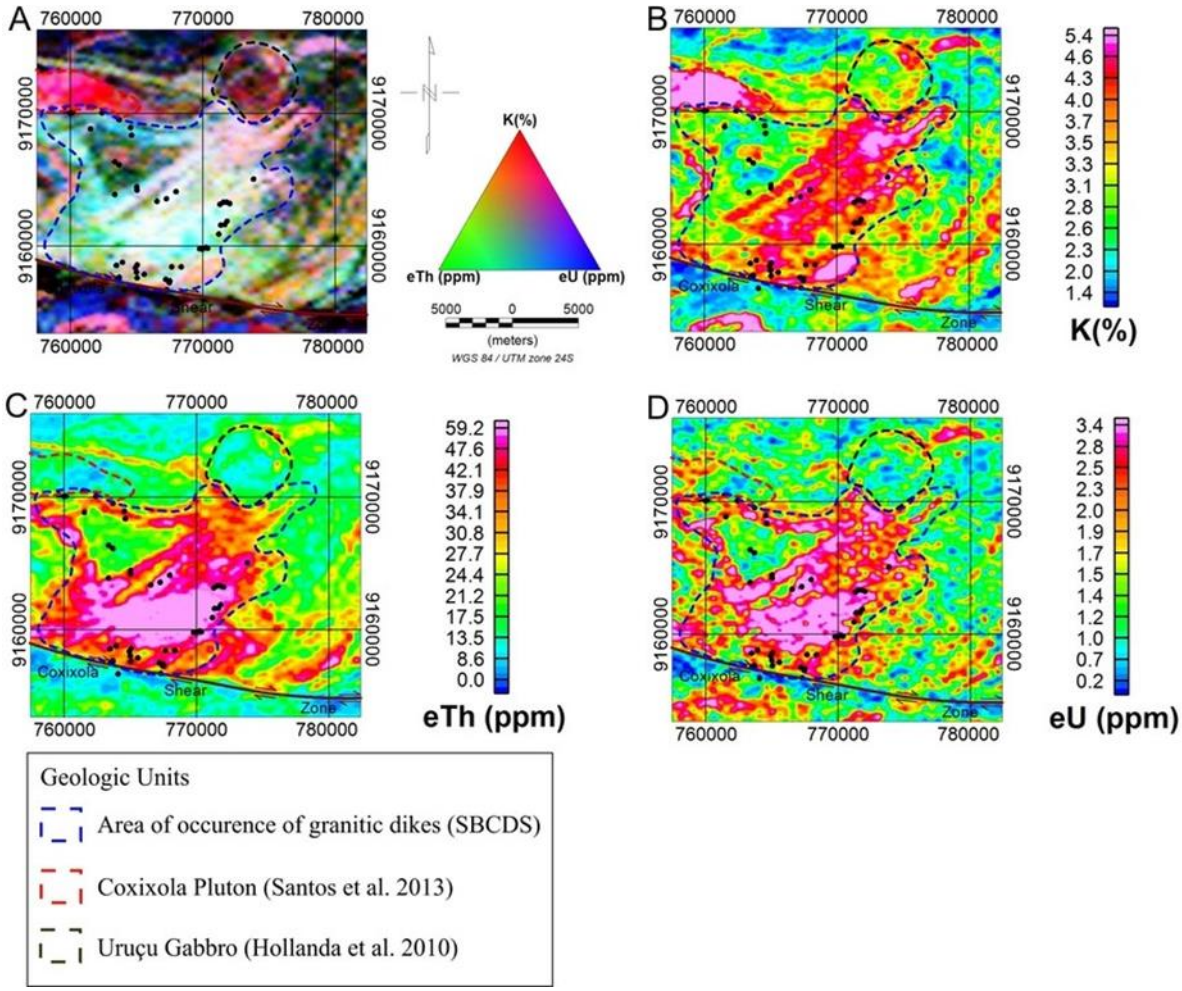

Although the Uruçu gabbro (Hollanda et al., 2010) (Figure 7 and figure 10) is coeval with the SBCDS, its composition differs distinctively from the ferroan plutons. This gabbroic intrusion was generated from partial melting of mantle sources, and K, Th and U are not geochemically compatible with these rocks. Hence, gamma spectrometric signature presents low to medium values of eTh (8 – 20ppm) and eU (0.2 – 1.2ppm), as well as, medium values of K (2.3 – 3%).

Medium values of K are either related to assimilation and mixing processes with granitoids of the SBCDS, or with the K-enriched nature of the lithospheric mantle beneath the Borborema Province, which leads widespread to generation of K-rich mafic to intermediate rocks (Silva Filho et al., 1993; Ferreira et al., 1997; Neves and Mariano, 1997, 2004; Neves et al., 2000; Mariano et al., 2001; Hollanda et al., 2003; Guimarães et al., 2005).

5.6.4 Prata Complex

From the ternary image of radioelements distribution, it is possible to identify the three distinct domains described by Guimarães et al. (2005) (Fig. 11a,b,c,d).

Figura 27 - Gamma-ray spectrometric maps of the Prata Complex: a) Ternary (RGB), b) K(%), c) eTh (ppm), d) eU (ppm)

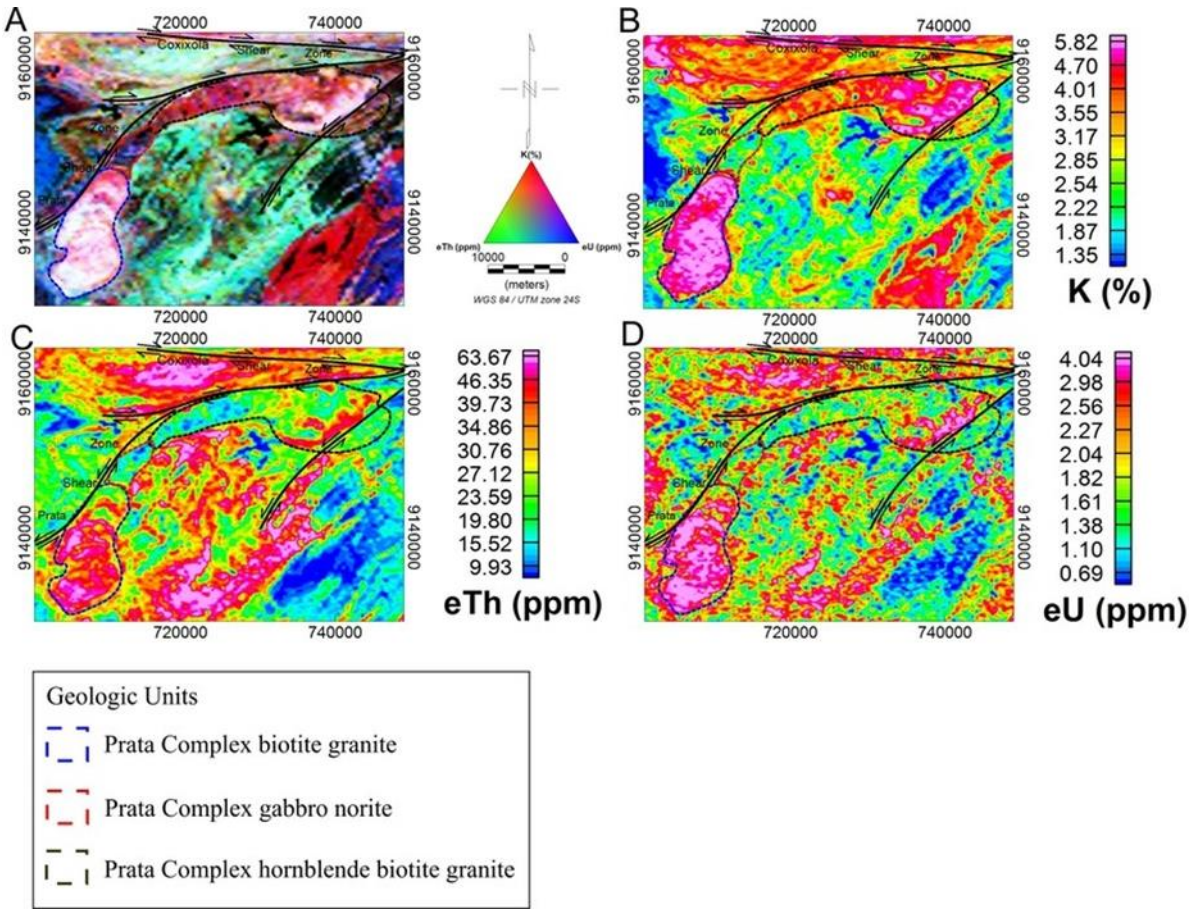

The southern pluton exhibits high contents of K (~6%), eTh (27 – 60ppm) and eU (2–4ppm), which is related to mineral abundances with high percentages of microcline (~50%), biotite (10%) and allanite (1.5%) (Mello, 1997).

The central sector is dominated by low contents of K (1 – 2%) and eTh (9 – 20ppm) and low to medium counts of eU (1 – 2ppm). Guimarães et al. (2005) described this region as mafic

rocks of comprising norites with depleted in incompatible elements signatures, probably related to the rise of astenospheric mantle in an extensional setting.

The north pluton is heterogeneous and characterized by medium to high values of K (3 – 5%) and variable contents of eU (0.5 – 4ppm) and eTh (10 – 46ppm). The west part of this pluton has medium contents of K and eU, and low contents of eTh, as the east has a region of high contents of the K, eTh and eU. The north pluton comprises hbl-bt granites, minor amounts of biotite (~6%) and allanite (0.5%). Minor radioelements concentration in this granitic intrusion is probably related to its mineralogical composition and widespread presence of dioritic enclave swarms.

5.7 DISCUSSION

Overall ferroan granitoids gamma spectrometric signatures reflect their LIL and HFS ele- ments enriched nature, with high abundances of K, eTh and eU. However, some these intrusions are associated with diorites and gabbros, exhibiting features of mixing, mingling, hybridization, resulting in remarkably heterogenous intrusions with different gamma spectrometric patterns.

Deformational processes can also change the radioelements distribution. For example, in the Queimadas pluton, a NE-SW dextral sense shear zone disrupts the granitic body and shear in brittle-ductile conditions are associated with K decrease in contact with this intrusion.

Geochemical differences between granites, diorites and gabbros are exhibited in gamma spectrometric maps. For instance, diorites and grabbros have lower contents of K2O (2-3%), Th (1 – 7 ppm) and U (0.5 – 3 ppm), than the ferroan granites K2O (4.2 – 6.4)%, Th (16 – 40 ppm) and U (2 – 5 ppm), feature also observed in gamma spectrometric maps (Gabbros and Diorites: K, 1 – 3%; eTh, 5 – 20ppm; eU, 0.2 – 2ppm; Granites: K, 3 – 6%; eTh, 15 – 60ppm; eU, 2 – 4ppm).

5.8 CONCLUSION

Gamma spectrometric signatures of ferroan intrusions on a regional scale are related to their general aspects as cohesive group of intrusions (LILE and HFSE rich). When observed individually, and in detail, gamma ray signatures are rather related to petrological and deforma- tional processes that acted during or posterior to the emplacement of these granitic intrusions (mineralogical composition, mingling, assimilation, hybridization).

Geochemical analyses and gamma spectrometric maps exhibit good correspondence and concentration intervals overlap. Diorites and norites exhibit lower contents of K, eTh and eU, similar behavior was identified in incompatible elements normalized patterns.

5.9 ACKNOWLEDGEMENTS

We are grateful for the Brazilian Geological Survey (CPRM) who allowed us to use and publish geophysical data from the projects Borda Leste do Planalto da Borborema and Pernambuco-Paraíba aerogeophysical surveys. This work was supported by Fundação de Amparo à Ciência e Tecnologia do estado de Pernambuco (FACEPE); under grant [IBPG-1074-1.07/15].

5.10REFERENCES

Accioly A.C.A., McReath I., Santos E.J., Guimarães I.P., Vannuci R. and Bottazzi R. 2000. The Passira meta-anorthositic complex and its tectonic implication, Borborema Province, Brazil. 31 International Geological Congress. International Union of Geological Sciences, Abstracts, Rio de Janeiro

Almeida C.N., Guimaraes I.P. and Silva Filho, A.F. 2002. A-type post-collisional granites in the Borborema Province – NE Brazil: The Queimadas Pluton. Gondwana Research. 5 (3), 667–681

Almeida F.F.M., Hasui Y., Brito Neves B.B. and Fuck, R. 1981. Brazilian structural provinces: an introduction. Earth-Science Reviews. 17, 1-29.

Almeida F.F.M., Leonardos Jr. O.H., Valença J. 1967. Review on granitic rocks of Northeast South America, Proceedings of the Symposium on Northeastern South America Granites, Recife, IUGS/UNESCO, p. 41

Amorim J.V.A, Guimarães I.P, Farias D.J.S., Lima J.V, Santos L. and Ribeiro V.B, 2018. Late-Neoproterozoic ferroan granitoids of the Transversal Subprovince, Borborema Province, NE Brazil: Petrogenesis and Geodynamic implications (submitted for publication)

Archanjo C.J., Launeau P., Hollanda M.H.B.M., Macedo J.W.P. and Liu D. 2009. Scattering of magnetic fabrics in the epizonal Cambrian alkaline granite of Meruoca (Ceará State, northeast Brazil). International Journal of Earth Sciences, 98, 1793–1807

Archanjo C.J., Viegas L.G.F., Hollanda M.H.B.M., Souza L.C. and Liu D. 2013, Timing of the HT/LP transpression in the Neoproterozoic Seridó Belt (Borborema Province, Brazil):

Constraints from UPb (SHRIMP) geochronology and implications for the connections between NE Brazil and West Africa: Gondwana Research, v. 23 (2), p. 701-714.

Baumgartner R., Romer R.L., Moritz R., Sallet R. and Chiaradia, M. 2006. Columbite tantalite-bearing granitic pegmatites from the Seridó Belt, northeastern Brazil: genetic constraints from U–Pb dating and Pb isotopes. Canadian Mineralogist 44, 69–86

Bea F. 1996. Residence of REE, Y, Th and U in granites and crustal protoliths; implications for the chemistry of crustal melts. Journal of Petrology 37, 521-552.

Bonin B., 2007. A-type granites and related rocks: evolution of a concept, problems and prospects. Lithos 97, 1-29

Brito Neves B. B., Santos E. J. and Van Schmus W. R. 2000. Tectonic History of the Borborema Province. In: Cordani U. G., Milani E. J., Thomaz Filho, A., Campos, D. A. (eds.) Tectonic evolution of South America. Rio de Janeiro, p. 151-182

Brito Neves B.B., Basei M.A.S., Passarelli C.R. and Santos E.J. 2003. Idades U-Pb em zircão de alguns granitos clássicos da Província Borborema. Bol. IG USP 3, 25-38.

Brito Neves B.B., Campos Neto M.C., Van Schmus W.R. and Santos, E.J., 2001. O "Sistema Pajeú-Paraíba" e o "Maciço" Sao José do Campestre no leste da Borborema. Revista Brasileira Geocencias 31 (2), 173–184

Brito Neves B.B., Van Schmus W.R., Santos E.J., Campos Neto M.C. and Kozuch, M., 1995. O evento Cariris Velhos na Província Borborema: integração de dados, implicações e perspectivas. Rev. Bras. Geociên. 25, 279-296

CPRM, 2008. Projeto Aerogeofísico Borda Leste do Planalto da Borborema. Consórcio LASA Engenharia e Prospecções S.A./ PROSPECTORS Aerolevantamentos e Sistemas Ltda.

CPRM, 2010. Projeto Aerogeofísico Pernambuco - Paraíba - Riogrande do Norte. Consórcio LASA Engenharia e Prospecções S.A./ PROSPECTORS Aerolevantamentos e Sistemas Ltda.

De Wit M.J., Jeffery M., Bergh H. and Nicolaysen L. 1998. Geological Map of Sectors of Gondwana, Reconstructed to Their Disposition 150 Ma. American Association of Petroleum Geologists, Tulsa, USA

Eby G.N. 1992. Chemical subdivision of the A-type granitoids: petrogenetic and tectonic implications. Geology 20, 641-644

Ferreira V.P., Sial A.N., Long L.E. and Pin, C., 1997. Isotopic signatures of Neoproterozoic to Cambrian ultrapotassic syenitic magmas, northeastern Brazil: implications for enriched mantle source. Int. Geol. Rev. 39, 660-669

Flinders J. and Clemens J. D. 1996. Non-linear dynamics, chaos, complexity and enclaves in granitoid magmas. Trans. R. Soc. Edinburgh Earth Sci. 87, 217–223.

Frost C.D., Frost B.R. 2011. On Ferroan (A-type) Granitoids: their Compositional Variability and Modes of Origin. Journal of Petrology, 52, 39-53

Guimarães I.P., Brito M.F.L., Lages G.A., Silva Filho A.F., Santos L. and Brasilino

R.G. 2016. Tonian granitic magmatism of the Borborema Province: A review. Journal of South American Earth Sciences, 68, 97-112

Guimarães I.P., Silva Filho A.F., Almeida C.N., Van Schmus W.R., Araújo J.M.M., Melo S.C. and Melo E.B. 2004. Brasiliano (Pan-African) granitic magmatism in the Pajeú-Paraíba belt, Northeast Brazil: an isotopic and geochronological approach. Precambrian Research 135, 23–53.

Guimarães I.P., Silva Filho A.F., Melo S.C. and Macambira M.B. 2005. Petrogenesis of A-type granitoids from Alto Moxotó and Alto Pajeú terranes of the Borborema Province, NE Brazil: constraints from geochemistry and isotopic compositions. Gondwana Research 8, 347–362.

Guimaraes I.P., Silva Filho A.F., Araújo D.B., Almeida C.N. and Dantas E., 2009. Trans- alkaline magmatism in the Serrinha-Pedro Velho complex, Borborema province, NE Brazil and its correlations with the magmatism in eastern Nigeria. Gondwana Res. 15, 98-110

Guimaraes I.P., Van Schmus W.R., Brito Neves B.B., Bittar S.M., Silva Filho A.F. and Armstrong R., 2012. U-Pb zircon ages of orthogneisses and supracrustal rocks of the Cariris Velhos belt: onset of Neoproterozoic rifting in the Borborema Province, NE Brazil. Precambrian Res. 192-195, 52-77.

Guimarães I.P., Silva Filho A.F. and Armstrong R., 2017. Origin and age of coeval gabbros and leucogranites in the northern supbrovince of the Borborema Province, NE Brazil. J. S. Am. Earth Sci., 76, 71-93.

Hollanda M.H.B.M., Archanjo C.J., Souza L.C., Armstrong R. and Vasconscelos P.M. 2010. Cambrian mafic o felsic magmatism and its connections with transcurrent shear zones of the Borborema Province (NE Brazil): Implications for the late assembly of West Gondwana.

Hollanda M.H.B., Pimentel M.M. and Jardim de Sá E.F., 2003. Paleoproterozoic subduction- related metasomatic signatures in the lithospheric mantle beneath NE Brazil: inferences from trace element and Sr–Nd–Pb isotopic compositions of Neoproterozoic high-K igneous rocks. Journal of South American Earth Sciences 15, 885–900

Hollanda M.H.B., Souza Neto J.A., Archanjo C.J., Stein H. and Maia A.C.S. 2017. Age of the granitic magmatism and the W-Mo mineralizations in skarns of the Seridó belt (NE Brazil) based on zircon U-Pb (SHRIMP) and Re-Os determinations. JOURNAL OF SOUTH AMERICAN EARTH SCIENCES, v. 79, 1-11.

IAEA. 1991. Airborne gamma ray spectrometer surveying. Technical Reports Series nº 323. Viena: Intern. Atomic Energy Agency.

Jardim de Sá E.F., Macedo M.H.F., Torres H.H.F. and Kawashita, K., 1988. Geochronology of metaplutonics and the evolution of supracrustal belts in the Borborema province. In: VII Latino-americano Geological Congress. Extended Abstract, pp. 49-62

Johan Z., and Johan V. 1994. Oxyfl uorures de terres rares de la coupole granitique de Cínovec (Zinnwald), Repúblique tchèque. CR Academie Sciences de Paris 318, 1225-1231.

Johan Z. and Johan V. 2005. Accessory minerals of the Cínovec (Zinnwald) granite cupola, Czech Republic: indicators of petrogenetic evolution. Mineral Petrol 83: 113–150.

Kozuch M. 2003. Isotopic and Trace Element Geochemistry of Early Gneissic and Metavolcanic Rocks in the Cariris Velhos Orogen of the Borborema Province, Province, Brazil and Their Bearing Tectonic Setting. PhD thesis. Kansas University, 199pp

Lages G.A., Marinho M.S., Nascimento M.A.L., Medeiros V.C. and Dantas E.L., 2016. Geocronologia e aspectos estruturais e petrologicos do Pluton Bravo, Domínio Central da Província Borborema, Nordeste do Brasil: um granito transalcalino precoce no estágio pos-colisional da Orogenese Brasiliana. Brazilian Journal of Geology, 46 (1), 41-61

Lima J.V., Guimarães I.P., Santos L., Amorim J.V.A., Farias D.J.S. 2017. Geochemical and isotopic characterization of the granitic magmatism along the Remígio-Pocinhos shear zone, Borborema Province, NE Brazil. J. S. Am. Earth Sci., 75, 116- 133

Loiselle M.C. and Wones D.S. 1979. Characteristics and origin of anorogenic granites. Geological Society of America. Abstracts with programs 11, 468.

Louro V.H.A., Ribeiro V.B. and Mantovani M. S. M. 2013. Geophysical exploration of the Buraco da Velha deposit (RO, Brazil). 13th International Congress of the Brazilian Geophysical Society & EXPOGEf, at Rio de Janeiro, Brazil. DOI: 10.1190/sbgf2013-144

Mariano G., Neves S.P., Silva Filho A.F. and Guimarães I.P. 2001. Diorites of the high-K calc-alkalic Association: geochemistry and Sm–Nd data and Implications for the evolution of the Borborema Province, Northeast Brazil. International Geology Review 43, 921–929

Melo S.C. 1997. Petrologia e geoquímica dos granitóides do Complexo Prata a nordeste de Monteiro-PB. M.Sc. Thesis. Universidade Federal de Pernambuco, 88p.

Nakamura N. 1974. Determination of REE, Ba, Fe, Mg, Na, and K in carbonaceous and ordinary chondrites. Geochimica Cosmochimica Acta 38, 757-775

Nascimento M.A.L., Galindo A.C. and Medeiros V.C. 2015. Ediacaran to Cambrian magmatic suites in the Rio Grande do Norte domain, extreme Northeastern Borborema Province (NE of Brazil): Current knowledge: Journal of South American Earth Sciences, v. 58, p. 281-299.

Neves S.P. 2015. Constraints from zircon geochronology on the tectonic evolution of the Borborema Province (NE Brazil): widespread intracontinental Neoproterozoic reworking of a Paleoproterozoic accreationary orogeny. J. South Am. Earth Sci. 58, 150-164

Neves S.P., Bruguier O., Vauchez A., Bosch D., Silva J.M.R. and Mariano, G., 2006a. Timing of crust formation, deposition of supracrustal sequences, and Transamazonian and Brasi- liano metamorphism in the East Pernambuco belt (Borborema Province, NE Brazil): implications for western Gondwana assembly. Precambrian Res. 149, 197-216.

Neves S.P., Lages G.A., Brasilino R.G. and Miranda A.W.A., 2015. Paleoproterozoic accretionary and collisional processes and the build-up of the Borborema Province (NE Brazil): Geochronological and geochemical evidence from the Central Domain. J. S. Am. Earth Sci., 58, 165-187.

Neves S.P. and Mariano, G., 1997. High-K calc-alkalic plutons in Northeast Brazil: origin of the biotite diorite/quartz monzonite to granite association and implications for the evolution of the Borborema Province. Int. Geol. Rev., 39, 621–638

Neves S.P. and Mariano, G., 2004. Heat-producing elements-enriched continental mantle lithosphere and Proterozoic intracontinental orogens: insights from Brasiliano/PanAfrican Belts. Gondwana Research 7 (2), 427–436

Neves S.P., Vauchez A. and Archanjo, C.J., 1996. Shear zone-controlled magma emplacement or magma-assisted nucleation of shear zones? Insights from northeast Brazil. Tectonophysics, 262, 349-364.

Neves S.P., Vauchez A. and Feraud G., 2000. Tectono-thermal evolution, magma emplacement, and shear zone development in the Caruaru area (Borborema Province, NE Brazil). Precambrian Res. 99, 1–32

Ostrovsky E. A. 1975. Antagonism of radioactive elements in wallrock alteration fields and its use in aerogamma spectrometric prospescting. International Geology Review, 17, 461-468.

Pagel M. 1982. The mineralogy and geochemistry of uranium, thorium, and rare-earth elements in two radioactive granits in the Vosges, France. Mineralogical Magazine 46, 149-161.

Pryer L.L. and Robin P.Y.F. 1995. Retrograde metamorphic reactions in deforming granites and the origin of flame perthite. J Metam Geol 14,645–658

Ribeiro V. B., Mantovani M. S. M, and Louro V.H.A. 2013. Aerogamaespectrometria e suas aplicações no mapeamento geológico. Terrae Didática, 10, 29-51.

Riberio, V.B., Mantovani, M. S. M. 2016. Gamma Spectrometric and Magnetic Interpre- tation of Cabaçal Copper Deposit in Mato Grosso (Brazil): Implications for hydrothermal fluids remobilization. Journal of Applied Geophysics, 135.DOI10.1016/j.jappgeo.2016.10.016

Sá J.M., Bertrand J.M., Leterrier J. and Macedo M.H.F. 2002. Geochemistry and geochronology of pre-Brasiliano rocks from the Transversal Zone, Borborema Province, Northeast Brazil. J. South Am. Earth Sci. 14, 851-866

Santos E.J., 1995. O complexo granítico Lagoa das Pedras: Acresção e colisão na região de Floresta (Pernambuco) Província da Borborema. Doctor Thesis, Universidade de Sao Paulo, 220 pp.

Santos L., Guimarães I.P., Silva Filho A.F., Farias D.J.S., Lima J.V. and Antunes J.V. 2014. Magmatismo Ediacarano extensional na Província Borborema, NE Brasil: Pluton Serra Branca. Comunicações Geológicas, 101, Especial I, 199-203

Santos T.J.S., Fetter A.H., Hackspacher P.C. Van Schmus W.R. and Nogueira Neto J.A. 2008. Neoproterozoic tectonic and magmatic episodes in the NW sector of Borborema Province, NE Brazil, during assembly of Western Gondwana. Journal of South American Earth Sciences 25, 271–284

Sial A.N., 1986. Granite-types of Northeast Brazil: current knowledge. Rev. Bras. Geoci- encias 16, 54-72

Silva Filho A.F., Guimaraes I.P. and Thompson, R.N., 1993. Shoshonitic and ultrapo-tassic Proterozoic suites in the Cachoeirinha –Salgueiro fold Belt, NE Brazil: a transition from collisional to post-collisional magmatism. Precambrian Res., 62, 323–342

Silva Filho A.F., Guimarães I.P., Ferreira V.P., Armstrong R.A. and Sial A.N., 2010. Ediacaran Aguas Belas pluton, Northeastern Brazil: evidence on age, emplacement and magma sources during Gondwana amalgamation. Gondwana Res. 17, 676-687

Sun S.-s. and McDonough W.F. 1989. Chemical and isotopic systematics of oceanic basalts: implications for mantle composition and processes. Geological Society, London, Special Publications 42, 313-345.

Toteu S.F., Van Schmus W.R., Penaye J. and Michard A., 2001. New U–Pb and Sm–Nd data from north-central Cameroon and its bearing on pre-Pan African history of central Africa. Precambrian Research, 108, 45–73

Ulbrich, H.H.G.J., Ulbrich M.N.C., Ferreira F.J.F., Alves L.S., Guimarães G.B. and Fruchting A. 2009. Levantamentos Gamaespectrométricos em Granitos Diferenciados. I: Revisão da Metodologia e do Comportamento Geoquímico dos Elementos K, Th e U. Geologia USP: Série Cientifica, 9(1), 33-53.

Van Schmus W.R., Brito Neves B.B., Hackspacher P.C. and Babinski M. 1995. U/Pb and Sm/Nd geochronologic studies of Eastern Borborema Province, northeastern Brazil: initial conclusions. J. S. Am. Earth Sci. 8, 267-288

Van Schmus W.R., Kozuch M. and Brito Neves B.B. 2011. Precambrian history of the Zona transversal of the Borborema province, NE Brazil: insights from Sm/Nd and U/Pb geochronology. J. S. Am. Earth Sci. 31, 227-252

Van Schmus W.R., Oliveira E.P., Silva Filho A.F., Toteu S.F., Penaye J. and Guimaraes

I.P. 2008. Proterozoic links between the Borborema province, NE Brazil, and the central African fold belt. Geol. Soc. Lond. Special Publ. 294, 69-99.

Vauchez A., Neves S.P., Caby R., Corsini M., Egydio-Silva M., Arthaud M.H. and Amaro V. 1995. The Borborema shear zone system, NE Brazil. J. S. Am. Earth Sci. 8, 247–266

Whalen J.B., Currie K.L. and Chappell B.W., 1987. A-types granites: geochemical characteristics, discrimination and petrogenesis. Contributions Mineralogy Petrology 95, 407-419.

6 CONCLUSÕES

Granitos ferrosos da subprovíncia Transversal distinguem dois grupos geoquímicos, e intrudem em três estágios distintos da orogênese Brasiliana:

1) granitos levemente peraluminosos a metaluminosos, álcali-cálcicos, com micas pobres em annita, cristalizados sob condições de fugacidade de oxigênio intermediária. Este grupo marca processos de transição de ambientes tectônicos. O complexo Aroeiras marca a transição do evento colisional para o transcorrente (~585 Ma); enquanto os enxames de diques de Serra Branca - Coxixola e diques tardios leucocráticos que cortam o complex Aroeiras, marcam a transição da transcorrência para o uplift e transtensão, com o início do desenvolvimento de bacias intracratônicas (~545 Ma);

2) granitos metaluminosos a levemente peraluminosos, alcalinos a álcali-cálcicos, com mi- cas ricas em annita e cristalizados sob baixas fugacidades de oxigênio (Plúton Queimadas e Complexo Prata). Este grupo, está associado com ambientes extensionais bem desen- volvidos. Os granitoides do pluton Queimadas estão associados a adelgaçamento crustal heterogêneo de crosta previamente espessada, em ambientes pós-colisionais associados a transcorrência entre 570 - 550 Ma; e os granitóides do complexo Prata estão associados com transtensão contemporânea com a deposição de bacias intracratônicas e as últimas intrusões ferrosas da Província Borborema.

A geração de granitos ferrosos envolve marjoritariamente fusão parcial de rochas de afinidade TTG de idade Paleoproterozóica no embasamento da Província Borborema, e processos de assimilação, limitados. A presença de rochas máficas pode resultar em modificações nas composições dos granitos estudados, e está associada a transferência de calor.

Assinaturas gamaespectrométricas dos granitos ferrosos, refletem a natureza bastante diferenciada destas rochas (ricas em LILE e HFSE). O estudo em detalhe de mapas gama espectrométricos mostram que heterogeneidades exibidas nos mapas estão associadas a processos petrológicos e deformacionais que atuaram durante a evolução destes corpos (composição mineralogica, mistura, assimilação, hibridização).

Análises geoquímicas e mapas gamaespectrométricos mostram boas correspondências e intervalos de concentração equivalentes, o que validam a qualidade dos dados aerogeofísicos cedidos pela CPRM. Dioritos e noritos exibem menores valores de K, eTh e eU, e padrões de elementos incompatíveis mostraram comportamento similar.

REFERÊNCIAS

ABDEL-RAHMAN, A. M. Nature of biotites from alkaline, calc-alkaline, and peraluminous magmas. *Journal of Petrology*, v. 35, p. 525 – 541, 1994.

ACCIOLY, A. C. et al. The Passira meta-anorthositic complex and its tectonic implication, Borborema Province, Brazil. In: 31 INTERNATIONAL GEOLOGICAL CONGRESS, 2000, Rio de Janeiro. *International Union of Geological Sciences*. Rio de Janeiro, 2000.

ACCIOLY, A. C. A. et al. Geochronology and geochemistry of the meta-volcanic rocks from riacho do tigre complex, borborema province - northeastern Brazil. In: VII SSAGI SOUTH AMERICAN SYMPOSIUM ON ISOTOPE GEOLOGY, 2010, Brasília. Brasília, 2010.

AGENCY, V. I. A. E. *Airborne gamma ray spectrometer surveying*. [S.l.], 1991.

ALMEIDA, C. N.; GUIMARÃES, I. P.; SILVA FILHO, A. F. A-type post-collisional granites in the Borborema Province – NE Brazil: The Queimadas Pluton. *Gondwana Research.*, v. 3, n. 5, p. 667 – 681, 2002.

ALMEIDA, F. F. M. et al. Brazilian structural provinces: an introduction. *Earth-Science Reviews*, n. 17, p. 1 – 29, 1981.

ALMEIDA, F. F. M.; LEONARDOS JR., O. H.; VALENÇA, J. Review on granitic rocks of Northeast South America. In: SYMPOSIUM ON NORTHEASTERN SOUTH AMERICA GRANITES, 1967, Recife. *Proceedings*. Recife, 1967. p. 41 –.

ANDERSEN, T. et al. Granitic magmatism by melting of juvenile continental crust: new constraints on the source of Palaeoproterozoic granitoids in Fennoscandia from Hf isotopes in zircon. *Geology Society*, n. 166, p. 233 – 247, 2009.

ANDERSON, J. L.; SMITH, D. R. The effects of temperature and fO2 on the Al – in hornblende barometer. *American Mineralogist*, v. 80, p. 549 – 559, 1995.

ARAÚJO, C. E. G.; WEINBERG, R. F.; CORDANI, U. G. Extruding the Borborema Province (NE-Brazil): a two-stage Neoproterozoic collision process. *Terra Nova*, n. 26, p. 157 – 168, 2014.

ARCHANJO, C. J. et al. Scattering of magnetic fabrics in the epizonal Cambrian alkaline granite of Meruoca (Ceará State, northeast Brazil). *International Journal of Earth Sciences*, n. 98, p. 1793 – 1807, 2009.

ATTOH, K.; CORFU, F.; NUDE, P. M. U-Pb zircon age of deformed carbonatite and alkaline rocks in the Pan-African Dahomeyide suture zone, West Africa. *Precambrian Research*, n. 155, p. 251 – 260, 2007.

AZZOUNI-SEKKAL, A. et al. The "Taourirt" magmatic province, a marker of the closing stage of the Pan-African orogeny in the Touareg Shield: review of available data and Sr–Nd isotope evidence. *Journal of African Earth Sciences*, n. 37, p. 331 – 350, 2003.

BARBARIN, B. Granitoids: main petrogenetic classifications in relation to origin and tectonic setting. *Geological Journal*, n. 25, p. 227 – 238, 1990.

BARBARIN, B. A review of the relationships between granitoid types, their origins and their geodynamic environments. *Lithos*, n. 46, p. 605 – 626, 1999.

BAUMGARTNER, R. et al. Columbitetantalite-bearing granitic pegmatites from the Seridó Belt, northeastern Brazil: genetic constraints from U–Pb dating and Pb isotopes. *Canadian*

Mineralogist, n. 44, p. 69 – 86, 2006.

BEA, F. Residence of REE, Y, Th and U in granites and crustal protoliths; implications for the chemistry of crustal melts. *Journal of Petrology*, n. 37, p. 521 – 552, 1996.

BEA, F. et al. Zircon inheritance reveals exceptionally fast crustal magma generation processes in central Iberia during the Cambro-Ordovician. *Journal of Petrology*, n. 48, p. 2327 – 2339, 2007.

BOGAERTS, M.; SCAILLET, B.; AUWERA, J. V. Phase equilibria of the Lyngdal granodiorite (Norway): Implications for the origin of metaluminous ferroan granitoids. *Journal of Petrology*, n. 47, p. 2405 – 2431, 2006.

BONIN, B. A-type granites and related rocks: evolution of a concept, problems and prospects. *Lithos*, n. 97, p. 1 – 29, 2007.

BONIN, B.; DUBOIS, R.; GOHAU, G. *Le métamorphisme et al formation des granites. Évoution des idées et concepts actuels*. Paris: Fac Sciences Nathan-Université, 1997. 317p.

BOUVIER, A.; VERVOORT, J. D.; PATCHETT, P. J. The Lu-Hf and Sm-Nd isotopic composition of CHUR: constraints from unequilibrated chondrites and implications for the bulk composition of terrestrial planets. *Earth and Planetary Science Letters*, n. 273, p. 48 – 57, 2008.

BRITO, M. F. L.; MENDES, V. A.; PAIVA, I. P. Metagranitoide Serra das Flores: magmatismo Toniano (tipo-A) no Domínio Pernambuco-Alagoas, Nordeste do Brasil. In: 44º BRAZILIAN GEOLOGICAL CONGRESS, 2008, Curitiba. Curitiba, 2008.

CARVALHO, M. J. *Tectonic Evolution of the Maranco-Poço Redondo Domain*: Records of the Cariris Velhos and Brasiliano Orogenesis in the Sergipano Belt, NE Brazil. 2005. Tese (Doutorado) — Campinas University.

CAVALCANTE, J. C. et al. *Mapa Geológico do Estado do Ceará e Escala 1:500.000*. [S.l.], 2003.

CAXITO, F. A.; UHLEIN, A.; DANTAS, E. L. The Afeição augen-gneiss Suite and the record of the Cariris Velhos Orogeny (1000-960 Ma) within the Riacho do Pontal fold belt, NE Brazil. *Journal of South American Earth Sciences*, n. 51, p. 12 – 27, 2014.

CAXITO, F. A. et al. Neoproterozoic oceanic crust remnants in northeast Brazil. *Geology*, n. 42, p. 387 – 390, 2014.

CHAPPELL, B. W.; WHITE, A. J. R. Two contrasting granite types. *Pacific Geology*, n. 8, p. 173 – 174, 1974.

CLEMENS, J. D.; STEVENS, G. Melt segregation and magma interactions during crustal melting: Breaking out of the matrix. *Earth-Science Reviews*, n. 160, p. 333 – 349, 2016.

CRUZ, R. F.; ACCIOLLY, A. C. A. Petrografia, geoquímica e idade U/Pb do Ortognaisse Rocinha, no Domínio Pernambuco-Alagoas W da Província Borborema. *Estudos Geológicos*, v. 2, n. 23, 2013.

DANTAS, E. L. et al. Archean accretion in the Sao Jose do Campestre Massif, Borborema Province, Northeast Brazil. *Revista Brasileira de Geociências*, v. 2, n. 28, p. 221 – 228, 1998.

DANTAS, E. L. et al. The 3.4-3.5 Ga Sao Jose do Campestre massif, NE Brazil: remnants of the

oldest crust in South America. *Precambrian Research*, n. 130, p. 113 – 137, 2004.

DANTAS, E. L. et al. Crustal growth in the 3.4 to 2.7 Ga Sao Jose de Campestre Massif, Borborema Province, NE Brazil. *Precambrian Research*, n. 227, p. 120 – 156, 2013.

DOUCE, A. P. Generation of metaluminous A-type granites by lowpressure melting of calc-alkaline granitoids. *Geology*, n. 25, p. 743 – 746, 1997.

EBY, G. N. A-type granitoids: a review of their occurence and chemical characteristics and speculations on their petrogenesis. *Lithos*, n. 26, p. 115 – 134, 1990.

EBY, G. N. Chemical subdivision of the A-type granitoids: petrogenetic and tectonic implications. *Geology*, n. 20, p. 641 – 644, 1992.

FERRÉ, E. et al. PanAfrican, post-collisional, ferro-potassic granite and quartz–monzonite plutons of Eastern Nigeria. *Lithos*, n. 45, p. 255 – 279, 1998.

FERREIRA, V. P. et al. Isotopic signatures of Neoproterozoic to Cambrian ultrapotassic syenitic magmas, northeastern Brazil: implications for enriched mantle source. *International Geology Review*, n. 39, p. 660 – 669, 1997.

FERREIRA, V. P. et al. Contrasting sources and PeT crystallization conditions of epidote-bearing granitic rocks, Northeastern Brazil: O, Sr and Nd isotopes. *Lithos*, n. 121, p. 189 – 201, 2011.

FERREIRA, V. P.; SIAL, A. N.; SÁ, E. F. J. de. Geochemical and isotopic signatures of proterozoic granitoids in terranes of Borborema structural province, northeast Brazil. *Journal of South American Earth Sciences*, n. 11, p. 439 – 455, 1998.

FETTER, A. H. *U-Pb and Sm-Nd Geochronological Constraints on the Crustal Framework and Geologic History of Ceara State, NW Borborema Province, NE Brazil*: Implications for the Assembly of Gondwana. 1999. Tese (Doutorado) — Kansas University.

FETTER, A. H. et al. U-Pb and Sm-Nd geochronological constraints on the crustal evolution of basement architecture of Ceara state, NW Borborema province, NE Brazil: implications for the existence of the Paleoproterozoic supercontinent 'Atlantica'. *Revista Brasileira de Geociências*, n. 30, p. 102 – 106, 2000.

FLINDERS, J.; CLEMENS, J. D. Non-linear dynamics, chaos, complexity and enclaves in granitoid magmas. *Transactions of the Royal Society of Edinburgh: Earth Sciences*, n. 87, p. 217 – 223, 1996.

FROST, B. R. et al. A Geochemical Classification for Granitic Rocks. *Journal of Petrology*, v. 42, n. 11, p. 2033 – 2048, April 2001.

FROST, B. R.; LINDSLEY, D. H.; ANDERSEN, D. J. Fe-Ti oxide-silicate equilibria: assemblages with fayalitic olivine. *American Mineralogist*, n. 25, p. 727 – 740, 1988.

FROST, C. D.; FROST, B. R. High-K, iron-enriched rapakivi-type granites: the tholeiite connection. *Geology*, n. 25, p. 647 – 650, 1997.

FROST, C. D.; FROST, B. R. On Ferroan (A-type) Granitoids: their Compositional Variability and Modes of Origin. *Journal of Petrology*, n. 52, p. 39 – 53, 2011.

FROST, C. D.; FROST, B. R.; BEARD, J. S. On silica-rich granitoids and their eruptive equivalents. *American Mineralogist*, n. 101, p. 1268 – 1284, 2016.

GIOIA, S. M. C. L.; PIMENTEL, M. M. The Sm-Nd isotopic method in the geochronology laboratory of the university of Brasília. *Anais da Academia Brasileira de Ciências*, v. 2, n. 72, p. 219 – 245, 2000.

GOODENOUGH, K. M. et al. Postcollisional Pan-African granitoids and rare-metal pegmatites in western Nigeria: age, petrogenesis and the pegmatite conundrum. *Lithos*, n. 200, p. 22 – 34, 2014.

GRIFFIN, W. L. et al. The Hf isotope composition of cratonic mantle: LAM-MC-ICPMS analysis of zircon megacrysts in kimberlites. *Geochimica et Cosmochimica Acta*, n. 64, p. 133 – 147, 2000.

GUIMARÃES, I. P. et al. Tonian granitic magmatism of the Borborema Province: A review. *Journal of South American Earth Sciences*, n. 68, p. 97 – 112, 2016.

GUIMARAES, I. P. et al. U-Pb zircon ages of orthogneisses and supracrustal rocks of the Cariris Velhos belt: onset of Neoproterozoic rifting in the Borborema Province, NE Brazil. *Precambrian Research*, v. 192-195, p. 52 – 77, 2012.

GUIMARÃES, I. P. et al. Brasiliano (Pan-African) granitic magmatism in the Pajeú-Paraíba belt, Northeast Brazil: an isotopic and geochronological approach. *Precambrian Research*, n. 135, p. 23 – 53, 2004.

GUIMARÃES, I. P. et al. U-Pb SHRIMP data constraints on calc-alkaline granitoids with 1.3-1.6 Ga Nd TDM model ages from the central domain of the Borborema province, NE Brazil. *Journal of South American Earth Sciences*, n. 31, p. 383 – 396, 2011.

GUIMARÃES, I. P. et al. Trans-alkaline magmatism in the Serrinha-Pedro Velho complex, Borborema province, NE Brazil and its correlations with the magmatism in eastern Nigeria. *Gondwana Research*, n. 15, p. 98 – 110, 2009.

GUIMARÃES, I. P.; SILVA FILHO, A. F. da; ARMSTRONG, R. Origin and age of coeval gabbros and leucogranites in the northern supbrovince of the Borborema Province, NE Brazil. *Journal of South American Earth Sciences*, n. 76, p. 71 – 93, 2017.

GUIMARÃES, I. P. et al. Petrogenesis of A-type granitoids from Alto Moxotó and Alto Pajeú terranes of the Borborema Province, NE Brazil: constraints from geochemistry and isotopic compositions. *Gondwana Research*, n. 8, p. 347 – 362, 2005.

HAGEN-PETER, G.; COTTLE, J. M. Synchronous alkaline and subalkaline magmatism during the late Neoproterozoic–early Paleozoic Ross orogeny, Antarctica: Insights into magmatic sources and processes within a continental arc. *Lithos*, n. 262, p. 677 – 698, 2016.

HILDRETH, W.; HALLIDAY, A. N.; CHRISTIANSEN, R. L. Isotopic and chemical evidence concerning the genesis and contamination of basaltic and rhyolitic magma beneath the Yellowstone plateau volcanic field. *Journal of Petrology*, n. 32, p. 63 – 138, 1991.

HILL, M. et al. Geochemical characteristics and origin of the Lebowa granite suite, Bushveld Complex. *International Geology Review*, n. 38, p. 195 – 227, 1996.

HOLLAND, T.; BLUNDY, J. Non-ideal interactions in calcic amphiboles and their bearing on amphibole-plagioclase thermometry. *Contributions to Mineralogy and Petrology*, n. 116, p. 433 – 447, 1994.

HOLLANDA, M. H. B.; PIMENTEL, M. M.; SÁ, E. F. J. de. Paleoproterozoic subduction-

related metasomatic signatures in the lithospheric mantle beneath NE Brazil: inferences from trace element and Sr–Nd–Pb isotopic compositions of Neoproterozoic high-K igneous rocks. *Journal of South American Earth Sciences*, n. 15, p. 885 – 900, 2003.

HOLLANDA, M. H. B. M. et al. Detrital zircon ages and Nd isotope compositions of the Serido and Lavras da Mangabeira basins (Borborema Province, NE Brazil): evidence for exhumation and recycling associated with a major shift in sedimentary provenance. *Precambrian Research*, n. 258, p. 186 – 207, 2015.

HOLLANDA, M. H. B. M. et al. Cambrian mafic o felsic magmatism and its connections with transcurrent shear zones of the Borborema Province (NE Brazil): Implications for the late assembly of West Gondwana. *Precambrian Research*, v. 178, p. 1 – 14, 2010.

HOLLANDA, M. H. B. M. et al. Long lived Paleoproterozoic granitic magmatism in the Serido-Jaguaribe domain, Borborema Province NE Brazil. *Journal of South American Earth Sciences*, n. 32, p. 287 – 300, 2011.

HOLLANDA, M. H. B. M. et al. Age of the granitic magmatism and the W-Mo mineralizations in skarns of the Seridó belt (NE Brazil) based on zircon U-Pb (SHRIMP) and Re-Os determinations. *Journal of South American Earth Sciences*, v. 79, p. 1 – 11, 2017.

ISHIHARA, S. Magnetite-series and ilmenite-series granitic rocks. *Mining Geology*, n. 27, p. 293 – 305, 1977.

JOHAN, Z.; JOHAN, V. Oxyfl uorures de terres rares de la coupole granitique de Cínovec (Zinnwald), República tchèque. *Academie Sciences de Paris*, n. 318, p. 1225 – 1231, 1994.

JOHAN, Z.; JOHAN, V. Accessory minerals of the Cı´novec (Zinnwald) granite cupola, Czech Republic: indicators of petrogenetic evolution. *Mineralogy and Petrology*, n. 83, p. 113 – 150, 2005.

KILPATRICK, J. A.; ELLIS, D. J. C-type magmas: igneous charnockites and their extrusive equivalents. *Transactions of the Royal Society of Edinburgh: Earth Sciences*, n. 83, p. 155 – 164, 1992.

KING, P. L. et al. Characterization and origin of aluminous A-type granites from the Lachlan Fold Belt, Southeastern Australia. *Journal of Petrology*, n. 38, p. 371 – 391, 1997.

KISTERS, A. F. M. et al. Timing and kinematics of the Colenso Fault: The Early Paleozoic shift from collisional to extensional tectonics in the Pan-African Saldania Belt, South Africa. *South African Journal of Geology*, n. 105, p. 257 – 270, 2002.

KLEEMAN, G. J.; TWIST, D. The compositionally zoned sheet-like granite pluton of the Bushveld Complex: Evidence bearing on the nature of A-type magmatism. *Journal of Petrology*, n. 30, p. 1383 – 1414, 1989.

KOZUCH, M. *Isotopic and Trace Element Geochemistry of Early Neoproterozoic Gneissic and Metavolcanic Rocks in the Cariris Velhos Orogen of the Borborema Province, Brazil and Their Bearing Tectonic Setting*. 2003. Tese (Doutorado) — Kansas University.

L., P. L.; F., R. P. Y. Retrograde metamorphic reactions in deforming granites and the origin of flame perthite. *Journal of Metamorphic Geology*, n. 14, p. 645 – 658, 1995.

LAGES, G. A. et al. Geocronologia e aspectos estruturais e petrologicos do Pluton Bravo, Domínio Central da Província Borborema, Nordeste do Brasil: um granito transalcalino precoce

no estágio pos-colisional da Orogenese Brasiliana. *Brazilian Journal of Geology*, v. 1, n. 46, p. 41 – 61, 2016.

LEAKE, B. E. et al. Nomenclature of amphiboles: Report of the subcommittee on amphiboles of the International Mineralogical Association, Commission on new minerals and mineral names. *American Mineralogist*, n. 82, p. 1019 – 1037, 1997.

LIÉGEOIS, J. P.; BLACK, R. Pétrographie et géochronologie Rb–Sr de la transition calco-alcaline–alcaline fini-Panafricaine dans l'Adrar des Iforas (Mali): Accrétion crustale au Précambrien supérieur. *African geology*, p. 115 – 145, 1984.

LIMA, J. V. et al. Geochemical and isotopic characterization of the granitic magmatism along the Remígio-Pocinhos shear zone, Borborema Province, NE Brazil. *Journal of South American Earth Sciences*, n. 75, p. 116 – 133, 2017.

LOISELLE, M. C.; WONES, D. R. Characteristics and origin of anorogenic granites. In: ANNUAL MEETINGS OF THE GEOLOGICAL SOCIETY OF AMERICA AND ASSOCIATED SOCIETIES, 1979, San Diego. *Abstracts*. San Diego, 1979. v. 11, p. 468 –.

LOURO, V. H. A.; RIBEIRO, V. B.; MANTOVANI, M. S. M. Geophysical exploration of the Buraco da Velha deposit (RO, Brazil). In: 13TH INTERNATIONAL CONGRESS OF THE BRAZILIAN GEOPHYSICAL SOCIETY & EXPOGEF, 2013, Rio de Janeiro, RJ. Rio de Janeiro, RJ, 2013. p. 144 –.

LTDA, C. L. E. e Prospecções S.A./ PROSPECTORS Aerolevantamentos e S. *Projeto Aerogeofísico Borda Leste do Planalto da Borborema*. [S.l.], 2008.

LTDA, C. L. E. e Prospecções S.A./ PROSPECTORS Aerolevantamentos e S. *Projeto Aerogeofísico Pernambuco - Paraíba - Rio Grande do Norte*. [S.l.], 2010.

MANIAR, P. D.; PICCOLI, P. M. Tectonic discrimination of granitoids. *Geological Society of America Bulettin*, n. 101, p. 635 – 643, 1989.

MARIANO, G. et al. Diorites of the high-K calc-alkalic Association: geochemistry and Sm–Nd data and Implications for the evolution of the Borborema Province, Northeast Brazil. *International Geology Review*, n. 43, p. 921 – 929, 2001.

MARTINS, G.; OLIVEIRA, E. P.; LAFON, J. M. The Algodões amphibolite-tonalite gneiss sequence, Borborema Province, NE Brazil: Geochemical and geochronological evidence for Palaeoproterozoic accretion of oceanic plateau/back-arc basalts and adakitic plutons. *Gondwana Research*, n. 15, p. 71 – 85, 2009.

MARTINS, G. et al. Geochemistry and geochronology of the Algodões sequence, Ceará, NE Brazil: a paleoproterozoic magmatic arc in the Central Ceará domain of the Borborema Province? In: 40º CONGRESSO BRASILEIRO DE GEOLOGIA, 1998, Belo Horizonte. Belo Horizonte, 1998.

MATTEINI, M. et al. Combined U-Pb and Lu-Hf isotope analyses by laser ablation MC-ICP-MS: methodology and applications. *Anais da Academia Brasileira de Ciências*, v. 2, n. 82, p. 479 – 491, 2010.

MCKENZIE, D. Some remarks on the development of sedimentary basins. *Earth and Planetary Science Letters*, n. 40, p. 25 – 32, 1978.

MELO, S. C. *Petrologia e geoquímica dos granitóides do Complexo Prata a nordeste de*

Monteiro-PB. 1997. Dissertação (Mestrado) — Universidade Federal de Pernambuco.

MIYASHIRO, A. Volcanic rock series in island arcs and active continental margins. *Journal of American Science*, n. 274, p. 321 – 355, 1970.

MONIÉ, P.; CABY, R.; ARTHAUD, M. H. The Neoproterozoic Brasiliano Orogeny in Northeast Brazil: 40Ar/39Ar and petrostructural data from Ceará. *Precambrian Research*, n. 81, p. 241 – 264, 1997.

NAKAMURA, N. Determination of REE, Ba, Fe, Mg, Na, and K in carbonaceous and ordinary chondrites. *Geochimica et Cosmochimica Acta*, n. 38, p. 757 – 775, 1974.

NEVES, B. B. B. et al. Idades U-Pb em zircao de alguns granitos clássicos da Província Borborema. *Geologia USP Série Científica*, v. 3, p. 25 – 38, 2003.

NEVES, B. B. B. et al. O "Sistema Pajeú-Paraíba" e o "Maciço" Sao José do Campestre no leste da Borborema. *Revista Brasileira de Geociências*, v. 2, n. 31, p. 173 – 184, 2001.

NEVES, B. B. B.; SANTOS, E. J.; SCHMUS, W. R. V. Tectonic history of the Borborema Province, northeastern Brazil. *Tectonic Evolution of South America*, v. 1, p. 151 – 182, 2000.

NEVES, B. B. B. et al. O evento Cariris Velhos na Província Borborema: integração de dados, implicações e perspectivas. *Revista Brasileira de Geociências*, n. 25, p. 279 – 296, 1995.

NEVES, S. P. Proterozoic history of the Borborema Province (NE Brazil): correlations with neighboring cratons and Pan-African belts, and implications for the evolution of western Gondwana. *Tectonics*, n. 22, p. 1031 –, 2003.

NEVES, S. P. Atlantica revisited: new data and thoughts on the formation and evolution of a long-lived continente. *International Geology Review*, v. 53, p. 1377 – 1391, 2011.

NEVES, S. P. Constraints from zircon geochronology on the tectonic evolution of the Borborema Province (NE Brazil): widespread intracontinental Neoproterozoic reworking of a Paleoproterozoic accreationary orogeny. *Journal of South American Earth Sciences*, v. 58, p. 150 – 164, 2015.

NEVES, S. P. et al. Timing of crust formation, deposition of supracrustal sequences, and Transamazonian and Brasiliano metamorphism in the East Pernambuco belt (Borborema Province, NE Brazil): implications for western Gondwana assembly. *Precambrian Research*, n. 146, p. 197 – 216, 2006.

NEVES, S. P. et al. Paleoproterozoic accretionary and collisional processes and the build-up of the Borborema Province (NE Brazil): Geochronological and geochemical evidence from the Central Domain. *Journal of South American Earth Sciences*, n. 58, p. 165 – 187, 2015.

NEVES, S. P.; MARIANO, G. High-K calc-alkalic plutons in Northeast Brazil: origin of the biotite diorite/quartz monzonite to granite association and implications for the evolution of the Borborema Province. *International Geology Review*, n. 39, p. 621 – 638, 1997.

NEVES, S. P.; MARIANO, G. Heat-producing elements-enriched continental mantle lithosphere and Proterozoic intracontinental orogens: insights from Brasiliano/PanAfrican Belts. *Gondwana Research*, v. 2, n. 7, p. 427 – 436, 2004.

NEVES, S. P. et al. 70 m.y. of synorogenic plutonism in eastern Borborema Province (NE Brazil): temporal and kinematic constraints on the Brasiliano Orogeny. *Geodinamica Acta*, n. 19,

p. 213 – 237, 2006.

NEVES, S. P. et al. Intralithospheric differentiation and crustal growth: evidence from the Borborema province, northeastern Brazil. *Geology*, n. 28, p. 519 – 522, 2000.

NEVES, S. P.; VAUCHEZ, A.; ARCHANJO, C. J. Shear zone-controlled magma emplacement or magma-assisted nucleation of shear zones? Insights from northeast Brazil. *Tectonophysics*, n. 262, p. 349 – 364, 1996.

NEVES, S. P.; VAUCHEZ, A.; FERAUD, G. Tectono-thermal evolution, magma emplacement, and shear zone development in the Caruaru area (Borborema Province, NE Brazil). *Precambrian Research*, n. 99, p. 1 – 32, 2000.

OLIVEIRA, D. C.; MOHRIAK, W. U. Jaibaras trough: an important element in the early tectonic evolution of the Parnaíba interior sag basin, Northern Brazil. *Marine and Petroleum Geology*, n. 20, p. 351 – 383, 2003.

OLIVEIRA, E. P.; WINDLEY, B. F.; ARAÚJO, D. B. The Neoproterozoic Sergipano orogenic belt, NE Brazil: a complete plate tectonic cycle in western Gondwana. *Precambrian Research*, n. 181, p. 64 – 84, 2010.

ORDÓÑEZ-CASADO, B. *Geochronological studies of the Pre-Mesozoic basement of the Iberian Massif* : The Ossa Morena Zone and the Allochthonous Complexes within the Central Iberian Zone. 1998. Tese (Doutorado) — Swiss Federal Institute of Technology Zurich.

OSTROVSKY, E. A. Antagonism of radioactive elements in wallrock alteration fields and its use in aerogamma spectrometric prospescting. *International Geology Review*, n. 17, p. 461 – 468, 1975.

PAGEL, M. The mineralogy and geochemistry of uranium, thorium, and rare-earth elements in two radioactive granits in the Vosges, France. *Mineralogical Magazine*, n. 46, p. 149 – 161, 1982.

PEACOCK, M. A. Classification of igneous rock series. *Journal of Geology*, n. 25, p. 54 – 67, 1931.

PEARCE, J. Sources and setting of granitic rocks. *Episodes*, v. 4, n. 19, p. 120 – 125, 1996.

PEARCE, J. A.; HARRIS, N. B. W.; TINDLE, A. G. Trace element discrimination diagrams for the tectonic interpretation of granitic rocks. *Journal of Petrology*, n. 25, p. 956 – 983, 1984.

PEDROSA JR., N. C. et al. Structural framework of the Jaibaras Rift, Brasil, based on geophysical data. *Journal of South American Earth Sciences*, n. 58, p. 318 – 334, 2015.

PEREIRA, M. F. et al. Tracing the Cadomian magmatism with detrital/inherited zircon ages by in-situ U–Pb SHRIMP geochronology (Ossa-Morena Zone, SW Iberian Massif). *Lithos*, n. 123, p. 204 – 217, 2011.

PICHAVANT, M. et al. The Miocene-Pliocene Macsani Volcanics, SE Peru II. Geochemistry and origin of a felsic peraluminous magma. *Contributions to Mineralogy and Petrology*, n. 100, p. 325 – 338, 1988.

PIETRANIK, A. B. et al. Episodic, mafic crust formation from 4.5 to 2.8 Ga: new evidence from detrital zircons, Slave craton, Canada. *Geology*, v. 11, n. 36, p. 875 – 878, 2008.

PISTONE, M. et al. Textural and chemical consequences of interactions between hydrous mafic

and felsic magmas: an experimental study. *Contributions to Mineralogy and Petrology*, n. 171, p. 8 –, 2015.

PITCHER, W. S. *Nature and Origin of Granite*. London - Glasgow: Chapman and Hall, 1993. 321p.

RIBEIRO, V. B.; MANTOVANI, M. S. M.; LOURO, V. H. A. Aerogamaespectrometria e suas aplicações no mapeamento geológico. *Terrae Didática*, n. 10, p. 29 – 51, 2013.

RIBERIO, V. B.; MANTOVANI, M. S. M. Gamma Spectrometric and Magnetic Interpretation of Cabaçal Copper Deposit in Mato Grosso (Brazil): Implications for hydrothermal fluids remobilization. *Journal of Applied Geophysics*, v. 135, p. 223 – 231, 2016.

RICHARD, P.; SHIMIZU, N.; ALLEGRE, C. J. 143Nd/144Nd, a natural tracer: an application to oceanic basalts. *Earth and Planetary Science Letters*, n. 31, p. 269 – 278, 1976.

S., S. S.; F., M. W. Chemical and isotopic systematics of oceanic basalts: implications for mantle composition and processes. *Geological Society*, n. 42, p. 313 – 345, 1989.

SÁ, E. F. J. de et al. Geochronology of metaplutonics and the evolution of supracrustal belts in the Borborema province. In: VII LATINO-AMERICANO GEOLOGICAL CONGRESS, 1988. [S.l.], 1988. p. 49 – 62.

SÁ, J. M. et al. Geochemistry and geochronology of pre-Brasiliano rocks from the Transversal Zone, Borborema Province, Northeast Brazil. *Journal of South American Earth Sciences*, n. 14, p. 851 – 866, 2002.

SÁ, J. M.; MCREATH, I.; LETERRIER, J. Petrology, geochemistry and tectonic setting of Proterozoic Igneous suites of the Orós fold belt (Borborema Province, Northeast Brazil). *Journal of South American Earth Sciences*, n. 8, p. 299 – 314, 1995.

SANTOS, E. J. *O complexo granítico Lagoa das Pedras*: Acresção e colisão na região de Floresta (Pernambuco) Província da Borborema. 1995. Tese (Doutorado) — Universidade de Sao Paulo.

SANTOS, E. J.; MEDEIROS, W. C. Constraints from granitic plutonism on Proterozoic crustal growth of the Transverse Zone, Borborema Province, NE Brazil. *Revista Brasileira de Geociências*, v. 29, n. 1, p. 73 – 84, 1999.

SANTOS, L. et al. Magmatismo Ediacarano extensional na Província Borborema, NE Brasil: Pluton Serra Branca. *Comunicações Geológicas*, n. 101, p. 199 – 203, 2014.

SANTOS, L. C. M. L. et al. Early to late Paleoproterozoic magmatism in NE Brazil: the Alto Moxoto Terrane and its tectonic implications for the pre-Western Gondwana assembly. *Journal of South American Earth Sciences*, n. 58, p. 188 – 209, 2015.

SANTOS, T. J. S. et al. Neoproterozoic tectonic and magmatic episodes in the NW sector of Borborema Province, NE Brazil, during assembly of Western Gondwana. *Journal of South American Earth Sciences*, n. 25, p. 271 – 284, 2008.

SANTOS, T. J. S.; FETTER, A. H.; NOGUEIRA NETO, J. A. Comparisons between the northwestern Borborema Province, NE Brazil, and the southwestern Pharusian-Dahomey Belt, SW Central Africa. *Geological Society*, n. 294, p. 101 – 120, 2008.

SCHMUS, W. R. V.; KOZUCH, M.; NEVES, B. B. B. Precambrian history of the Zona

transversal of the Borborema province, NE Brazil: insights from Sm/Nd and U/Pb geochronology. *Journal of South American Earth Sciences*, n. 31, p. 227 – 252, 2011.

SCHMUS, W. R. V. et al. U/Pb and Sm/Nd geochronologic studies of Eastern Borborema Province, northeastern Brazil: initial conclusions. *Journal of South American Earth Sciences*, n. 8, p. 267 – 288, 1995.

SCHMUS, W. R. V. et al. Proterozoic links between the Borborema province, NE Brazil, and the central African fold belt. *Geological Society*, n. 294, p. 69 – 99, 2008.

SIAL, A. N. Granite-types of Northeast Brazil: current knowledge. *Revista Brasileira de Geociências*, n. 16, p. 54 – 72, 1986.

SIAL, A. N.; FERREIRA, V. P. Brasiliano age peralkalic plutonic rocks of the Central Structural Domain, Northeast Brazil. *Rendiconti della Società Italiana di Mineralogia e Petrologia*, n. 43, p. 307 – 342, 1988.

SIAL, A. N.; FERREIRA, V. P. Magma associations in ediacaran granitoids of the Cachoeirinha-Salgueiro and Alto Pajeú terranes, northeastern Brazil: Forty years of studies. *Journal of South American Earth Sciences*, n. 68, p. 113 – 133, 2015.

SIAL, A. N.; FERREIRA, V. P.; SANTOS, E. J. Magmatic Epidote-bearing Granitoids and Ultrapotassic Magmatism of the Borborema Province, NE Brazil. In: SECOND INTERNATIONAL SYMPOSIUM ON GRANITES AND ASSOCIATED MINERALIZATIONS (ISGAM), 1997, Salvador, BA. Salvador, BA, 1997. p. 33 – 54.

SIAL, A. N. et al. Geochronological and mineralogical constraints on depth of emplacement and ascension rates of epidote-bearing magmas from northeastern Brazil. *Lithos*, n. 105, p. 225 – 238, 2008.

SILVA FILHO, A.; GUIMARÃES, I. P.; THOMPSON, R. N. Shoshonitic and ultrapotassic Proterozoic suites in the Cachoeirinha –Salgueiro fold Belt, NE Brazil: a transition from collisional to post-collisional magmatism. *Precambrian Research*, n. 62, p. 323 – 342, 1993.

SILVA FILHO, A. F. et al. Ediacaran Aguas Belas pluton, Northeastern Brazil: evidence on age, emplacement and magma sources during Gondwana amalgamation. *Gondwana Research*, n. 17, p. 676 – 687, 2010.

SILVA FILHO, A. F. et al. Geochemistry, U-Pb geochronology, Sm-Nd and O isotopes of ca. 50my long Ediacaran High-K Syn-Collisional magmatism in the Pernambuco-Alagoas Domain, Borborema Province, NE Brazil. *Journal of South American Earth Sciences*, n. 68, p. 134 – 154, 2016.

SILVA, T. R. et al. Two-stage mantle derived granitic rocks and the onset of the Brasiliano orogeny: Evidence from Sr, Nd, and O isotopes. *Lithos*, n. 264, p. 189 – 200, 2016.

SKJERLIE, K. P.; JOHNSTON, A. D. Fluid-absent melting behavior of an F-rich tonalitic gneiss at mid-crustal pressures: Implications for the generation of anorogenic granites. *Journal of Petrology*, n. 34, p. 785 – 815, 1993.

SODERLUND, U. et al. The 176Lu decay constant determined by Lu-Hf and U-Pb isotope systematics of Precambrian mafic intrusions. *Earth and Planetary Science Letters*, n. 219, p. 311 – 324, 2004.

SOUZA, Z. S. et al. Calc-alkaline magmatism at the Archean-Proterozoic Transition: the Caico

complex basement (NE Brazil). *Journal of Petrology*, n. 48, p. 2149 – 2185, 2007.

STEVENS, G.; CLEMENS, J. D. Fluid–absent melting and the roles of fluids in the lithosphere: a slanted summary? *Chemical Geology*, v. 108, p. 1 – 17, 1993.

TAGNE-KAMGA, G. Petrogenesis of the Neoproterozoic Ngondo Plutonic complex (Cameroon, west central Africa): a case of late-collisional ferro-potassic magmatism. *Journal of African Earth Sciences*, n. 36, p. 149 – 171, 2003.

THOMPSON, R. N. Magmatism of the british tertiary volcanic province. *Scottish Journal of Geology*, n. 18, p. 50 – 107, 1982.

TOTEU, S. F. et al. New U–Pb and Sm–Nd data from north-central Cameroon and its bearing on pre-Pan African history of central Africa. *Precambrian Research*, n. 108, p. 45 – 73, 2001.

ULBRICH, H. H. G. J. et al. Levantamentos Gamaespectrométricos em Granitos Diferenciados. I: Revisão da Metodologia e do Comportamento Geoquímico dos Elementos K, Th e U. *Geologia USP: Série Cientifica*, v. 1, n. 9, p. 33 – 53, 2009.

VAUCHEZ, A. et al. The Borborema shear zone system, NE Brazil. *Journal of South American Earth Sciences*, n. 8, p. 247 – 266, 1995.

VERVOORT, J. D.; KEMP, A. I. S. Clarifying the zircon Hf isotope record of crust-mantle evolution. *Chemical Geology*, v. 425, p. 65 – 75, 2016.

VISONA, D.; LOMBARDO, B. Two-mica and tourmaline leucogranites from the Everest-Makalu region (Nepal-Tibet). Himalayan leucogranite genesis by isobaric heating? *Lithos*, n. 62, p. 125 – 150, 2002.

WATSON, E. B.; HARRISON, T. M. Zircon saturation revisited: temperature and composition effects in a variety of crustal magma types. *Earth and Planetary Science Letters*, n. 64, p. 295 – 304, 1983.

WEDEPOHL, K. H. Chemical composition and fractionation of the continental crust. *Geologische Rundschau*, v. 80, p. 207 – 223, 1991.

WHALEN, J. B.; CURRIE, K. L.; CHAPPELL, B. W. A-type granites: geochemical characteristics, discrimination and petrogenesis. *Contibutions to mineralogy and petrology*, n. 95, p. 407 – 419, 1987.

WHITE, A. J. R. Sources of Granitic Magma. In: ANNUAL MEETINGS OF THE GEOLOGICAL SOCIETY OF AMERICA AND ASSOCIATED SOCIETIES, 1979, San Diego. *Abstracts*. San Diego, 1979. v. 11, p. 539 –.

WIT, M. J. D. et al. *Geological Map of Sectors of Gondwana, Reconstructed to Their Disposition 150 Ma*. Tulsa, USA, 1998.

WONES, D. R. Mafic silicates as indicators of intensive variables in granitic magmas. *Mining Geology*, v. 31, p. 191 – 212, 1981.

WONES, D. R. Significance of the assemblage titanite + magnetite + quartz in Granitic rocks. *American Mineralogist*, n. 74, p. 744 – 749, 1989.

YOUNG, D. A. *Mind over Magma. The Story of Igneous Petrology*. Princeton and Oxford: Princeton University Press, 2003. 686p.

APÊNDICE A – DADOS DE ANÁLISE *IN SITU* POR MICROSSONDA ELETRÔNICA

A. 1 – BIOTITAS

Aroeiras Complex					
Sample	ARO1-8-1N	ARO1-8	ARO1-1-1	ARO1-1-2	ARO1-2
SiO2	34.01	34.17	35.16	34.64	33.48
TiO2	1.91	2.28	2.45	2.83	1.67
Al2O3	15.81	15.50	16.05	15.41	15.73
FeO	27.16	27.58	26.14	26.78	27.59
MnO	0.44	0.47	0.32	0.29	0.38
MgO	4.62	4.53	4.70	4.61	4.71
CaO	0.02	0.05	0.02	0.01	0.05
Na2O	0.10	0.07	0.09	0.09	0.12
K2O	9.15	9.16	9.32	9.22	8.97
F	0.23	0.23	0.36	0.32	0.12
Cl	0.15	0.12	0.09	0.13	0.11
BaO	0.02	0.17	0.11	0.10	0.10
Total	93.61	94.31	94.80	94.43	93.04
Cations on the basis of 24(O)					
Si	5.55	5.55	5.62	5.59	5.51
Al iv	2.45	2.45	2.38	2.41	2.49
Al vi	0.59	0.52	0.65	0.52	0.56
Ti	0.23	0.28	0.29	0.34	0.21
Fe	3.71	3.75	3.49	3.62	3.80
Mn	0.06	0.06	0.04	0.04	0.05
Mg	1.12	1.10	1.12	1.11	1.16
Ca	0.00	0.01	0.00	0.00	0.01
Na	0.03	0.02	0.03	0.03	0.04
K	1.91	1.90	1.90	1.90	1.88
Ba	0.00	0.01	0.01	0.01	0.01
OH*	3.84	3.85	3.79	3.81	3.91
F	0.12	0.12	0.18	0.16	0.06
Cl	0.04	0.03	0.03	0.03	0.03
Al total	3.04	2.97	3.02	2.93	3.05
Fe/Fe+Mg	0.77	0.77	0.76	0.77	0.77

Aroeiras Complex			
Sample	ARO1A-1	ARO1A-2	ARO1A-5
SiO2	34.94	34.91	34.54
TiO2	2.04	2.23	2.26
Al2O3	15.35	15.23	15.32
FeO	27.06	27.96	27.15
MnO	0.35	0.33	0.31
MgO	5.66	5.35	5.41
CaO	0.00	0.05	0.07
Na2O	0.07	0.06	0.03
K2O	9.23	9.02	9.00
F	0.40	0.26	0.54
Cl	0.14	0.11	0.10
BaO	0.17	0.22	0.20
Total	95.41	95.72	94.92
Cations on the basis of 24(O)			
Si	5.59	5.58	5.57
Al iv	2.41	2.42	2.43
Al vi	0.49	0.45	0.48
Ti	0.25	0.27	0.27
Fe	3.62	3.74	3.66
Mn	0.05	0.04	0.04
Mg	1.35	1.27	1.30
Ca	0.00	0.01	0.01
Na	0.02	0.02	0.01
K	1.88	1.84	1.85
Ba	0.01	0.01	0.01
OH*	3.76	3.84	3.70
F	0.20	0.13	0.28
Cl	0.04	0.03	0.03
Al total	2.90	2.87	2.91
Fe/Fe+Mg	0.73	0.75	0.74

Aroeiras Complex						
Sample	ARO1B-4	ARO1B-6-1	ARO1B-6-2	ARO1B-4-N	ARO1B-1-1	ARO1B-1-2
SiO2	35.57	34.68	35.02	34.87	34.80	35.07
TiO2	2.14	2.19	2.42	2.47	1.89	2.22
Al2O3	14.78	14.63	15.05	14.86	15.74	15.31
FeO	25.36	25.02	25.39	24.97	25.11	25.37
MnO	0.37	0.24	0.31	0.33	0.27	0.33
MgO	6.16	6.19	6.21	6.17	5.99	5.99
CaO	0.05	0.06	0.04	0.04	0.02	0.00
Na2O	0.05	0.08	0.08	0.05	0.07	0.06
K2O	8.97	8.96	9.11	9.08	8.92	9.06
F	0.32	0.35	0.40	0.55	0.44	0.53
Cl	0.13	0.11	0.11	0.12	0.12	0.12
BaO	0.28	0.16	0.18	0.17	0.19	0.21
Total	94.17	92.66	94.32	93.67	93.56	94.28
Cations on the basis of 24(O)						
Si	5.71	5.66	5.62	5.64	5.62	5.64
Al iv	2.29	2.34	2.38	2.36	2.38	2.36
Al vi	0.50	0.48	0.47	0.47	0.61	0.54
Ti	0.26	0.27	0.29	0.30	0.23	0.27
Fe	3.40	3.42	3.41	3.38	3.39	3.41
Mn	0.05	0.03	0.04	0.05	0.04	0.04
Mg	1.47	1.50	1.49	1.49	1.44	1.43
Ca	0.01	0.01	0.01	0.01	0.00	0.00
Na	0.01	0.03	0.03	0.02	0.02	0.02
K	1.83	1.86	1.86	1.87	1.84	1.86
Ba	0.02	0.01	0.01	0.01	0.01	0.01
OH*	3.80	3.79	3.77	3.69	3.74	3.70
F	0.16	0.18	0.20	0.28	0.23	0.27
Cl	0.04	0.03	0.03	0.03	0.03	0.03
Al total	2.80	2.81	2.85	2.83	3.00	2.90
Fe/Fe+Mg	0.70	0.69	0.70	0.69	0.70	0.70

Aroeiras Complex					
Sample	ARO1B-2-1N	ARO1B-2-2N	ARO1B-2	ARO1B-7-N	ARO1B-7
SiO2	34.89	35.30	34.86	34.93	34.79
TiO2	2.67	2.19	3.00	2.16	1.62
Al2O3	14.49	15.07	14.58	14.97	15.10
FeO	25.06	25.09	25.62	25.57	25.54
MnO	0.25	0.31	0.28	0.29	0.31
MgO	6.17	6.25	5.73	6.12	6.58
CaO	0.00	0.02	0.01	0.01	0.02
Na2O	0.09	0.07	0.07	0.07	0.05
K2O	9.03	9.13	8.93	9.23	9.29
F	0.62	0.41	0.44	0.48	0.63
Cl	0.18	0.13	0.12	0.14	0.11
BaO	0.20	0.20	0.23	0.13	0.17
Total	93.64	94.18	93.86	94.10	94.22
Cations on the basis of 24(O)					
Si	5.66	5.67	5.64	5.64	5.62
Al iv	2.34	2.33	2.36	2.36	2.38
Al vi	0.43	0.52	0.41	0.48	0.49
Ti	0.33	0.26	0.36	0.26	0.20
Fe	3.40	3.37	3.46	3.45	3.45
Mn	0.03	0.04	0.04	0.04	0.04
Mg	1.49	1.50	1.38	1.47	1.59
Ca	0.00	0.00	0.00	0.00	0.00
Na	0.03	0.02	0.02	0.02	0.02
K	1.87	1.87	1.84	1.90	1.91
Ba	0.01	0.01	0.01	0.01	0.01
OH*	3.63	3.76	3.74	3.72	3.65
F	0.32	0.21	0.23	0.24	0.32
Cl	0.05	0.03	0.03	0.04	0.03
Al total	2.77	2.85	2.78	2.85	2.87
Fe/Fe+Mg	0.70	0.69	0.71	0.70	0.69

Aroeiras Complex				
Sample	ARO41-1	ARO41-2	ARO41-3	ARO41-4
SiO2	35.07	34.88	34.95	34.63
TiO2	2.58	1.97	2.26	2.76
Al2O3	15.39	15.44	15.36	15.22
FeO	29.79	29.60	30.06	29.44
MnO	0.38	0.42	0.37	0.39
MgO	4.64	4.97	4.56	4.49
CaO	0.02	0.00	0.01	0.08
Na2O	0.03	0.07	0.02	0.05
K2O	9.80	9.87	9.67	9.71
F	0.21	0.41	0.18	0.45
Cl	0.11	0.09	0.11	0.07
BaO	0.10	0.09	0.11	0.07
Total	98.13	97.81	97.65	97.36
Cations on the basis of 24(O)				
Si	5.48	5.49	5.50	5.48
Al iv	2.52	2.51	2.50	2.52
Al vi	0.32	0.35	0.34	0.31
Ti	0.30	0.23	0.27	0.33
Fe	3.89	3.89	3.95	3.89
Mn	0.05	0.06	0.05	0.05
Mg	1.08	1.17	1.07	1.06
Ca	0.00	0.00	0.00	0.01
Na	0.01	0.02	0.01	0.01
K	1.95	1.98	1.94	1.96
Ba	0.01	0.01	0.01	0.00
OH*	3.86	3.77	3.88	3.76
F	0.11	0.20	0.09	0.22
Cl	0.03	0.02	0.03	0.02
Al total	2.84	2.86	2.85	2.84
Fe/Fe+Mg	0.78	0.77	0.79	0.79

Aroeiras Complex				
Sample	ARO41-5	ARO41-6	ARO41-7	ARO41-8
SiO2	35.10	34.79	34.89	34.88
TiO2	2.41	2.72	2.90	2.80
Al2O3	15.78	15.33	15.31	15.56
FeO	29.61	29.41	29.44	29.03
MnO	0.40	0.44	0.40	0.34
MgO	4.63	4.37	4.21	4.50
CaO	0.04	0.02	0.00	0.00
Na2O	0.03	0.06	0.04	0.05
K2O	9.76	9.78	9.94	9.80
F	0.36	0.46	0.43	0.42
Cl	0.07	0.10	0.10	0.13
BaO	0.12	0.09	0.13	0.15
Total	98.31	97.57	97.80	97.65
Cations on the basis of 24(O)				
Si	5.47	5.49	5.49	5.48
Al iv	2.53	2.51	2.51	2.52
Al vi	0.37	0.34	0.33	0.36
Ti	0.28	0.32	0.34	0.33
Fe	3.86	3.88	3.87	3.81
Mn	0.05	0.06	0.05	0.05
Mg	1.08	1.03	0.99	1.05
Ca	0.01	0.00	0.00	0.00
Na	0.01	0.02	0.01	0.02
K	1.94	1.97	2.00	1.96
Ba	0.01	0.01	0.01	0.01
OH*	3.80	3.74	3.76	3.76
F	0.18	0.23	0.22	0.21
Cl	0.02	0.03	0.03	0.03
Al total	2.90	2.85	2.84	2.88
Fe/Fe+Mg	0.78	0.79	0.80	0.78

Serra Branca – Coxixola dike swarms					
Sample	MA05_Biot_1	MA05_Biot_2	MA05_Biot_3	MA05_Biot_4	MA05_Biot_5
SiO2	36.14	35.88	35.41	35.32	35.51
TiO2	3.17	2.72	2.83	2.60	2.59
Al2O3	14.64	14.96	14.76	14.68	14.53
FeO	24.39	23.85	25.56	24.70	24.64
MnO	0.26	0.27	0.27	0.25	0.27
MgO	8.23	8.62	7.46	8.05	8.44
CaO	0.07	0.05	0.07	0.05	0.07
Na2O	0.05	0.07	0.06	0.05	0.06
K2O	9.57	9.58	9.48	9.76	9.51
F	0.93	0.87	0.72	0.89	0.98
Cl	0.13	0.10	0.13	0.09	0.11
BaO	0.34	0.40	0.53	0.50	0.48
Total	97.92	97.36	97.28	96.95	97.18
Cations on the basis of 24(O)					
Si	5.53	5.51	5.50	5.51	5.51
Al iv	2.47	2.49	2.50	2.49	2.49
Al vi	0.17	0.22	0.21	0.21	0.17
Ti	0.36	0.31	0.33	0.30	0.30
Fe	3.12	3.06	3.32	3.22	3.20
Mn	0.03	0.03	0.04	0.03	0.04
Mg	1.88	1.97	1.73	1.87	1.95
Ca	0.01	0.01	0.01	0.01	0.01
Na	0.01	0.02	0.02	0.02	0.02
K	1.87	1.88	1.88	1.94	1.88
Ba	0.02	0.02	0.03	0.03	0.03
OH*	3.52	3.55	3.61	3.54	3.49
F	0.45	0.42	0.35	0.44	0.48
Cl	0.03	0.03	0.03	0.02	0.03
Al total	2.64	2.71	2.70	2.70	2.66
Fe/Fe+Mg	0.62	0.61	0.66	0.63	0.62

Serra Branca – Coxixola dike swarms				
Sample	MA05_Biot_6	MA05_Biot_7	MA05_Biot_8	MA05_Biot_9
SiO2	35.86	35.60	35.60	35.38
TiO2	3.09	3.00	2.83	2.80
Al2O3	14.41	14.83	15.11	14.69
FeO	25.04	25.42	25.74	25.38
MnO	0.27	0.30	0.31	0.33
MgO	8.11	7.74	7.50	7.58
CaO	0.05	0.02	0.06	0.07
Na2O	0.07	0.04	0.05	0.07
K2O	9.53	9.57	9.61	9.55
F	0.77	0.77	0.82	0.84
Cl	0.11	0.16	0.11	0.10
BaO	0.33	0.40	0.47	0.46
Total	97.64	97.86	98.21	97.25
Cations on the basis of 24(O)				
Si	5.52	5.49	5.48	5.51
Al iv	2.48	2.51	2.52	2.49
Al vi	0.13	0.19	0.22	0.20
Ti	0.36	0.35	0.33	0.33
Fe	3.22	3.28	3.31	3.30
Mn	0.04	0.04	0.04	0.04
Mg	1.86	1.78	1.72	1.76
Ca	0.01	0.00	0.01	0.01
Na	0.02	0.01	0.01	0.02
K	1.87	1.88	1.89	1.90
Ba	0.02	0.02	0.03	0.03
OH*	3.59	3.58	3.57	3.56
F	0.38	0.38	0.40	0.41
Cl	0.03	0.04	0.03	0.03
Al total	2.61	2.70	2.74	2.69
Fe/Fe+Mg	0.63	0.65	0.66	0.65

A. 2 – ANFIBÓLIOS

Aroeiras Complex						
Sample	ARO1-6-N	ARO1-6-B	ARO1-7-1B	ARO1-7-N	ARO1-7-2B	ARO1-3-B
SiO2	40.18	39.75	40.29	40.22	38.96	39.75
TiO2	1.29	1.03	1.23	0.89	1.02	1.17
Al2O3	9.78	10.39	9.75	10.65	11.62	9.75
FeO	26.09	26.49	25.74	26.23	26.12	26.58
MnO	0.74	0.72	0.68	0.74	0.72	0.69
MgO	3.89	3.68	4.06	3.63	3.45	4.04
CaO	10.79	10.77	10.79	10.78	10.84	10.74
Na2O	1.12	1.06	1.46	1.20	1.30	1.61
K2O	1.39	1.44	1.33	1.53	1.60	1.45
F	0.24	0.11	0.16	0.18	0.36	0.18
Cl	0.17	0.21	0.19	0.26	0.27	0.19
BaO	0.03	0.00	0.00	0.00	0.02	0.02
Total	95.70	95.66	95.66	96.33	96.27	96.17
Cations on the basis of 23(O)						
Si	6.45	6.38	6.48	6.42	6.25	6.38
Al iv	1.55	1.62	1.52	1.58	1.75	1.62
Al vi	0.31	0.34	0.33	0.42	0.45	0.23
Ti	0.16	0.12	0.15	0.11	0.12	0.14
Fe3+	0.58	0.70	0.46	0.57	0.59	0.61
Fe2+	2.93	2.85	3.00	2.93	2.92	2.96
Mn	0.10	0.10	0.09	0.10	0.10	0.09
Mg	0.93	0.88	0.97	0.86	0.82	0.97
Ca	1.86	1.85	1.86	1.84	1.86	1.85
Na	0.35	0.33	0.45	0.37	0.40	0.50
K	0.28	0.29	0.27	0.31	0.33	0.30
F	0.12	0.06	0.08	0.09	0.18	0.09
Cl	0.05	0.06	0.05	0.07	0.07	0.05
OH*	1.83	1.89	1.87	1.84	1.74	1.86
Total	17.49	17.48	17.59	17.53	17.60	17.65
(Ca+Na) (B)	2.00	2.00	2.00	2.00	2.00	2.00
Na (B)	0.14	0.15	0.14	0.16	0.14	0.15
(Na+K) (A)	0.49	0.48	0.59	0.53	0.60	0.65
Mg/(Mg+Fe2)	0.24	0.24	0.24	0.23	0.22	0.25
Fe3/(Fe3+Alvi)	0.65	0.67	0.58	0.57	0.57	0.73

Aroeiras Complex							
Sample	ARO1A-1-B.1	ARO1A-1-B.2	ARO1A-4	ARO1A-4-B	ARO1A-3-B.1	ARO1A-3-B.2	ARO1A-3-N
SiO2	39.66	39.36	40.68	40.32	40.10	39.63	40.08
TiO2	1.00	1.09	1.32	1.26	1.07	1.04	1.70
Al2O3	11.12	11.12	10.43	10.53	11.06	11.36	9.98
FeO	26.44	26.63	26.08	25.72	26.80	26.75	26.32
MnO	0.39	0.45	0.46	0.42	0.48	0.48	0.49
MgO	4.10	4.24	4.85	4.47	3.99	4.20	4.51
CaO	10.94	11.04	11.03	10.88	10.94	10.97	10.74
Na2O	1.22	1.32	1.49	1.12	1.15	1.53	1.33
K2O	1.45	1.47	1.37	1.36	1.43	1.53	1.35
F	0.14	0.22	0.46	0.30	0.16	0.26	0.18
Cl	0.23	0.20	0.18	0.19	0.18	0.20	0.18
BaO	0.00	0.00	0.00	0.00	0.00	0.00	0.00
Total	96.70	97.15	98.33	96.57	97.35	97.95	96.85
Cations on the basis of 23(O)							
Si	6.28	6.22	6.34	6.38	6.30	6.22	6.33
Al iv	1.72	1.78	1.66	1.62	1.70	1.78	1.67
Al vi	0.36	0.29	0.26	0.34	0.35	0.32	0.19
Ti	0.12	0.13	0.15	0.15	0.13	0.12	0.20
Fe3+	0.74	0.79	0.68	0.68	0.77	0.75	0.75
Fe2+	2.76	2.73	2.72	2.72	2.76	2.76	2.72
Mn	0.05	0.06	0.06	0.06	0.06	0.06	0.07
Mg	0.97	1.00	1.13	1.05	0.93	0.98	1.06
Ca	1.86	1.87	1.84	1.84	1.84	1.85	1.82
Na	0.38	0.40	0.45	0.34	0.35	0.47	0.41
K	0.29	0.30	0.27	0.27	0.29	0.31	0.27
F	0.07	0.11	0.22	0.15	0.08	0.13	0.09
Cl	0.06	0.05	0.05	0.05	0.05	0.05	0.05
OH*	1.87	1.83	1.73	1.80	1.87	1.82	1.86
Total	17.53	17.57	17.56	17.46	17.48	17.62	17.50
(Ca+Na) (B)	2.00	2.00	2.00	2.00	2.00	2.00	2.00
Na (B)	0.14	0.13	0.16	0.16	0.16	0.15	0.18
(Na+K) (A)	0.53	0.57	0.56	0.46	0.48	0.62	0.50
Mg/(Mg+Fe2)	0.26	0.27	0.29	0.28	0.25	0.26	0.28
Fe3/(Fe3+Alvi)	0.67	0.73	0.73	0.67	0.69	0.70	0.80

Aroeiras Complex						
Sample	ARO1A-1-B	ARO1A-1-N	ARO1A-2-B	ARO1A-2	ARO1A-4-B	ARO1A-4-N
SiO2	40.33	40.84	40.39	40.84	40.14	40.69
TiO2	1.14	1.25	1.49	1.44	1.51	1.61
Al2O3	10.78	10.57	11.11	10.36	10.69	9.92
FeO	26.87	26.60	26.24	26.44	26.05	26.24
MnO	0.42	0.50	0.43	0.44	0.40	0.49
MgO	4.09	4.32	4.28	4.57	4.60	4.65
CaO	11.14	10.99	11.05	11.03	10.99	11.06
Na2O	1.31	1.40	1.19	1.34	1.53	1.33
K2O	1.40	1.38	1.44	1.32	1.40	1.25
F	0.14	0.28	0.18	0.23	0.24	0.21
Cl	0.17	0.17	0.20	0.19	0.15	0.17
BaO	0.00	0.00	0.00	0.00	0.00	0.00
Total	97.79	98.30	98.01	98.19	97.70	97.60
Cations on the basis of 23(O)						
Si	6.33	6.37	6.30	6.36	6.30	6.38
Al iv	1.67	1.63	1.70	1.64	1.70	1.62
Al vi	0.32	0.31	0.35	0.27	0.27	0.22
Ti	0.13	0.15	0.17	0.17	0.18	0.19
Fe3+	0.65	0.65	0.65	0.68	0.63	0.65
Fe2+	2.88	2.82	2.77	2.77	2.79	2.79
Mn	0.06	0.07	0.06	0.06	0.05	0.06
Mg	0.96	1.00	0.99	1.06	1.08	1.09
Ca	1.87	1.84	1.85	1.84	1.85	1.86
Na	0.40	0.42	0.36	0.41	0.47	0.40
K	0.28	0.27	0.29	0.26	0.28	0.25
F	0.07	0.14	0.09	0.11	0.12	0.10
Cl	0.04	0.05	0.05	0.05	0.04	0.04
OH*	1.89	1.81	1.86	1.84	1.84	1.85
Total	17.55	17.53	17.50	17.51	17.59	17.51
(Ca+Na) (B)	2.00	2.00	2.00	2.00	2.00	2.00
Na (B)	0.13	0.16	0.15	0.16	0.15	0.14
(Na+K) (A)	0.55	0.53	0.50	0.51	0.59	0.51
Mg/(Mg+Fe2)	0.25	0.26	0.26	0.28	0.28	0.28
Fe3/(Fe3+Alvi)	0.67	0.67	0.65	0.72	0.70	0.75

Aroeiras Complex						
Sample	ARO1B-3-4B	ARO1B-3-N	ARO1B-3-B	ARO1B-3-2B	ARO1B-7	ARO1B-7-B
SiO2	39.98	41.62	40.04	41.02	41.08	40.45
TiO2	1.18	1.06	0.71	0.99	0.91	1.29
Al2O3	8.82	9.23	10.21	9.79	9.69	8.93
FeO	24.10	24.17	24.40	24.38	25.08	23.39
MnO	0.54	0.44	0.44	0.45	0.55	0.51
MgO	5.13	5.23	4.63	5.15	5.07	5.53
CaO	10.83	11.18	11.14	11.06	11.18	10.88
Na2O	1.20	1.09	1.28	1.24	1.23	1.23
K2O	1.25	1.29	1.36	1.35	1.36	1.24
F	0.24	0.08	0.15	0.24	0.37	0.01
Cl	0.15	0.14	0.20	0.15	0.18	0.18
BaO	0.00	0.00	0.00	0.00	0.00	0.01
Total	93.41	95.52	94.56	95.82	96.69	93.65
Cations on the basis of 23(O)						
Si	6.54	6.63	6.48	6.52	6.50	6.56
Al iv	1.46	1.37	1.52	1.48	1.50	1.44
Al vi	0.24	0.36	0.43	0.36	0.31	0.27
Ti	0.14	0.13	0.09	0.12	0.11	0.16
Fe3+	0.50	0.35	0.36	0.46	0.54	0.43
Fe2+	2.79	2.86	2.94	2.79	2.78	2.74
Mn	0.07	0.06	0.06	0.06	0.07	0.07
Mg	1.25	1.24	1.12	1.22	1.19	1.34
Ca	1.90	1.91	1.93	1.88	1.89	1.89
Na	0.38	0.34	0.40	0.38	0.38	0.39
K	0.26	0.26	0.28	0.27	0.28	0.26
F	0.12	0.04	0.08	0.12	0.19	0.00
Cl	0.04	0.04	0.06	0.04	0.05	0.05
OH*	1.84	1.92	1.87	1.84	1.77	1.95
Total	17.54	17.51	17.62	17.54	17.55	17.54
(Ca+Na) (B)	2.00	2.00	2.00	2.00	2.00	2.00
Na (B)	0.10	0.09	0.07	0.12	0.11	0.11
(Na+K) (A)	0.54	0.51	0.62	0.54	0.55	0.54
Mg/(Mg+Fe2)	0.31	0.30	0.28	0.30	0.30	0.33
Fe3/(Fe3+Alvi)	0.68	0.50	0.46	0.56	0.64	0.62

Serra Branca – Coxixola dike Swarms

Sample	MA05_Amp_1	MA05_Amp_2	MA05_Amp_3	MA05_Amp_4
SiO2	40.20	40.26	40.75	34.79
TiO2	1.91	1.29	1.45	2.74
Al2O3	12.24	12.44	12.13	15.69
FeO	24.32	24.08	25.26	27.03
MnO	0.46	0.47	0.44	0.26
MgO	5.56	5.53	4.95	6.73
CaO	11.28	11.26	11.10	0.05
Na2O	1.43	1.23	1.19	0.04
K2O	1.72	1.74	1.75	9.61
F	0.35	0.27	0.33	0.59
Cl	0.11	0.14	0.11	0.15
BaO	0.00	0.00	0.00	0.00
Total	99.58	98.71	99.46	97.68
		Cations on the basis of 23(O)		
Si	6.14	6.18	6.23	5.69
Al iv	1.86	1.82	1.77	2.31
Al vi	0.35	0.43	0.42	0.72
Ti	0.22	0.15	0.17	0.34
Fe3+	0.62	0.68	0.69	0.00
Fe2+	2.49	2.41	2.54	3.70
Mn	0.06	0.06	0.06	0.04
Mg	1.27	1.27	1.13	1.64
Ca	1.85	1.85	1.82	0.01
Na	0.42	0.37	0.35	0.01
K	0.34	0.34	0.34	2.01
F	0.17	0.13	0.16	0.31
Cl	0.03	0.04	0.03	0.04
OH*	1.80	1.83	1.81	1.65
Total	17.61	17.56	17.51	18.46
(Ca+Na) (B)	2.00	2.00	2.00	0.02
Na (B)	0.15	0.15	0.18	0.01
(Na+K) (A)	0.61	0.56	0.51	2.01
Mg/(Mg+Fe2)	0.34	0.34	0.31	0.31
Fe3/(Fe3+Alvi)	0.64	0.61	0.62	0.00

Serra Branca – Coxixola dike swarms				
Sample	MA05_Amp_5	MA05_Amp_6	MA05_Amp_7	MA05_Amp_8
SiO2	40.65	40.57	40.51	41.06
TiO2	1.68	1.40	1.45	1.61
Al2O3	12.29	12.08	12.19	12.02
FeO	23.72	23.82	23.43	23.99
MnO	0.43	0.46	0.43	0.48
MgO	5.86	5.61	5.69	5.58
CaO	11.22	11.18	11.15	11.27
Na2O	1.41	1.38	1.29	1.34
K2O	1.74	1.72	1.72	1.61
F	0.33	0.40	0.28	0.34
Cl	0.11	0.13	0.10	0.11
BaO	0.00	0.00	0.00	0.00
Total	99.44	98.76	98.23	99.41
Cations on the basis of 23(O)				
Si	6.19	6.24	6.24	6.26
Al iv	1.81	1.76	1.76	1.74
Al vi	0.40	0.43	0.45	0.42
Ti	0.19	0.16	0.17	0.18
Fe3+	0.61	0.58	0.57	0.55
Fe2+	2.42	2.49	2.45	2.51
Mn	0.06	0.06	0.06	0.06
Mg	1.33	1.29	1.31	1.27
Ca	1.83	1.84	1.84	1.84
Na	0.42	0.41	0.39	0.40
K	0.34	0.34	0.34	0.31
F	0.16	0.19	0.14	0.16
Cl	0.03	0.04	0.03	0.03
OH*	1.81	1.77	1.84	1.81
Total	17.59	17.59	17.56	17.55
(Ca+Na) (B)	2.00	2.00	2.00	2.00
Na (B)	0.17	0.16	0.16	0.16
(Na+K) (A)	0.59	0.59	0.56	0.55
Mg/(Mg+Fe2)	0.36	0.34	0.35	0.34
Fe3/(Fe3+Alvi)	0.60	0.57	0.56	0.56

APÊNDICE B – DADOS DE ELEMENTOS MAIORES E TRAÇOS

Sample	ARO-01A	ARO-05A	ARO-43A	ARO-43B	ARO-45	ARO-46	ARO-75	ARO-100	ARO-101B	ARO-101C	ARO-101D	ARO-102A	ARO-102B	ARO-104	MA-03	MA-10A	MA-11	MA-18	MA-50
SiO2	72.51	69.88	52.44	70.92	71.14	51.31	70.3	66.38	65.62	67.59	53	52.93	66.56	65.49	72.74	72.64	73.24	72.96	71.77
TiO2	0.18	0.367	2.03	0.28	0.32	2.22	0.29	0.54	0.67	0.52	1.77	2.5	0.52	0.58	0.23	0.2	0.19	0.28	0.22
Al2O3	14.18	14.35	14.65	14.41	13.92	14.5	14.43	15.83	15.41	14.71	14.9	14.29	14.92	14.84	13.95	13.77	13.76	13.86	13.88
Fe2O3	1.98	3.61	14.33	2.49	2.94	14.63	3.08	4.35	5.11	4.47	13.75	12.96	4.96	5.74	1.86	1.91	1.5	2.11	2.32
MnO	0.04	0.053	0.19	0.05	0.05	0.21	0.06	0.06	0.06	0.05	0.19	0.18	0.07	0.09	0.02	0.03	0.02	0.03	0.03
MgO	0.28	0.49	1.84	0.34	0.43	2.47	0.35	0.86	0.9	0.73	1.86	2.7	0.73	0.75	0.29	0.24	0.24	0.25	0.21
CaO	1.57	1.93	4.77	1.42	1.61	5.15	1.38	2.78	2.5	2.33	4.72	5.39	2.47	2.56	1.03	1.1	0.94	1.05	1.19
Na2O	3.37	3.61	3.86	3.55	3.46	3.81	3.99	3.42	3.89	3.36	3.66	3.5	3.61	3.51	2.97	2.98	2.93	3.07	3.19
K2O	5.22	4.77	3.85	5.5	4.91	3.14	4.96	4.22	4.09	4.59	3.62	2.97	4.38	4.61	5.87	5.91	5.82	5.63	5.86
P2O5	0.03	0.128	1.22	0.06	0.08	1.57	0.15	0.16	0.23	0.18	1.17	1.16	0.19	0.25	0.05	0.05	0.05	0.05	0.06
LOI					0.8		0.7	0.8	1	0.9	0.8	0.9	1	1.1					
Total	99.36	99.188	99.18	99.02	99.66	99.01	99.69	99.4	99.48	99.43	99.44	99.48	99.41	99.52	99.01	98.83	98.69	99.29	98.73
Trace-element compositions (ppm)																			
Ba	1540	1572.6	1901.2	1701	1326	1564	1342	2660	2021	2079	2187	1530	2318	2225	851	662	730	667	620
Sr	255.2	267.9	415.2	219.2	180	432.5	169.1	348.6	272	255.2	419.3	446.4	241.2	251.7	182.7	142.9	154	104.8	99.5
Rb	95	101	56.1	95	116.2	60.4	129.7	96.1	103.9	100.1	56.2	63.2	89.7	91.6	219.5	204.1	228	267.7	237.2
Th	12.2	13.4	6.3	17.7	17.8	6.1	21.4	19.2	18.4	22.7	7	6.1	20.1	16.7	32.8	43.6	43.4	63	39.9
Ni	2.2	2.6	4.7	3.8	4.1	8.6	3	6.7	5.9	3.2	4.1	12.2	6.2	5.9	<20	<20	<20	<20	<20
Y	36.5	38.8	78.7	25.8	25	63.7	34.3	35	37.1	40.1	76.9	59.9	48	43.4	13.4	14.7	15.6	22.7	12.2
Nb	18.8	19.8	41.1	16	19.4	39.9	31.4	19.9	24.9	26.2	41.1	37	29.9	29.2	14.6	17.3	16.9	24.3	19.1
Zr	201.3	201	903	291	285.7	640.9	324.2	453.3	463.3	501.5	801.8	654.4	549.8	595.5	219.8	190.4	183.1	266.5	236.9
Hf	5.8	5.8	18.1	7.7	8.1	14.6	8	11.5	11.1	11.6	16.8	14.3	12.9	13.8	6.5	6.4	5.1	7.6	7.2
Ta	1	1	2.1	0.8	0.8	2.4	1.6	0.7	0.9	1.1	2.2	2.1	1.7	1.1	0.7	0.8	1.2	1	0.8
La	55.2	72.5	87.9	84.8	87.1	92	85.2	134.8	131.2	139.8	110	87.5	128.1	112.5	97.4	103.5	94	157.7	141.7
Ce	109.9	129.7	181.8	152.7	163.9	190.5	157.2	241.2	237.7	267.7	224.1	182.4	240.3	216.2	173.9	188.2	161.1	273.9	275.0
Nd	40.4	53.38	94.1	57	56.6	89.6	51.7	86.6	87	98.4	103.3	84.3	87.5	83.9	58.2	64.1	52.7	87.4	81.8
Sm	8	8.5	16.6	9.05	8.83	16.71	9.05	12.87	13.25	14.72	19.14	15.58	13.83	13.86	8.09	9.56	7.55	12.84	11.02
Eu	1.62	1.68	4.38	1.73	1.36	4.3	1.21	2.16	2.14	2.11	4.86	3.97	2.25	2.33	0.72	0.61	0.61	0.79	0.81
Gd	6.86	7.4	15.65	6.7	6.68	15.23	7.61	9.88	10.91	11.6	17.6	14.23	11.09	11.46	5.28	6.52	5.49	8.86	7.14
Tb	1.16	1.2	2.55	1.02	1.06	2.45	1.27	1.26	1.34	1.5	2.46	1.96	1.47	1.53	0.58	0.73	0.69	1.01	0.68
Dy	6.55	6.65	13.79	4.73	5.26	12.58	6.21	7.21	7.66	8.65	14.23	11.71	8.9	8.73	2.95	3.3	3.42	4.84	2.84
Er	3.58	3.54	7.41	2.69	2.74	7.62	3.95	3.33	3.56	4.22	7.62	5.89	4.78	4.31	1.22	1.42	1.4	1.98	1.01
Yb	3.43	3.74	6.7	2.57	2.42	6.59	3.55	2.9	3.5	3.74	7.44	5.42	4.49	4.05	1.18	1.29	1.34	1.65	0.67
Lu	0.5	0.51	0.98	0.39	0.36	1.02	0.53	0.46	0.48	0.53	1.08	0.83	0.69	0.59	0.18	0.21	0.21	0.25	0.11

APÊNDICE C – DADOS U-PB EM LA-ICP-MS

MA50

	Isotopic ratios						Ages (Ma)						Rho	Th/U	Conc. (%)
Grain spot	$^{207}Pb/^{206}Pb$		$^{207}Pb/^{235}U$	± (1σ)	$^{206}Pb/^{238}U$	± (1σ)	$^{207}Pb/^{206}Pb$	± 1σ (Ma)	$^{207}Pb/^{235}U$	± 1σ (Ma)	$^{206}Pb/^{238}U$	± 1σ (Ma)			
5.sSMPABC029	0.061	1.20E-03	0.805	0.014	0.096	8.40E-04	637.82	41.68	599.8	8.08	590.4	4.92	0.49	0.73	98.41
5.sSMPABC052	0.061	1.08E-03	0.791	0.012	0.094	7.50E-04	635.35	37.69	591.7	7.03	580.8	4.44	0.51	0.41	98.12
5.sSMPABC040	0.061	9.10E-04	0.786	0.010	0.094	7.10E-04	632.87	31.93	589.2	5.78	578.1	4.2	0.59	0.60	98.08
5.sSMPABC067	0.061	1.55E-03	0.786	0.019	0.094	8.90E-04	633.58	53.78	588.7	10.54	577.7	5.27	0.40	0.27	98.10
5.sSMPABC046	0.061	1.33E-03	0.783	0.016	0.094	8.40E-04	626.84	46.64	586.9	8.98	577	4.94	0.45	0.41	98.28
5.sSMPABC048	0.061	7.80E-04	0.780	0.008	0.093	6.80E-04	627.55	27.35	585.5	4.62	574.9	3.99	0.70	0.33	98.16
5.sSMPABC049	0.060	8.10E-04	0.780	0.009	0.095	7.10E-04	594.90	29.38	585.4	5.05	583.2	4.18	0.66	0.41	99.62
5.sSMPABC028	0.060	9.30E-04	0.778	0.010	0.094	7.20E-04	605.02	33.22	584.1	5.95	579	4.25	0.57	0.47	99.12
5.sSMPABC069	0.060	8.40E-04	0.777	0.009	0.094	7.10E-04	606.46	30.07	583.9	5.25	578.4	4.16	0.64	0.51	99.05
5.sSMPABC044	0.061	8.00E-04	0.773	0.008	0.093	6.70E-04	622.57	28.2	581.5	4.79	571.2	3.97	0.67	0.71	98.20
5.sSMPABC054	0.060	7.80E-04	0.769	0.008	0.092	6.70E-04	620.79	27.57	579	4.64	568.6	3.95	0.69	0.77	98.17
5.sSMPABC066	0.059	7.40E-04	0.768	0.008	0.094	6.90E-04	570.78	27.11	578.8	4.49	581	4.05	0.72	0.74	100.38
5.sSMPABC058	0.060	1.46E-03	0.767	0.017	0.093	9.00E-04	602.85	51.92	578.2	9.98	572.2	5.32	0.43	0.53	98.95
5.sSMPABC045	0.059	7.00E-04	0.765	0.007	0.094	6.70E-04	576.66	25.47	577.1	4.08	577.4	3.93	0.77	0.53	100.05
5.sSMPABC026	0.060	1.00E-03	0.763	0.011	0.092	7.20E-04	610.41	35.44	575.9	6.4	567.4	4.24	0.54	0.56	98.50
5.sSMPABC042	0.060	7.70E-04	0.763	0.008	0.093	6.80E-04	588.72	27.84	575.6	4.67	572.5	4.03	0.69	0.58	99.46
5.sSMPABC047	0.060	1.02E-03	0.761	0.012	0.093	7.60E-04	591.99	36.68	574.4	6.66	570.4	4.46	0.54	0.72	99.30
5.sSMPABC034	0.059	7.00E-04	0.761	0.007	0.094	6.80E-04	562.66	25.7	574.3	4.14	577.5	3.99	0.77	0.77	100.55
5.sSMPABC056	0.059	7.20E-04	0.757	0.007	0.093	6.60E-04	574.46	26.15	572.5	4.19	572.2	3.9	0.74	0.30	99.95
5.sSMPABC031	0.059	7.50E-04	0.757	0.008	0.093	6.80E-04	557.84	27.44	572.1	4.53	575.8	4.01	0.70	0.21	100.64
5.sSMPABC050	0.060	8.10E-04	0.755	0.009	0.092	6.80E-04	586.90	29.2	571.3	4.94	567.6	4.02	0.65	0.78	99.35
5.sSMPABC027	0.059	7.30E-04	0.753	0.008	0.092	6.70E-04	575.93	26.66	570.1	4.35	568.8	3.95	0.73	0.71	99.77
5.sSMPABC018	0.060	7.70E-04	0.752	0.008	0.091	6.70E-04	595.62	28.34	569.1	4.63	562.7	3.96	0.69	0.64	98.86
5.sSMPABC021	0.060	1.55E-03	0.749	0.018	0.090	8.50E-04	612.92	54.59	567.8	10.45	556.7	5.05	0.39	0.37	98.01
5.sSMPABC025	0.061	1.41E-03	0.747	0.016	0.089	8.20E-04	638.88	48.86	566.7	9.24	549.2	4.88	0.43	0.54	96.81
5.sSMPABC055	0.060	7.90E-04	0.747	0.008	0.091	6.60E-04	597.43	28.48	566.6	4.75	559.2	3.92	0.67	0.51	98.68
5.sSMPABC059	0.060	8.30E-04	0.747	0.009	0.090	6.70E-04	618.29	29.54	566.4	5.02	553.8	3.95	0.65	0.45	97.72
5.sSMPABC070	0.060	9.90E-04	0.746	0.011	0.090	6.90E-04	620.79	34.99	566	6.29	552.7	4.07	0.53	0.58	97.59
5.sSMPABC033	0.060	7.80E-04	0.746	0.008	0.091	6.70E-04	589.08	27.97	565.9	4.64	560.3	3.94	0.69	0.42	99.00
5.sSMPABC051	0.059	2.29E-03	0.746	0.028	0.092	1.16E-03	567.10	82.37	565.8	16.03	566.5	6.84	0.34	0.60	100.12
5.sSMPABC143	0.060	1.19E-03	0.746	0.014	0.091	7.90E-04	585.44	42.9	565.8	7.95	561.3	4.67	0.47	0.64	99.20
5.sSMPABC019	0.061	7.50E-04	0.746	0.007	0.089	6.50E-04	628.98	26.55	565.8	4.35	550.4	3.84	0.73	0.31	97.20
5.sSMPABC032	0.059	7.90E-04	0.743	0.008	0.091	6.80E-04	578.86	28.73	563.9	4.8	560.3	4	0.67	0.76	99.36
5.sSMPABC024	0.060	1.46E-03	0.742	0.017	0.090	8.60E-04	595.26	52.32	563.5	9.77	556.2	5.09	0.42	0.48	98.69
5.sSMPABC041	0.059	7.90E-04	0.739	0.008	0.091	6.90E-04	565.99	28.74	561.8	4.91	561.1	4.07	0.67	0.54	99.88
5.sSMPABC023	0.060	7.10E-04	0.736	0.007	0.089	6.50E-04	590.54	25.51	559.8	4.07	552.5	3.84	0.77	0.75	98.68
[illegible]	[illegible]	[illegible]	[illegible]	[illegible]	[illegible]	[illegible]	[illegible]	[illegible]	[illegible]	[illegible]	[illegible]	[illegible]	[illegible]	[illegible]	[illegible]
5.sSMPABC014	0.059	1.21E-03	0.735	0.014	0.090	7.70E-04	583.25	43.7	559.3	8.03	553.6	4.53	0.46	0.46	98.97
5.sSMPABC016	0.060	1.20E-03	0.735	0.013	0.089	7.50E-04	595.26	43.25	559.3	7.81	550.8	4.46	0.46	0.89	98.46
5.sSMPABC142	0.059	1.67E-03	0.731	0.019	0.090	9.00E-04	569.31	60.42	557.2	11.42	554.6	5.35	0.38	0.49	99.53
5.sSMPABC020	0.061	1.83E-03	0.726	0.020	0.086	9.10E-04	646.27	63.02	554.3	12.02	532.8	5.38	0.38	0.77	95.96
5.sSMPABC013	0.058	1.22E-03	0.723	0.014	0.090	7.80E-04	532.03	45.85	552.6	8.21	557.8	4.59	0.45	0.46	100.93
5.sSMPABC053	0.059	8.20E-04	0.722	0.008	0.089	6.60E-04	551.15	30.13	552.1	5	552.5	3.92	0.63	0.62	100.07
5.sSMPABC139	0.059	8.30E-04	0.717	0.009	0.089	6.70E-04	548.54	30.68	549.2	5.12	549.6	3.97	0.62	0.68	100.07
5.sSMPABC057	0.060	1.03E-03	0.716	0.011	0.086	6.90E-04	610.77	36.5	548.5	6.38	533.9	4.1	0.53	0.22	97.27
5.sSMPABC131	0.059	1.91E-03	0.716	0.022	0.089	9.80E-04	553.01	69.48	548.1	13.06	547.5	5.78	0.36	0.38	99.89
5.sSMPABC137	0.059	1.00E-03	0.716	0.011	0.088	7.00E-04	568.94	36.38	548.1	6.33	543.6	4.13	0.53	0.80	99.17
5.sSMPABC140	0.059	1.21E-03	0.715	0.013	0.089	7.60E-04	552.64	44.28	547.8	7.96	547	4.48	0.46	0.42	99.85
5.sSMPABC060	0.059	1.02E-03	0.713	0.011	0.088	6.80E-04	564.51	37.08	546.7	6.38	543.3	4.02	0.51	0.64	99.37
5.sSMPABC128	0.059	9.50E-04	0.711	0.010	0.088	7.00E-04	559.33	34.86	545.5	6.05	542.4	4.14	0.56	0.67	99.43
5.sSMPABC135	0.059	1.61E-03	0.708	0.018	0.087	9.00E-04	566.36	58.46	543.8	10.85	538.6	5.32	0.40	0.71	99.03
5.sSMPABC129	0.058	1.10E-03	0.701	0.012	0.087	7.20E-04	547.04	40.76	539.5	7.13	538	4.24	0.49	0.46	99.72
5.sSMPABC043	0.059	1.02E-03	0.700	0.011	0.086	7.20E-04	556.36	37.57	538.6	6.49	534.7	4.24	0.54	0.58	99.27
5.sSMPABC132	0.059	1.10E-03	0.691	0.012	0.086	6.90E-04	552.27	40.98	533.5	7.06	529.4	4.09	0.47	0.95	99.23
5.sSMPABC130	0.058	2.31E-03	0.684	0.026	0.085	1.07E-03	541.05	84.94	529.4	15.59	527.1	6.34	0.33	0.45	99.56
5.sSMPABC133	0.058	1.83E-03	0.681	0.020	0.085	8.90E-04	542.18	67.7	527.4	12.23	524.3	5.32	0.35	0.53	99.41
5.sSMPABC134	0.058	2.16E-03	0.680	0.024	0.085	1.05E-03	537.67	79.64	527	14.47	524.7	6.25	0.35	0.59	99.56
5.sSMPABC017	0.059	1.69E-03	0.677	0.018	0.084	8.60E-04	554.50	61.47	524.8	11.05	518.3	5.11	0.38	0.21	98.75

ARO103

Grain spot	Isotopic ratios						Ages (Ma)						Rho	Th/U	Conc. (%)
	$^{207}Pb/^{206}Pb$		$^{207}Pb/^{235}U$	± (1σ)	$^{206}Pb/^{238}U$	± (1σ)	$^{207}Pb/^{206}Pb$	± 1σ (Ma)	$^{207}Pb/^{235}U$	± 1σ (Ma)	$^{206}Pb/^{238}U$	± 1σ (Ma)			
004-Z01	0.129	0.239	5.660	0.902	0.319	0.869	2080	4	1925	8	1785	14	0.96	0.12	93
005-Z02	0.162	0.211	10.018	0.696	0.449	0.663	2473	4	2436	6	2393	13	0.94	0.45	98
007-Z04	0.060	0.474	0.812	0.820	0.098	0.669	605	10	604	4	603	4	0.78	0.35	100
008-Z05	0.060	0.876	0.782	1.062	0.095	0.600	588	19	586	5	586	3	0.50	0.21	100
013-Z08	0.118	0.390	4.154	0.721	0.255	0.606	1931	7	1665	6	1462	8	0.80	0.07	88
014-Z09	0.130	0.323	6.707	0.747	0.373	0.674	2105	6	2074	7	2043	12	0.88	0.66	99
016-Z11	0.060	1.162	0.767	1.517	0.092	0.976	617	25	578	7	568	5	0.84	0.39	98
017-Z12	0.072	0.881	1.110	1.614	0.112	1.353	986	18	758	9	683	9	0.83	0.23	90
018-Z13	0.060	0.425	0.811	0.789	0.098	0.664	606	9	603	4	602	4	0.81	0.21	100
019-Z14	0.064	0.808	0.925	1.257	0.105	0.963	734	17	665	6	645	6	0.75	0.27	97
020-Z15	0.109	1.505	4.631	1.717	0.308	0.825	1785	27	1755	14	1729	13	0.71	0.54	99

APÊNDICE D – DADOS U-PB EM SHRIMP

ARO1

Grain spot	% $^{206}Pb_c$	ppm U	ppm Th	$^{232}Th/^{238}U$	ppm $206Pb^*$	(1) $^{206}Pb/^{238}U$ Age	(1) $^{207}Pb/^{206}Pb$ Age	% Dis.	(1) $^{207}Pb^*/^{206}Pb^*$	±%	(1) $^{207}Pb^*/^{235}U$	±%	(1) $^{206}Pb^*/^{238}U$	±%	err corr
ARO1-4.1	1,00	2072	512	0,26	125	439 ±7	505 ±24	+14	0,05736	1,1	0,557	2,1	0,0704	1,8	0,9
ARO1-3.1	10,75	88	74	0,88	6	483 ±8	567 ±432	+15	0,05901	19,8	0,633	19,9	0,0778	1,7	0,1
ARO1-11.1	1,08	893	315	0,36	63	508 ±5	571 ±29	+11	0,05911	1,3	0,669	1,7	0,0821	1,0	0,6
ARO1-16.1	1,52	1430	348	0,25	102	515 ±5	564 ±34	+9	0,05891	1,5	0,675	1,9	0,0831	1,1	0,6
ARO1-8.1	1,76	404	324	0,83	29	526 ±5	548 ±64	+4	0,05849	2,9	0,685	3,1	0,0850	1,0	0,3
ARO1-17.1	0,60	603	87	0,15	44	526 ±5	542 ±31	+3	0,05833	1,4	0,684	1,8	0,0851	1,0	0,6
ARO1-21.1	0,57	259	131	0,52	19	528 ±5	578 ±39	+9	0,05930	1,8	0,699	2,1	0,0854	1,1	0,5
ARO1-13.1	3,54	449	211	0,48	33	531 ±6	575 ±78	+8	0,05923	3,6	0,701	3,8	0,0859	1,3	0,3
ARO1-15.1	0,51	666	285	0,44	49	534 ±5	568 ±27	+6	0,05902	1,3	0,703	1,6	0,0864	1,0	0,6
ARO1-20.1	1,19	1135	370	0,34	84	535 ±5	557 ±33	+4	0,05873	1,5	0,701	1,8	0,0865	1,0	0,5
ARO1-19.1	0,25	353	171	0,50	27	542 ±5	576 ±24	+6	0,05924	1,1	0,716	1,5	0,0877	1,0	0,7
ARO1-2.1	0,68	624	210	0,35	47	541 ±5	524 ±36	-3	0,05784	1,6	0,698	1,9	0,0875	1,0	0,5
ARO1-9.1	1,60	330	150	0,47	25	544 ±6	622 ±59	+13	0,06051	2,7	0,734	2,9	0,0880	1,1	0,4
ARO1-1.1	1,42	662	279	0,43	50	543 ±5	529 ±52	-3	0,05798	2,4	0,703	2,6	0,0880	1,0	0,4
ARO1-5.1	0,47	582	181	0,32	44	545 ±5	545 ±30	-0	0,05841	1,4	0,711	1,7	0,0883	1,0	0,6
ARO1-18.1	0,26	2448	735	0,31	186	548 ±6	567 ±11	+4	0,05899	0,5	0,721	1,3	0,0887	1,2	0,9
ARO1-6.1	0,18	629	306	0,50	48	548 ±5	562 ±18	+3	0,05885	0,8	0,720	1,3	0,0888	1,0	0,8
ARO1-7.1	4,15	175	169	1,00	13	549 ±6	519 ±152	-6	0,05770	6,9	0,707	7,0	0,0889	1,2	0,2
ARO1-12.1	0,31	631	158	0,26	49	553 ±7	603 ±19	+9	0,05997	0,9	0,741	1,6	0,0896	1,3	0,8
ARO1-14.1	2,84	49	40	0,84	8	1115 ±15	1383 ±63	+21	0,08805	3,3	2,293	3,6	0,1889	1,5	0,4
ARO1-10.1	0,71	37	26	0,73	9	1600 ±23	1601 ±41	+0	0,09876	2,2	3,836	2,7	0,2817	1,6	0,6

NA 97

Grain.Spot	% $^{206}Pb_c$	ppm U	ppm Th	$^{232}Th/^{238}U$	ppm $^{206}Pb^*$	(1) $^{206}Pb/^{238}U$ Age	(1) $^{207}Pb/^{206}Pb$ Age	% Dis.	(1) $^{207}Pb^*/^{206}Pb^*$	±%	(1) $^{207}Pb^*/^{235}U$	±%	(1) $^{206}Pb^*/^{238}U$	±%	err corr
2,1	0,18	199	148	0,77	15.4	555.3 ± 6.3	533 ± 40	-4	0.0581	1.8	0.72	2.2	0.09	1.2	,548
3,1	5,35	2959	682	0,24	160	372.4 ± 4.1	601 ± 170	38	0.0599	7.7	0.491	7.7	0.05948	1.1	,148
4,1	0,00	178	167	0,97	14.6	586.7 ± 8.1	667 ± 38	12	0.0618	1.8	0.812	2.3	0.0953	1.4	,633
4,2	0,12	319	238	0,77	24.2	544.3 ± 7.8	550 ± 37	1	0.05854	1.7	0.711	2.2	0.0881	1.5	,661
5,1	0,72	48	58	1,25	3.66	549 ±11	511 ± 110	-7	0.0575	5.2	0.706	5.5	0.089	2	,368
6,1	1,26	36	45	1,29	2.9	568 ±14	480 ± 250	-18	0.0567	11	0.721	12	0.0922	2.6	,220
7,1	1,35	865	110	0,13	66.6	546.2 ± 5.8	542 ± 65	-1	0.0583	3	0.711	3.2	0.08843	1.1	,345
7,2	0,19	584	215	0,38	44.5	546.4 ± 5.9	545 ± 35	0	0.05841	1.6	0.712	2	0.08846	1.1	,575
8,1	0,50	105	120	1,18	8.02	546.2 ± 8.4	585 ± 100	7	0.0595	4.8	0.725	5.1	0.0884	1.6	,316
9,1	11,76	609	297	0,50	51.8	540 ±14	350 ±1100	-54	0.054	49	0.65	49	0.0874	2.8	,057
10,1	0,00	151	139	0,95	11.8	561.4 ± 9.2	540 ± 43	-4	0.0583	2	0.731	2.6	0.091	1.7	,657
10,2	0,05	608	291	0,49	47.6	562.5 ± 6	556 ± 22	-1	0.05869	1	0.738	1.5	0.0912	1.1	,743
11,1	0,81	57	45	0,82	4.22	529 ±12	565 ± 170	6	0.0589	7.7	0.694	8.1	0.0855	2.4	,300
12,1	0,58	78	56	0,74	6.02	549.9 ± 9.1	534 ± 120	-3	0.0581	5.4	0.713	5.7	0.0891	1.7	,304
13,1	0,12	541	446	0,85	40.8	541.7 ± 8.1	532 ± 27	-2	0.05806	1.2	0.702	2	0.0877	1.6	,781
14,1	0,00	145	109	0,78	11.4	567.1 ± 7.7	598 ± 45	5	0.0599	2.1	0.759	2.5	0.092	1.4	,567
15,1	3,61	310	246	0,82	24.2	541.4 ± 8.1	645 ± 280	16	0.0612	13	0.739	13	0.0876	1.6	,118
15,2	4,35	363	235	0,67	28.6	541.9 ± 7	549 ± 180	1	0.0585	8.3	0.707	8.4	0.0877	1.3	,159

APÊNDICE E – DADOS LU-HF

MA 50

Sample	$^{176}Lu/^{177}Hf$ (raw)	±2SE	$^{176}Hf/^{177}Hf$ (corr.)	±2SE	t, Age (Ma)	ε Hf (t)	T_{DM} (Ma)
MA50.1	0,000465182	3,06533203	0,281733632	29,01169472	524,8	-24,0542679	2051
MA50.2	0,001032692	6,251180647	0,281755589	14,69999151	527,4	-23,41889081	2052
MA50.3	0,000708182	4,256177265	0,281748697	17,89355932	529,4	-23,50608449	2044
MA50.4	0,000870894	5,295689738	0,281758637	20,51734296	533,5	-23,12315018	2039
MA50.5	0,001236347	14,08660866	0,281766923	25,00246364	538,6	-22,85069319	2047
MA50.6	0,000523797	3,149484509	0,281734238	21,24914865	539,5	-23,73365989	2054
MA50.7	0,00064666	3,940836613	0,281756409	21,75900416	543,8	-22,89952016	2030
MA50.8	0,000835329	5,018065786	0,281727236	24,83779608	545,5	-23,96393526	2080
MA50.9	0,000948206	5,768261749	0,281767538	26,46951165	546,7	-22,55208293	2031
MA50.10	0,000500415	3,374060375	0,281719584	17,09282887	547,8	-24,06353247	2072
MA50.11	0,000447396	2,703308328	0,281789294	16,29332561	548,1	-21,56950399	1975
MA50.12	0,001245779	7,498772087	0,281767235	26,85302172	548,1	-22,6409823	2047
MA50.13	0,00112715	7,04222394	0,281704768	20,12108286	548,5	-24,80107138	2127
MA50.14	0,001077919	6,475477955	0,281740986	29,80370167	549,2	-23,48581236	2074
MA50.15	0,000452376	2,8558821	0,281723952	17,16187651	552,1	-23,79769303	2064
MA50.16	0,000504232	3,047539188	0,281704783	17,00902823	552,6	-24,48454225	2093
MA50.17	0,000801043	5,966762615	0,281722645	23,84505896	554,3	-23,92429777	2084
MA50.18	0,000747234	4,504435333	0,281745307	18,53931723	557,2	-23,03947162	2050

APÊNDICE F – DADOS SM-ND

Sample	$^{147}Sm/^{144}Nd$	$^{143}Nd/^{144}Nd$	$^{143}Nd/^{144}Nd_i$	$\varepsilon Nd_{(t)}$	T_{DM}
ARO-01A	0.1075	0.511572	0.511160	-14.15	2.15
ARO-06	0.1108	0.511692	0.511267	-12.05	2.04
ARO-08A	0.1186	0.511741	0.511286	-11.68	2.13

ANEXO – CARTAS DE SUBMISSÃO DE ARTIGO EM PERIÓDICO

Figura 28 – Carta de submissão ao periódico International Geology Review

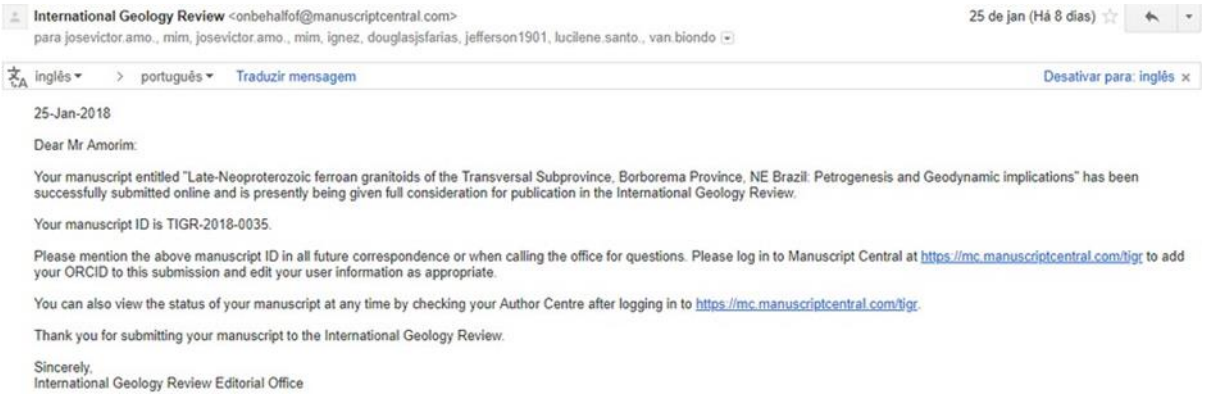

International Geology Review <onbehalfof@manuscriptcentral.com> 25 de jan (Há 8 dias)
para josevictor.amo., mim, josevictor.amo., mim, ignez, douglasjsfarias, jefferson1901, lucilene.santo., van.biondo

inglês > português Traduzir mensagem Desativar para: inglês

25-Jan-2018

Dear Mr Amorim:

Your manuscript entitled "Late-Neoproterozoic ferroan granitoids of the Transversal Subprovince, Borborema Province, NE Brazil: Petrogenesis and Geodynamic implications" has been successfully submitted online and is presently being given full consideration for publication in the International Geology Review.

Your manuscript ID is TIGR-2018-0035.

Please mention the above manuscript ID in all future correspondence or when calling the office for questions. Please log in to Manuscript Central at https://mc.manuscriptcentral.com/tigr to add your ORCID to this submission and edit your user information as appropriate.

You can also view the status of your manuscript at any time by checking your Author Centre after logging in to https://mc.manuscriptcentral.com/tigr.

Thank you for submitting your manuscript to the International Geology Review.

Sincerely,
International Geology Review Editorial Office

Figura 29 – Carta de submisão ao periódico Near Surface Geophysics

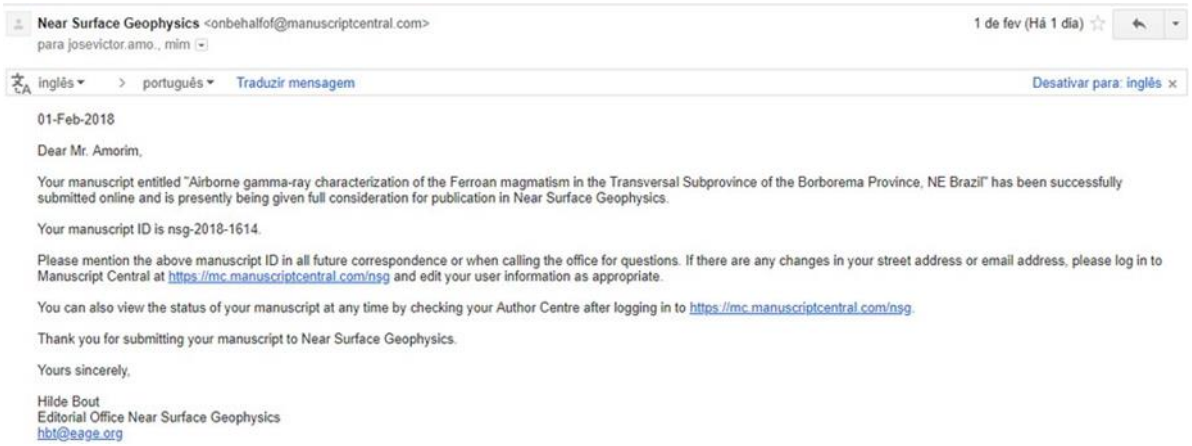

Near Surface Geophysics <onbehalfof@manuscriptcentral.com> 1 de fev (Há 1 dia)
para josevictor.amo., mim

inglês > português Traduzir mensagem Desativar para: inglês

01-Feb-2018

Dear Mr. Amorim,

Your manuscript entitled "Airborne gamma-ray characterization of the Ferroan magmatism in the Transversal Subprovince of the Borborema Province, NE Brazil" has been successfully submitted online and is presently being given full consideration for publication in Near Surface Geophysics.

Your manuscript ID is nsg-2018-1614.

Please mention the above manuscript ID in all future correspondence or when calling the office for questions. If there are any changes in your street address or email address, please log in to Manuscript Central at https://mc.manuscriptcentral.com/nsg and edit your user information as appropriate.

You can also view the status of your manuscript at any time by checking your Author Centre after logging in to https://mc.manuscriptcentral.com/nsg.

Thank you for submitting your manuscript to Near Surface Geophysics.

Yours sincerely,

Hilde Bout
Editorial Office Near Surface Geophysics
hbt@eage.org